ISBN: 978-9949-46-022-8

Current Researches in Science and Mathematics Sciences

Cetinje 2020

Current Researches in

Science and Mathematics Sciences

Editor
Dr. Canan Demir

Cetinje 2020

Current Researches in Science and Mathematics Sciences

Editor

Dr. Canan Demir

Cetinje 2020

Editor

Dr. Canan Demir

First Edition •© June 2020 /Cetinje-Montenegro

ISBN • 978-9949-46-022-8

web: www.ivpe.me

Tel. +382 41 234 709

e-mail: office@ivpe.me

Ivpe Cetinje, Montenegro

PREFACE

"Current Researches in Science and Mathematics Sciences" is serving an academic forum for both academics and researchers working in such fields. mathmematic and natural sciences research is an interdisciplinary by nature. So it covers several fields Besides, have been used as a research method for the contemporary issues relevant to mathmematic and natural sciences.In this book, the academics working in different fields share their results with the scientific community. Thus more researchers will be aware of these studies and have some new ideas for their future studies. The selected articles have been reviewed and approved for publication by referees. It is hoped that the book will be of interest and of value to academics and researchers.

We would like to take this opportunity to thank all our colleagues and writers for their efforts.

CONTENTS

PREFACE……..I

CONTENTS…….II

REFEREE BOARD……...IV

CHAPTER I

Arzu Özgen

MOLECULAR IDENTIFICATION OF ALLIUM SCHOENOPRASUM AND ITS ANTIOXIDANT AND ANTIMICROBIAL ACTIVITY,,,,,……1

CHAPTER II

Deniz Çakar & Seçil Akilli Şimşek & Y. Zekai Katircioğlu & Salih Maden

BIOLOGICAL CONTROL OF CHESTNUT CANKER CAUSED BY CRYPHONECTRIA PARASITICA (MURR.) BY HYPOVIRULENT STRAINS AT SELECTED ORCHARDS IN IZMIR AND AYDIN PROVINCES OF TURKEY…….12

CHAPTER III

Serap Çetinkaya

AN INTRODUCTION TO THE STRUCTURAL AND FUNCTIONAL METHODOLOGY FOR FRAGMENT tRNA MOLECULES……..40

CHAPTER IV

Elif Ayşe Erdoğan Eliuz

ANTIFUNGAL ACTIVITY OF BORIC ACID AND CITRIC ACID MIXTURE AS A SANITIZER AGENT……...59

CHAPTER V

Altuğ Mert Sevim & Barbaros Akkurt

USE OF SONOGASHIRA CARBON-CARBON COUPLING TO GIVE WAY TO NEW PHTHALOCYANINE MACROCYCLES..71

CHAPTER VI

Altuğ Mert Sevim & Barbaros Akkurt

ON THE HECK REACTION: A LITERATURE SURVEY WITH SOME ARTICLES IN 2020……..89

CHAPTER VII

Mustafa Biriken & Rifat Battaloğlu

DETERMINATION OF FATTY ACID COMPONENTS OF SOME TROPICAL FRUITS BY MICROWAVE ASSISTED ANALYSIS METHOD AND COMPARISON WITH TRADITIONAL METHOD……...107

CHAPTER VIII

Mehtap Düz

HYBRID (FUSION-FISSION) REACTORS…….113

REFEREE BOARD

Prof. Dr. Ali Fazıl YENİDÜNYA, Sivas Cumhuriyet University, Turkey

Prof. Dr. Mehmet ALTUN, İstanbul University Cerrahpaşa, Turkey

Prof. Dr. Mustafa NİZAMLIOĞLU, İstanbul Gelişim University, Turkey

Prof. Dr. Rıdvan KARAPINAR, Burdur Mehmet Akif Ersoy University, Turkey

Prof. Dr. Tanja SOLDATOVIĆ, Novi Pazar State University, Serbia

Prof. Dr. Zana C. DOLICANIN, Novi Pazar State University, Serbia

Assoc. Prof. Dr. Firudin AGAYEV, Institute of Technology Sciences, Azerbaijna

Asst. Prof. Dr. Dhia Hadi HUSSAİN, Mustansiriyah University, Iraq

Dr. Aydan Altıkulaç, Muğla Sıtkı Koçman University, Turkey

Dr. Canan DEMİR, Van Yüzüncü Yıl University, Turkey

MOLECULAR IDENTIFICATION OF *ALLIUM SCHOENOPRASUM* AND ITS ANTIOXIDANT AND ANTIMICROBIAL ACTIVITY

Arzu Özgen*

1. Introduction

Allium, which is one of the largest genera, is a perennial flowering herbaceous plant (Rattanachaikunsopon and Phumkhachorn, 2008; Zdravković-Korać et al., 2010; Vlase et al., 2012; Parvu et al., 2014). According to the classification of the APG III (Angiosperm Phylogeny Group), it is placed in the *Amaryllidaceae* family and *Allioideae* subfamily (Timité et al., 2013; Gardens Royal Botanic, 2017).

Nowadays, the classification forms of APG which is based on the molecular data are accepted. Thus, it is possible to explain the evolutionary relationships of the plants world and to classify the species more reliably. Studies have shown that the error rate of the systematic morphologies based on the previous studies is very high. In other words, classical taxonomy does not take into account the changes in the genomic level and, in most cases, leads to erroneous results (Angiosperm Phylogeny Group, 1998; Angiosperm Phylogeny Group II, 2003). Over the centuries, *Allium* species have been widely used as ethnomedicine for the prevention of various diseases as well as their use as vegetables and spices (Barazani et al., 2004; Kim et al., 2016).

Members of the *Allium* genus are known as very good sulfur compounds producers (Timité et al., 2013) and contain chemical compounds that are important for human health, such as anthocyanins, flavonoids, phenols, tannins and carotenoids (Vina and Cerimele, 2009). It has been supported by studies that various pharmacological activities such as antioxidant, anti-inflammatory, antimicrobial, anticancer, anti-HIV, anticoagulant, neuroprotection, immunomodulation, antitubercular and anti-allergy are related to the presence of these important compounds (Ariga and Seki, 2006; Kaiser et al., 2009; Vlase et al., 2012). Chives, which have limited studies in the literature, are members of the Amaryllidaceae family along with leeks, shallots, onions and garlics (Singh et al., 2018; Rattanachaikunsopon and Phumkhachorn, 2008).

* Asst. Prof. Dr. Department of Medical Services and Techniques, Vocational School of Health Sciences, Istanbul Gelisim University, İstanbul, Turkey. E-mail: aozgen@gelisim.edu.tr

Chives grow naturally in many places of the world including Turkey. They are used in cheese production process and in traditional meals in many places of the world. It has positive effects on health such as regulation of blood pressure by decreasing it and antimicrobial activity especially against fungi (Rattanachaikunsopon and Phumkhachorn, 2008). There are many epidemiological studies regarding to disease preventing effects of natural foods. The biochemical studies showed that *Allium* species contain minerals, vitamins, lipids, amino acids (Singh et al., 2018) and different antioxidants. All parts of chives, especially the leaves, have a significant nutritional value (Stajner et al., 2008; Stajner and Popovic, 2009). Chives leaves that contain high amounts of superoxide dismutase (SOD) activity, free thiol and carotenoid have beneficial effects that cannot be ignored in processes such as tumor development, cardiovascular diseases and aging associated with free radicals (Zdravkovic´-Korac et al., 2010).

In this study, the determination of the chives species, which grow naturally in Sultan Murat Plateau in the eastern Black Sea Region (Turkey) with an altitude of 2100 meters and were identified at the molecular level for the first time, with the ITS nucleotide sequence was carried out and the obtained data were entered the international gene bank and its antioxidant and antibacterial effects were investigated.

2. Materials and methods

Plant material

Chives were collected from Sultan Murat Plateau with an altitude of 2100 meters in August 2017. The collected plant materials were dried in an area with no direct sunlight and light air flow.

Bacterial strains

The bacterial strains used in this study were obtained from Acıbadem Mehmet Ali Aydınlar University, Faculty of Medicine, Department of Microbiology. In antibacterial activity assays, the Gram (+) bacteria (*Staphylococcus aureus* ATCC 95923, *Staphylococcus epidermidis* ATCC 12228) and Gram (-) bacteria (*Pseudomonas aeruginosa* ATCC 27853, *Klebsiella pneumonia* ATCC 700603, *Escherichia coli* ATCC 25922, *Proteus mirabilis* ATCC 27853, *Salmonella Typhimurium* ATCC 14028, *Acinetobacter baumannii* ATCC BAA 747) were used.

Ethanol extraction procedure

200 mg of dried and powdered plant leaves were weighed and kept for 10 min in 5 ml ethanol (absolute) in ultrasonic bath (35 kHz and 37 °C). Samples were centrifuged at 6000xg for 15 minutes. The supernatant phase was taken and passed through Whatmann paper. It has been put in

incubator at 37 °C for complete removal of ethanol. The extracts were stored at 4 ° C until use.

Total genomic DNA isolation of the chives

The finely chopped plant leaves were disinfected with 70% ethanol for 3 min to remove the microorganisms that they may contain on their surfaces. The plant leaves were passed through the sterile purified water and then subjected to the bead-beating process of the ZymoBIOMICS DNA Miniprep Kit (D4303). The following steps were carried out according to the defined procedure in the kit. The concentration of the obtained genomic DNA was measured with the nanodrop.

Amplification of ribosomal RNA (rRNA) internal spacer (ITS) regions and sequence analysis

ITS DNA regions of chives were amplified by polymerase chain reaction (PCR). The primers were ITS4 Reverse 5'-TCCTCCGCTTATTGATATGC-3'; ITS5 Forward 5'-GGAAGTAAAAGTCGTAACAAGG-3'. The 50 µl of PCR reaction contained 0.2 mM dNTP mix, 0.2 µM of each primer, 10 ng DNA, 5X Phusion HF buffer (contains 7.5 mM $MgCl_2$ which provides 1.5 mM $MgCl_2$ in final concentration) and 0.02 U/µL of Phusion DNA polymerase (Thermo Scientific) in the BIO-RAD T100-Thermal Cycler. The PCR conditions were follows; An initial denaturation and enzyme activation step of 30 seconds at 98°C was followed by 35 cycles amplification at the following conditions; 10 seconds at 98°C, 30 seconds 53°C and 40 seconds 72°C and 10 minutes extension at 72°C completed the protocol. The PCR product was separated in 1% agarose gel at 80 V voltage for 45 min and visualized on BIO-RAD ChemiDoc MP Imaging System. ITS DNA region fragment was excised and purified using the Zymo Gel DNA Recovery Kit (D4007) and purified ITS DNA amplicon concentration was measured using Thermo Scientific Varioskan Flash Multimode Reader (Thermo Scientific) and then ligated into pJET1.2/blunt cloning vector (Thermo Scientific). The ligation product was transformed into the *E. coli* DH5α competent cells and the positive clone was confirmed by the restriction enzyme digestion (*Bgl*II) and sequenced at the Macrogen Company. The nucleotide sequence data was searched with the National Center for Biotechnology Information (NCBI) database using Basic Local Alignment Search Tool (BLAST). The ITS DNA sequence of chive was registered to the GenBank and the accession number was acquired.

Antioxidant activity

The antioxidant activity of the chives was examined according to 1,1-diphenyl-2-picryl-hydrazil (DPPH) radical-scavenging assay using the

Brand-Williams method (Brand-Williams, 1995). 20 mg/L of the DPPH solution was prepared to be dissolved in ethanol. In the following step, the serial dilutions of the plant extract were prepared as 100, 250, 500,750 and 1000 µg/ml. 0.75 ml of each plant dilutions were added on 1.5 ml of the DPPH solution. This mixture was incubated in a dark place in the room temperature for 30 minutes. The absorbance of the mixture was measured at 517 nm. Ethanol was used as the blank and 100, 250, 500, 750, 1000 µg/ml concentrations of the Butylated hydroxyanisole (BHA), butylated hydroxytoluene (BHT) and ascorbic acid solutions were used as the standard antioxidants.

Antioxidant activity of chives was calculated by the following way:

DPPH Scavenging Effect (%) = $[(A_0-A_1)/A_0 \times 100]$,

Where A_0 is the absorbance of the control reaction and A_1 is the absorbance in the presence of the chives extract or standards.

The antimicrobial activity

Disk-diffusion assay

The Antibacterial activities of the chives extract obtained by ethanol extraction were determined by the disc-diffusion susceptibility test using a solid medium (Russell and Furr, 1977; Irobi et al., 1994). The chives extract was dissolved in the DMSO to a final concentration of 30 mg/ml. Eight G (+) and G (-) bacterial species were grown in Luria-Bertani (LB) broth medium at 37 ° C for 16 hours at 200 rpm in the dry air incubator. The liquid cultures were used in order to get 10^8 CFU/ml bacteria (CLSI 2012). 100 µl of the bacteria suspensions were inoculated on the LB agar with the help of a sterile L-spreader. The sterile discs (Whatmann No:1, 6 mm in diameter) were placed on the petri dishes. Then, the disks impregnated with the chives extracts (300 µg/disc). Appropriate antibiotic disks were used as positive controls for each bacterial strain. For the negative control, the disks impregnated with DMSO were used. Bacteria were incubated at 37 °C for 24 hours and the results of the dimeters of inhibition zones were measured in millimeters. The experiments were repeated twice.

Determination of minimum inhibitory concentration of chives extract

The minimum inhibitory concentration of chives extract against bacteria was studied by broth micro dilution assay using 96-well cell culture plates (NCCLS 2002). 10^8 CFU/ml of bacteria grown in broth culture for 12 hours were prepared as suspensions. The plant extract was dissolved in 10% DMSO to a concentration of 500 µg/ml. Into the each

well of a 96-well plate, 95 µl of LB broth and serial dilutions of plant extracts (from 500 µg/ml to 7.8125 µg/ml) were placed and 5 µl of bacteria cultures were added. 195 µl of LB broth agar and 5 µl of bacteria were used as the negative control. For the positive control, the standard antibiotics were used. The 96-well plate was put on a shaker at 300 rpm for 20 minutes and incubated at 37 °C for 24 hours. Microbial growth was measured at 600 nm using the Thermo Scientific Varioskan Flash Multimode Reader (Thermo Scientific). The study was repeated twice. Minimum inhibitory concentration (MIC) was defined as the lowest concentration that inhibits the bacterial growth.

3. Results and discussion

In recent years, molecular phylogeny studies have been used in the classification of plants and this contribution is too high to deny. Comparisons at the molecular level increase the accuracy of phylogenetic results and plant nuclear genomic DNA and organelle DNA were found to be the most suitable sites for these results (Uncu et al., 2015). rRNA genes and spacer regions are important sources for reaching the genetic informations of all living beings (Dixon and Hillis, 1993). These DNA regions are composed of large and small subunits and highly conserved in eukaryotes (Caetano-Anollés, 2002).

Therefore, the spacer regions of RNA loci are important for the classification of the plants as for the other living beings (Poczai and Jaakko, 2010). Eukaryotic genomic DNA have two different ITS regions named ITS1 and ITS2 regions which are found between the 18S rRNA, 5.8S rRNA and 26S rRNA genes and the 5.8 rDNA exon which locates between the ITS1 and ITS2 regions that highly conserved (Wheeler and Honeycutt, 1988). This region contains 500-700 bp in angiosperms (Baldwin, 1995).

In this study, the 744 bp long PCR products of chives obtained using ITS4 and ITS5 primers were cloned into pJet1.2/ blunt cloning vector, confirmed by restriction enzyme cleavage (Fig. 1) and sequenced with Sanger dideoxy sequencing method. The DNA nucleotide sequences obtained as a result of sequencing were determined to be *Allium schoenoprasum* (Chives) at 99% similarity level compared with different *A. schoenoprasum* species (Accesion number: KF419377.1, Accesion number: GQ412234.1, Accesion number: KU145490.1) from NCBI GenBank and the accession number MH174936.1 was taken from the gene bank.

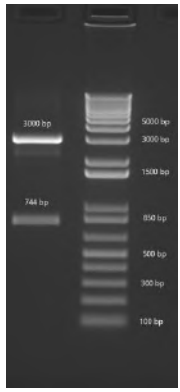

Figure 1: PCR product of chives cloned into pJet1.2/ blunt cloning vector, confirmed by restriction enzyme cleavage. 1 % agarose gel electrophoresis of M: 1 kb marker DNA ladder (Invitrogen), 3000 bp: pJet1.2/ blunt cloning vector, 744 bp: PCR product of chives (ribosomal RNA (rRNA) internal transcribed spacer (ITS) regions).

Nowadays, interest in natural herbal products with antioxidant properties is increasing and the use of antioxidant compounds in plants for food preservation is a viable and healthy alternative to compared with non-popular synthetic antioxidants. (Chen et al., 2013; Mnayer et al., 2014).

Chives have antioxidant and antibacterial properties because they contain various flavonoids, lipids, fatty acids, steroids, anthocyanins, miscellaneous and various minerals such as potassium, magnesium and sodium, sulfur compounds and their precursors with polyphenols and dietary fibers (Nencini et al., 2007; Haro et al., 2017; Singh et al., 2018). In 2004, Stajner et al. have supported the antioxidant activities of various enzymes of Chives such as superoxide dismutase, SOD, catalase, C-ase, peroxidase, P-ase, glutathione peroxidase, GP-ase and reported that all organs of the plant, especially the leaves, could be used as a natural antioxidant source.

In 2014, Dima Mnayer et al. have determined the rate of DPPH inhibition of the chive essential oil in 2 mg/ml, 4 mg/ml, 8 mg/ml concentrations as 39.05 ± 0.33, 45.15 ± 0.11 and 57.34 ± 1.14, respectively. In this study, the antioxidant activity of *A. schoenoprasum* obtained by ethanol extraction was determined using DPPH. 21% at 0.1 mg/ml, 31% at 0.25 mg/ml, 39% at 0.5 mg/ml, 41% at 0.75 mg/ml and 50% at 1 mg/ml were determined (Fig. 2).

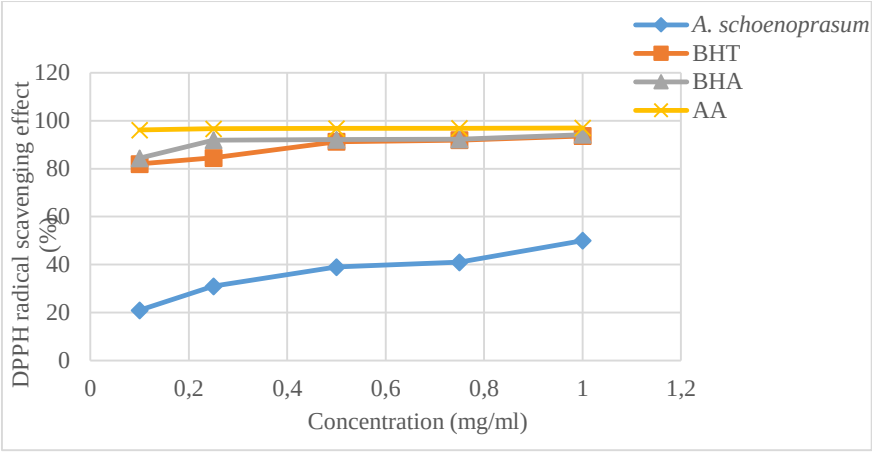

Figure 2: DPPH scavenging activity of the extract from *A. schoenoprasum.*

Lipid oxidation and microbial changes are among the causes of the deterioration quality, safety and shelf life of foods, and the presence of pathogens in foods may be responsible for serious diseases that may cause death. Allium-derived antibacterial compounds inhibit the microbial growth by reacting with the sulfhydryl (SH) groups of cellular proteins of microorganisms (Kyung, 2012). The antibacterial activity of chives is associated with the sulfur compounds such as diallyldisulfide, diallyltrisulfide and diallyltetrasulfide (Rattanachaikunsopon and Phumkhachorn, 2008).

In this study, we investigated the antibacterial activity of *A. schoenoprasum* obtained by ethanol extraction against (*Staphylococcus aureus* ATCC 25923, *Staphylococcus epidermidis* ATCC 12228) and Gram (-) bacteria (*P. aeruginosa ATCC* 27853, *K. pneumonia* ATCC 700603, *E. coli* ATCC 25922, *P. mirabilis* ATCC 27853, *S. Typhimurium ATCC* 14028, *A. baumannii* ATCC BAA 747) by the disc diffusion and MIC assay. The results are given in Suppl. Table 1. According to the results, Chives extract formed an inhibition zone between 7 mm and 8 mm on bacteria. Similar results were obtained in the study of Dima Mnayer et al in 2014. In the MIC study, the MIC value of the chives extract on *P. aeruginosa ATCC 27853* was determined as 31.25 µg/ml and 7.8125 µg/ml for *K. pneumonia ATCC 700603.*

Table 1. Antibacterial activity of *A. schoenoprasum* extract against the bacterial strains assayed

Pathogens	Plant Extract (EtOH)		Antibiotics	
	Disc diffusion[a](300 µg/disc)	Minimal Inhibition Concentration (µg/ml)	Disc diffusion[c]	Minimal Inhibition Concentration (µg/ml)
S. aureus ATCC 25923	8 mm	ND	33 mm (AM)	10 (AM)
S. epidermidis ATCC 12228	7 mm	ND	30 mm (VA)	30 (VA)
P. aeruginosa ATCC 27853	7 mm	31,25	20 mm (AK)	20 (AK)
K. pneumonia ATCC 700603	8 mm	7,8125	20 mm (FOX)	30 (FOX)
E. coli ATCC 25922	7 mm	ND	20 mm (AMC)	20/10 (AMC)
P. mirabilis ATCC 27853	ND[b]	ND	20 mm (FOX)	30 (FOX)
S. Typhimurium ATCC 14028	8 mm	ND	23 mm (SXT)	1,25/23,75 (SXT)
A. baumannii ATCC BAA 747	8 mm	ND	24 mm (AM)	10 (AM)

[a] Inhibition Diameter (mm) [2] Including Disk Diameter of 6.0 mm

[b] ND: Not Detected

[c] AM: ampicillin (10 µg/ml); VA: vancomycin (30 µg/ml); AK: amikacin (30 µg/ml); FOX: cefoxitin (30 µg/ml); AMC: amoxicillin-clavulanate (20/10 µg/ml); SXT: trimethoprim-sulphamethoxazole (1,25/23,75 µg/ml)

When the data obtained from the study are evaluated, it is important to use the antioxidant and antibacterial properties of Chives as a protective and bacterial growth inhibitor in foods as other natural antioxidants and antibacterial plants.

Acknowledgments

This work was financially supported by the Department of Medical Microbiology, Faculty of Medicine, Acıbadem Mehmet Ali Aydınlar University, İstanbul, Turkey.

References

Angiosperm Phylogeny Group (1998), "An ordinal classification for the families of flowering plants", *Annals of the Missouri Botanical Garden*, 85: 531-55.

Angiosperm Phylogeny Group II (2003), "An update of the Angiosperm Phylogeny Group classification for the orders and families of flowering plants", *Botanical journal of the Linnean Society*, 141: 399-436.

Ariga, T. & Seki, T. (2006), "Antithrombotic and anticancer effects of garlic-derived sulfur compounds: a review", *Biofactor,* 26: 93-103.

Baldwin, B.G., Sanderson, M.J., Porter, J.M., Wojciechowski. M.F., Campbell, C.S., & Donoghue, M.J. (1995), "The ITS region of nuclear ribosomal DNA: a valuable source of evidence on angiosperm phylogeny", *Annals of the Missouri Botanical Garden*, 82: 247-277.

Barazani, O., Dudai, N., Khadka, U.R., & Golan-Goldhirsh, A. (2004), "Cadmium accumulation in *Allium schoenoprasum* L. grown in an aqueous medium", *Chemosphere*, 57: 1213-1218.

Brand-Williams, W., Cuvelier M.E., & Berset, C. (1995), "Use of a free radical method to evaluate antioxidant activity", *Food Science and Technology–Lebensmittel Wissenschaft und Technologie*, 28: 25-30.

Caetano-Anollés, G. (2002), "Tracing the evolution of RNA structure in ribosomes", *Nucleic Acids Research,* 30: 2575-2587.

Chen, W., Sudji, I.R., Wang, E., Joubert, E., van Wyk, B.E., & Wink, M. (2013), "Ameliorative effect of spalathin from rooibos (*Aspalathus linearis*) on acute oxidative stress in *Caenorhabditis elegans*", *Phytomedicine*, 20: 380-386.

Clinical and Laboratory Standards Institute, (2012), "Methods for dilution antimicrobial susceptibility tests f or bacteria that grow aerobically; approved standard", 9. Edition, *CLSI document* M07-A9, Wayne, 68 s.

Dixon, M.T. & Hillis, D.M. (1993), "Ribosomal RNA secondary structure: compensatory mutations and implications for phylogenetic analysis", *Molecular Biology and Evolution*, 10: 256-267.

Gardens, Royal Botanic. (2017), "Kew and Missouri Botanical Garden, The Plant List: a working list of all plant species".

Haro, G., Sinaga, S.M., Iksen, I., Nerdy, N., & Theerachetmongkol, S. (2017), "Protective effects of chives leaves (*Allium schoenoprasum* L.) infusion against ethylene glycol and ammonium chloride induced nephrolithiasis in rats", *Journal of Applied Pharmaceutical Science*, 7: 222-225.

Irobi, O.N., Moo-Young, M., Anderson, W.A., & Daramola, S.O. (1994), "Antimicrobial activity of bark extracts of *Bridelia ferruginea* (Euphorbiaceae)", *Journal of Ethnopharmacology*, 43: 185-190.

Kaiser, P., Youssouf, M.S., Tasduq, S.A., Singh, S., Sharma, S.C., Singh, G.D., Gupta, V.K., Gupta, B.D., & Johri, R.K. (2009), "Anti-allergic effects of herbal product from *Allium cepa* (Bulb)", *Journal of Medicinal Food*, 12: 374-382.

Kim, S., Kim, D.B., Lee, S., Park, J., Shin, D., & Yoo, M. (2016), "Profiling of organosulphur compounds using HPLCPDA and GC/MS system and antioxidant activities in hooker chive (*Allium hookeri*)", *Natural Product Research*, 30: 2798-2804.

Kyung, K.H. (2012), "Antimicrobial properties of allium species", *Current Opinion in Biotechnology*, 23: 142-147.

Mnayer, D., Fabiano-Tixier, A.S., Petitcolas, E., Hamieh, T., Nehme, N., Ferrant, C., & Chemat, F. (2014), "Chemical composition, antibacterial and antioxidant activities of six essentials oils from the Alliaceae family", *Molecules*, 19: 20034-20053.

National Committee for Clinical Laboratory Standards, (2002), "Performance Standards for Antimicrobial Susceptibility Testing", 12. Edition, Informational Supplement M100-S12, *NCCLS*, Wayne, PA.

Nencini, C., Cavallo, F., Capasso, A., Franchi, G.G., Giorgio, G., & Micheli, L. (2007), "Evaluation of antioxidative properties of *Allium* species growing wild in Italy", *Phytotherapy Research*, 21: 874-878.

Parvu, A.E., Parvu, M., Vlase, L., Miclea, P., Mot, A.C., & Silaghi-Dumitrescu, R. (2014), "Anti-inflammatory effects of *Allium schoenoprasum* L. Leaves", *Journal of Physiology and Pharmacology*, 65: 309-315.

Poczai, P. & Jaakko, H. (2010), "Nuclear ribosomal spacer regions in plant phylogenetics: problems and prospects", *Molecular Biology Reports*, 37: 1897-1912.

Rattanachaikunsopon, P. & Phumkhachorn, P. (2008), "Diallyl sulfide content and antimicrobial activity against food-borne pathogenic bacteria of chives (*Allium schoenoprasum*)", *Bioscience, Biotechnology, and Biochemistry*, 72: 2987-2991.

Russell, A.D. & Furr, J.R. (1977), "The antibacterial activity of a new chloroxylenol preparation containing ethylenediamine tetraacetic acid", *The Journal of Applied Bacteriology*, 43: 253-260.

Singh, V., Chauhan, G., Krishan, P., & Shri, R. (2018), "*Allium schoenoprasum* L.: a review of phytochemistry, pharmacology and future directions", *Natural Product Research*, 32: 2202-2216.

Štajner, D., Čanadanović-Brunet, J., & Pavlović, A. (2004). *Allium schoenoprasum* L., as a natural antioxidant. *Phytotherapy Research*, 18: 522-524.

Stajner, D., Igic, R., Popovic, B.M., & Malencic, Dj. (2008), "Comparative study of antioxidant properties of wild growing and cultivated *Allium* species", *Phytotherapy Research*, 22: 113-117.

Stajner, D. & Popovic, B.M. (2009), "Comparative study of antioxidant capacity in organs of different *Allium* species", *Central European Journal of Biology*, 4: 224-228.

Timité, G., Mitaine-Offer, A.C., Miyamoto, T., Tanaka, C., Mirjolet, J.F., Duchamp, O., & Lacaille-Dubois, M.A. (2013), "Structure and cytotoxicity of steroidal glycosides from *Allium schoenoprasum*", *Phytochemistry*, 88:61-66

Uncu, A.O., Uncu, A.T., Celık, I., Doganlar, S., & Frary, A. (2015), "A primer to molecular phylogenetic analysis in plants", *Critical Reviews in Plant Sciences*, 34: 454-468.

Vina, S.Z.& Cerimele, E.L. (2009), "Quality changes in fresh chives (*Allium schoenoprasum* L.) during refrigerated storage", *Journal of Food Quality*, 32: 747-759.

Vlase, L., Parvu, M., Parvu, E.A., & Toiu, A. (2012), "Chemical constituents of three *Allium* species from Romania", *Molecules*, 18: 114-127.

Wheeler, W.C. & Honeycutt, R.L. (1988), "Paired sequence difference in ribosomal RNAs: evolutionary and phylogenetic implications", *Molecular Biology and Evolution*, 5: 90-96.

Zdravković-Korać, S., Milojević, J., Tubić, L., Ćalić-Dragosavac, D., Mitić, N., & Vinterhalter, B. (2010), "Somatic embryogenesis and plant regeneration from root sections of *Allium schoenoprasum* L", *Plant Cell, Tissue and Organ Culture*, 101: 237-244.

BIOLOGICAL CONTROL OF CHESTNUT CANKER CAUSED BY *CRYPHONECTRIA PARASITICA* (MURR.) BY HYPOVIRULENT STRAINS AT SELECTED ORCHARDS IN IZMIR AND AYDIN PROVINCES OF TURKEY*

Deniz Çakar* & ***Seçil Akıllı Şimşek*****
Y. Zekai Katırcıoğlu** & ***Salih Maden******

INTRODUCTION

Chestnut is encountered by a serious disease, not only causing great damage but killing the trees on some conditions, everywhere in the world where chestnut grows. The disease, known as chestnut canker or chestnut blight, is caused by a fungus named as *Cryphonectria parasitica* (Murrill.). This disease is also present in the Aegean Region of Turkey, found in all of the chestnut growing areas of Turkey (Erincik et al., 2003; Döken et al., 2004; Çeliker and Onoğur, 2009; Erincik et al., 2011; Akıllı Şimşek et al., 2019). In the Aegean region, particularly in İzmir and Aydın provinces, about 5000 ha chestnut forests were mostly converted to chestnut orchards by the villagers by removing the other trees and grafting them to good quality varieties, besides new orchards have been set up by grafted saplings. Healthy, well-cared orchards used to provide a profitable income to the farmers but this was impaired by some diseases especially by chestnut canker.

The most common and effective control method applied for chestnut cancer is the biological control accomplished by using hypovirulent isolates. Hypovirulence is caused by viruses infecting the pathogen fungus and decreasing its virulence (MacDonald and Fulbright, 1991; Bisiach et al., 1995). Hypovirulence appeared in some countries naturally but in some places it has been spread by artificial inoculations (Heiniger and Rigling,

---

*This work is derived from the master's thesis by Deniz Çakar. The topic it is "*Determination of the Effectiveness of Different Methods Used for the Application of Hypovirulent Isolates for the Biological Control of Chestnut Canker (Cryphonectria parasitica)* (Kestane Kanseri (*Cryphonectria parasitica*)'nin Biyolojik Mücadelesinde Kullanılan Hipovirülent İzolatların Uygulanmasında Değişik Yöntemlerin Etkinliğinin Araştırılması)

** (Researcher); Forestry Research Institute of Western Black Sea Region, Bolu, Turkey, denizcakar@ogm.gov.tr

*** (Prof. Dr.) Çankırı Karatekin University, Çankırı, Turkey, secilakilli@gmail.com

**** (Prof. Dr.) Ankara University, Ankara, Turkey, katirci@agri.ankara.edu.tr

***** (Prof. Dr.) Ankara University, Ankara, Turkey, salihmaden@hotmail.com

1994). Hypovirulence appeared first in Italy in 1950's by formation of healing cankers (Heiniger and Rigling, 1994). Afterwrads, healing cankers have been observed in the many other countries and the fungus obtained from those cankers was found infected by dsRNA viruses. Hypovirulence in Turkey was first detected 30 years after the first record of the disease in 1968 (Robin and Heiniger, 2001).

There have been some countries having chestnut canker but no natural hypovirulence till now, such as Portugal (Bragança et al., 2007), Spain (Castano et al., 2015; Zamora et al., 2012), Bulgaria (Risteski et al., 2013), Romania (Adamcikova et al., 2015), Northern Switzerland (Hoegger et al., 2000) and Aegean region of Turkey (Erincik et al., 2011).

Bryner and Rigling (2011) pointed out that hypovirulence was not only correlated with the intensity of virus but environmental factors also affected it.

When the virulent *C. parasitica* infected by the hypovirus, the pathogen loses it virulence and the cankers on the infected tree heals by formation of new calli. Such cankers appear slightly swollen and darker in colour, for this reason they are called as healing cankers and they do not cause any damage to the trees (Milgroom and Cortesi, 2004).

Information on the presence of hypovirulence, its effectiveness, and vegetative compatibility (vc) types of the pathogen is of the most importance for a successful biological control (Anagnostakis et al., 1986; MacDonald and Fulbright, 1991; Heiniger and Rigling, 1994; Cortesi and Milgroom, 1998; Robin et al., 2010). High variation of vc types in a population will influence the success of the biological control (Anagnostakis et al., 1986; Heiniger and Rigling, 1994; Robin et al., 2000; Cortesi et al., 2001).

Hypovirulence treatments yielded successful results in Europe. Treatment is generally achived by drilling wells with a cork borer around the cankers and by placing compatible hypovirulent culture disks or hypovirulent pastes in the wells. Hypovirulence treatment is more effective especially when young cankers with thin barks which are easy to handle, are treated (Robin et al., 2000; Hoegger et al., 2003). Hypovirulence treatment is more difficult on the cankers when they are so big, take place on the upper parts of the trees and have old thick barks. Although healing appears on the hypovirulence treated cankers, spread of hypovirulence does not occur always (Milgroom and Cortesi, 2004). There are some factors affecting the spread of hyopovirulence. Among these; application of as many treatments as possible (Heiniger and Rigling, 2009; Diamandis et al., 2014), and selection of an effective biocontrol agent (MacDonald

and Fulbright, 1991). Subtypes of hypovirus CHV-1 may affect the growth and sporulation of the pathogen fungus at different rates (Bryner and Rigling, 2011; Robin et al., 2010). It was mentioned that; although subtypes F1 and F2 reduced the growth of the fungus significantly, subtype I was found more efficient for prevention of canker growth and spread of hypovirulence (Akıllı et al., 2013; Robin et al., 2010; Rigling and Prospero, 2017).

Variation on vc types also affects the distribution of hypovirus. Because of the diversity on vc types in North Eastern America, hypovirulence treatment was not found so effective (Milgroom and Cortesi, 2004). In North America, natural hypovirulence was only observed at some chestnut stands in Michigan and Ontario (Milgroom and Cortesi, 2004). In Macedonia; treatment of cankers with CHV-1 prevented canker development and caused a recession on tree deaths (Sotirowski et al., 2011). In Romania; biological control studies carried out on new coming sprouts on the heavily infected trees for five years by disk application of hypovirulent strains gave successful results (Chira et al., 2017). In Spain; Effectiveness of CHV-1 subtype F isolates on canker growth was evaluated on both cut–stems and on trees in the forest. On the studies on cut-stems; strains of hypoviruses did not prevent canker growth on Eu-1 vc types, but four hypovirulent isolates of vc type Eu-11 retarded canker growth. Field applications of hypovirulent isolates of both vc types were effective in Leon province but not in Zamora. This study showed that hypovirulent subtype F isolates were effective controlling chestnut canker in 33 Leon but not so in Zamora province (Zamora et al, 2012, 2014). Using hypovirulent isolates transformed by French hypovirus, in Slovakia, about 32% success was obtained (Juhásová et al., 2005). Hypovirulence applications in Italy were observed for fifteen years and along with healing, spread of the hypovirus was also determined (Turchetti and Marsei, 2008). In France, biological control studies were performed on 200 cankers at about 20 ha area by inoculating hypovirulent isolates and healing was observed after 4 years. In a similar study in Italy, on 233 cankers, good results were obtained (Heiniger and Rigling, 1994). Biological control programs with transmissible hypovirulence were established in France, Italy, Greece, and Switzerland (Bisiach et al., 1991; Calza, 1993; Robin et al., 2000; Heiniger and Rigling, 2009).

Since *Cryphonectria parasitica* (Murr.) Barr. has caused serious damage on chestnut also in Turkey, biological control studies have been put into practice. The prevalence of the disease in Black Sea region was determined by many researchers (Coşkun et al., 1999; Gürer et al., 2001) and also by a project work supported by Scientific Research Projects Department of Ankara University with the project no 2006/07 111 01, in

detail. With the project work, TCP/TUR/3201 funded by FAO, "Support to Turkish Government in development and implementation of a Feasibility Study (FS) for management of chestnut blight in chestnuts and other hardwoods" disease situation and precautions to be taken was determined. Afterwards; a new project, 'TCP/TUR/615676 FAO-Management of Chestnut Blight and Increased Capacity for Improving Forest Health and Vitality' was put into practice. With this project, biological control studies were started at the selected locations. At the selected 3 sites the cankers showed healing. A laboratory, funded by FAO, responsible for biological control of chestnut canker was established at the Insttitute of Western Black Sea Forestry Research Institute in Bolu (FAO, 2014). This laboratory undertakes biological control studies at various locations in Turkey. In the areas like İzmir and Aydın where there is no hypovirulence, Chestnut cankers were treated by hypovirulent isolates of Eu-1 (Turkish origin), Eu-12 (Macedonian origin) prepared by this laboratory. On the other hand, Çeliker et al. (2017) used an Eu-1 hypovirulent isolate at Haciisalar village of Turgutlu-Manisa to treat virulent cankers by disk method and found it effective.

Hypovirulent treatment of the cankers to the drilled wells by application of culture disk or paste is time consuming and bears some difficulty, especially for big cankers and the ones taking place on upper parts of the trees not easy to reach. There is very few studies to make it more applicable. Kunova et al. (2016), tested a new method for the cankers not easily reached. They made a new formulation, a pellet formulation consisting polyethylene glycol and hydroxypropil to be launched by air rifle. They observed healing on the treated canker by this way. This method might be an alternative to the conventional method by the ease of application.

For the biological control of chestnut blight with hypovirulent isolates; the widely accepted method is drilling wells on the intact tissue on the peripheries of the cankers at 2-3 cm space and filling them with either culture disks of the hypovirulent culture or pastes prepared from the culture. In this study, the above mentioned method was used at chestnut grooves in İzmir. The first aim of this study is to see the effectiveness of this hypovirulent treatment by using two different vc types of *Cryphonectria parasitica*, Eu-1 and Eu-12, with paste application, which has not been tested in this region and also in Turkey so far. Along with this application method; three other methods thought to be more applicable were also tested. This study was carried out in İzmir and Aydın provincial areas where no hypovirulence has been observed so far.

MATERIALS AND METHODS

Collection of canker samples and mapping their locations

In order to hypovirulence treatment, the canker vc types have to be known along with their bigness and positions on the trees. Before collection of samples to identify their vc types, the areas were visited and the chestnut trees having suitable cankers to work with were selected, and their GPS coordinates recorded. From the cankers planned to hypovirulent application, 165 bark samples from 12 different locations of Beydağ, Kiraz, Ödemiş, and Tire counties of İzmir were taken in April 2015. Thirty canker samples were also collected from an orchard about 60 ha having 20 years old chestnut trees at Malgaç Mustafa village of Sultanhisar County, in Aydın province in 2016. The samples were taken from the peripheries of the active cankers near the intact tissue by removing the bark, 1.0 cm in diameter, with a cork-borer from the two end points up and below and from the centre. The samples were placed between paper towels, kept in cool boxes, and brought to the laboratory, with the relevant information on them. In order to find out the natural spread of the hypovirulent treatment, a control canker around the two treated cankers was planned to leave untreated, but this could not be achieved everywhere because of the difficulty to find suitable cankers.

Isolation of *Cryphonectria parasitica* from bark samples

Total 195 bark samples, 165 being from İzmir and 30 from Aydın, were disinfected in 1% sodium hypochloride for three min. and dried between paper towels. The bark disks were cut into two pieces transversely, about 2 x 2 mm were dissected from the adjacent tissue of the intact and diseased portions and they were plated on PDAmb (PDA 40g, methionin 100mg, biotin 1mg, distilled water 1000ml) medium. The plates were incubated at 26 ℃, with 12-hour dark and light cycles for 7 days. Monospore isolates were obtained by taking small mycelial tips under a stereomicrocope, and they were grown on agar slants in tubes and stored at 4 ℃ in a refrigerator and at -20 ℃ in 15% glycerine in cryo-vials.

Determination of hypovirulence

Hypovirulence was determined by cultural aspects of the isolates. For this, 154 isolates of *Cryphonectria parasitica* obtained from 165 samples from İzmir province and 24 isolates from Aydın were grown on PDAmb medium for 7 days at 25 ^{0}C in dark and 5 days in diffuse light in the lab. After that culture morphology of the isolates was evaluated visually for determination of hypovirulence. The isolates which grew orange in color with profuse sporulation were admitted as virulent, while

whitish ones with very sparse sporulation were accepted as hypovirulent.

Determination of vc types of *Cryphonecteria parasitica* isolates

In order to determine the vc types of 178 *Cryphonectria parasitica* isolates, first a small amount of sporulation from the isolate of unknown vc type was removed from the cultures grown on PDAmb with a sterile needle and placed on the medium together with the known European vc types Eu-1 and Eu-12, at 2 mm apart. The inoculated cultures were kept as mentioned above for hypovirulence. The isolates formed barrage zones with or without sporulation with the mating isolate were admitted as incompatible with the known Eu vc type while the ones not formed were as compatible. The procedure was repeated twice.

Transformation of virulent isolates to hypovirulence

In order to obtain hypovirulent isolates to be used in the forest, one virulent isolate from each location was transformed to hypovirulence by inoculating the virulent and hypovirulent isolates in the same vc type as mentioned above for determination of virulence. When the orange isolate was converted to white, the local isolate was admitted as transformed to hypovirulence and those isolates were used for hypovirulence treatment (Anagnostakis et al., 1986; Bissegger et al., 1997). As a source of hypovirulence, an isolate previously obtained from Zonguldak (Z-1, Eu-1 vc type) and a Macedonian isolate (M-7055, Eu-12 vc type) obtained from Swiss Federal Institute for Forest, Snow and Landscape Research WSL were used. These local transformed isolates were used for bio-control studies.

Preparation of hypovirulent paste

In order to facilitate the hypovirulence treatment a paste formulation was prepared. For this; hypovirulent isolates were grown on acidified PDAmb medium (pH 4.5) in 9 cm diameter Petri plates at 2-3 mm thickness. When the hypovirulent cultures covered the whole dish, about 10 dished were placed in a sterile jar and macerated by a hand blender in a sterile cabin. The inoculum in the jars was kept 3-4 days until use and mixed by a swerving motion. The obtained paste was diluted with sterile water at 1:1 rate to obtain a diluted paste suitable for brush application.

Applications of hypovirulent isolates in İzmir province

Since most of the cankers are scraped by the farmers, in Izmir, suitable cankers for treatment were not found easily. For this reason, in this region, hypovirulent treatment was only done as filling the wells (**Figure 1a**) drilled on the bark at 2-3 cm distance around the cankers by hypovirulent

paste (**Figure 1b**) to 154 cankers in July 2015. After placing the hypovirulent paste, the wells were closed by the bark disks and the treated area was wrapped by painter's tape in 5 cm width to keep the treated surface humide (**Figure 1c**). The hypovirulent paste prepared as mentioned before was sent to the farmers in jars (**Figure 1d**).

Hipovirulence treatments in Aydın province

Three different hypovirulent treatments, to six cankers each, were done at an orchard near Malgaç Mustafa Village of Sultanhisar county in Aydın: i) This application was the same as done in İzmir, ii) Canker peripheries were wounded by striking with an instrument having 5 nails (**Figure 1e**) and diluted paste was smeared on the wounded surfecae by a brush, iii)

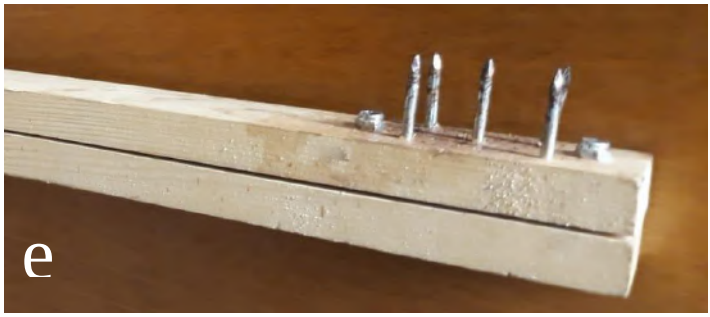

Figure 1. Application of hypovirulent paste to the cankers in İzmir. a) Drilled wells around a canker, b) Filling of the paste to the wells, c) Wrapping the treated canker with a painter's teyp, d) Hypovirulent paste sent to the farmers, e) The instrument used for wounding

Diluted paste was smeared on unwounded canker surface. Treated cankers were wrapped as mentioned for İzmir.

Fungicide treatment to the wounded cankers by a device with nails.

This treatment was done on 6 cankers. For the treatment cankers were wounded by striking the peripheries of the canker 3-4 four times with a devive having nails 2-3 cm apart, than the fungicide (Switch 62 WG; cyprodinil 37.5% + fludioxonil 25%) was sprayed on the wounded surface untill run off, at the rate of 50 g /100 l.

Evaluation of the treatments

The treated cankers were examined 3, 6, and 12 monts after the application and they are visually evaluated by calli formation around the cankers. Bark samples were collected around the treated and control cankers and hypovirulence was evaluated by looking at the colours of the cultures.

RESULTS

Evaluation of the causal agents of the cankers and their distribution

From the 165 samples collected from 12 different locations of İzmir in April 2015, 154 *Cryphonectria parasitica* isolates were obtained (**Table 1**). All the *C. parasitica* isolates from İzmir and Aydın provinces were found virulent, in other words they produced orange pigmentation on PDAmb medium (**Figure 2**).

Cryphonectria parasitica was not isolated from 11 of the samples out of 165 colected from İzmir; instead other fungi such as *Cytospora* sp., *Aureobasidium* sp., and *Penicillium* spp. From the 30 samples collected from an orchard in Aydın, 24 *C. parasitica* was isolated, and from the remaning six samples, on the other hand, *Paecilomyces* sp., *Cytospora* sp., *Penicillium* sp., and *Curvularia* sp. were isolated.

In order to determine vc types of the isolates obtained, they were matched with the known vc types of Eu-1 and Eu-12, which are the most commonly found vc types in Turkey so far. The uncompatible isolates produced distinct barrage zones with the matching ones while the compatible ones did not produce but merged each other (**Figure 2**).

Majority of İzmir isolates were belong to Eu-12 vc type (108 out of 154, 70%), while 46 (29%) were Eu-1. The same trend occurred in Aydın province; out of 24 isolates, 16 were Eu-12 and 8 were Eu-1 (**Table 1**).

Figure 2. Orange colour growth of virulent isolates of *Cryphonectria parasitica*. Barrage zones produced by some İzmir isolates with Eu-1 vc type show incompatible reaction (**a, b**)

Table 1. The locations where the bark samples were collected, number of bark samples examined and vc types of *Cryphonectria parasitica* obtained

Province/ County	Location	No of the bark samples	Number of isolates per vc type obtained	
			Eu-1	Eu-12
İzmir / Ödemiş	Kemer	10	-	10
	Güneyköy	15	2	13
	Bıçakçı	25	-	20
	Küçükören	20	5	15
	Küre	13	-	10
İzmir / Beydağ	Çomaklar	25	11	14
	Çamlık	10	4	5
İzmir / Kiraz	Örencik	10	6	3
	Ahmetler	7	6	-
	Bağlan	10	8	2
	Çatak	10	4	6
İzmir / Tire	Dallık	10	-	10
Aydın / Sultanhisar	Malgaç Mustafa	30	8	16
TOTAL		**195**	**54**	**124**

No incompatible isolates to vc types Eu-1 and Eu-12 were obtained in the study area being vc type Eu-12 was the most widespread one. The distribution of the vc types are shown in the map (**Figure 3**).

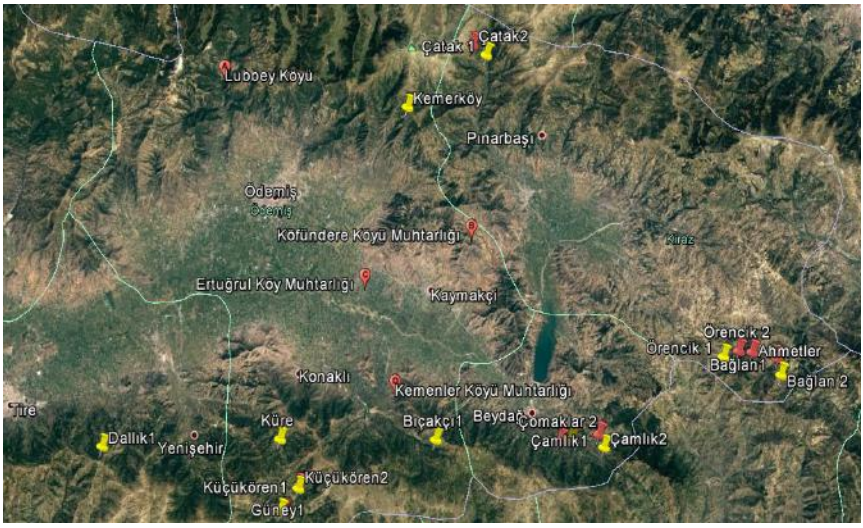

Figure 3. Distribution of the vc types of *Cryphonectria parasitica* in İzmir. Yellow marks show Eu-12 and red ones Eu-1

Hypovirus transmission to the local virulent isolates used for canker treatment was successfuly done from Z-1 for Eu-1 and M-7055 for Eu-12 vc types; obtained from Zonguldak and from Swiss Federal Institute for Forest, Snow and Landscape Research WSL (Macedonia origin) respectively (**Figure 4**).

Figure 4. Transmission of hypovirus to one of the virulent isolates of İzmir. The isolate on the right are completely transformed to hypovirulence

Evaluation of the treatments in İzmir

For the evaluation of hypovirulent treatments, cankers were visually examined for new calli formation and new canker growth above the treated areas after 3., 6. and 12 months of treatment. Fiftyone of the treated cankers could not be found in situ since they had been either scaped (**Figure 5 a, b**) or cut down by the farmers who thought that the treatment was unsuccessful. Some of the villagers could not differenciate the callus formation from the active canker, some thought that the application was insufficient because of Goat moth (*Cossus cossus*) damage which caused a severe bark harm (**Figure 5 c, d**).

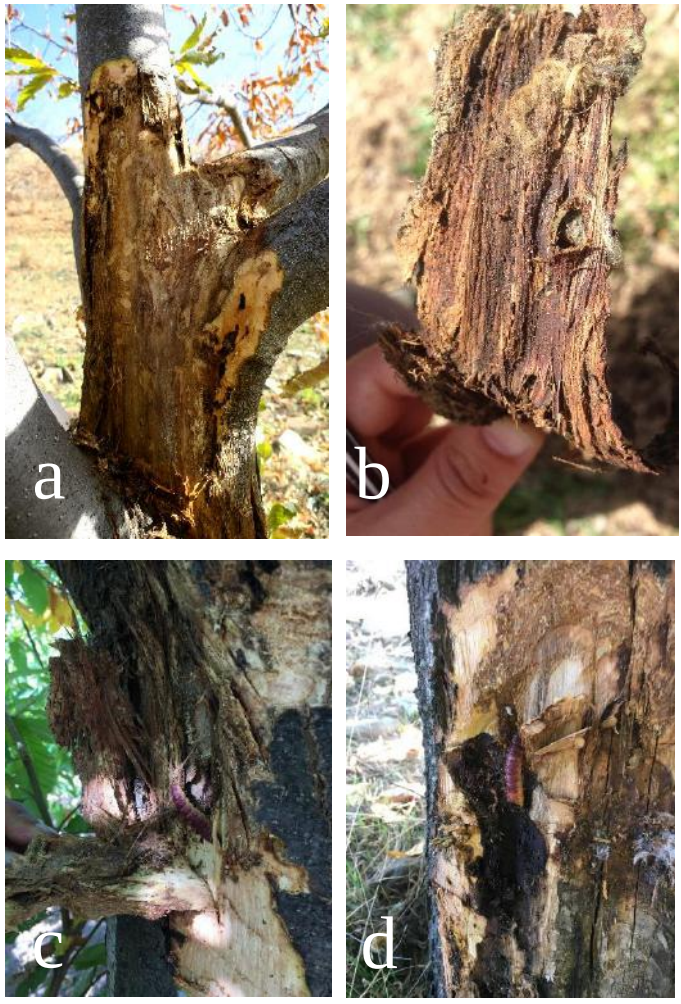

Figure 5. Various aspects of treated cankers impairing the onset of hypovirulence. a) A scrapeed canker, b) Bark pieces of the scraped canker found on the ground. c, d) *Cossus cossus* damage on the treated cankers

Almost all the treated cankers produced new calli at varying degrees, some of them being completely healed (**Figure 6 a, b, c, e**), some of them partially healed due to escape from the edge of the application (**Figure 6 d**).

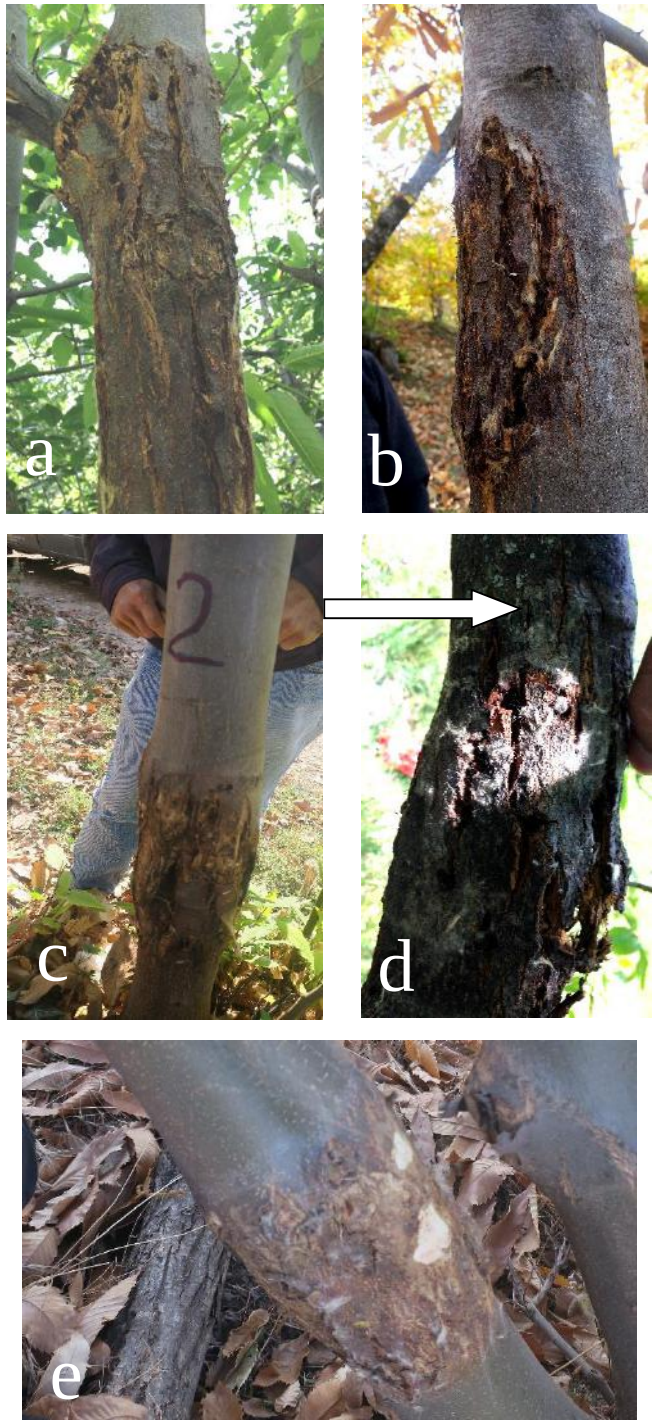
a
b
c
d
e

Figure 6. Progress of healing on some cankers. a), b) and c) Calli formation around the cankers after 6 monts from treatment, d) A canker showing ascape from treatment (arrow) and e) a completely healed canker

When bark samples were taken from the healing cankers, reisolations mostly yielded hypovirulent isolates in other words white colonies (F**igure 7**).

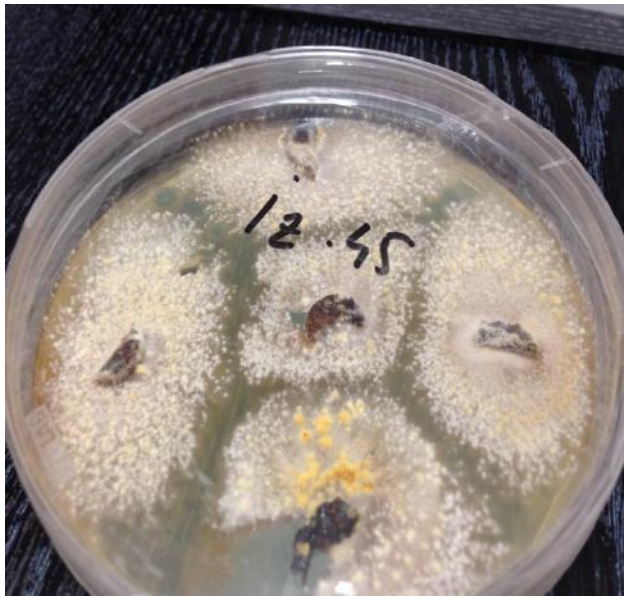

Figure 7. White colony growth of *Cryphonectria parasitica* from treated and healed cankers

Some untreated cankers adjacent to the treated trees were selected as controls in order to evaluate the transmission of the hypovirulence, which were observed during the study. Still, many of the cankers remained as control, were removed by the farmers and a few of them were evaluated. Only one control canker out of ten was fount healed.

Evaluation of various canker treatments in Aydın, Sultanhisar

Calli formation was started on four of the six cankers treated as hypovirulent paste to the wells after 6 months from the treatment; four cankers were completely healed and two cankers showed calli formation

after 18 months but Goat moth damage prevented the complete healing process (**Table 2, Figure 8).**

Table 2. Status of the cankers treated by hypovirulent paste application to the wells drilled around the cankers

No of the trees	Status of the cankers treated by hypovirulent paste in two years					
	November, 2016			October, 2017		
	Calli formation		Condition of the cankers	Calli formation		Condition of the cankers
	+	-		+	-	
*P1	X		Calli formation started, Goat moth damage severe	X		Canker healed. The branch died since the canker was too big
P2		X	No calli formation observed.	X		New calli formation observed, Goat moth damage present.
P3		X	Further canker development present, no Goat moth damage observced	X		Calli formation started, further growth of canker present due to Goat moth damage
P4	X		Calli formation started, Goat moth damage present	X		Canker completely healed
P5	X		Calli formation started	X		Canker completely healed
P6	X		Calli formation started	X		Canker completely healed

*P; hypovirulent paste application

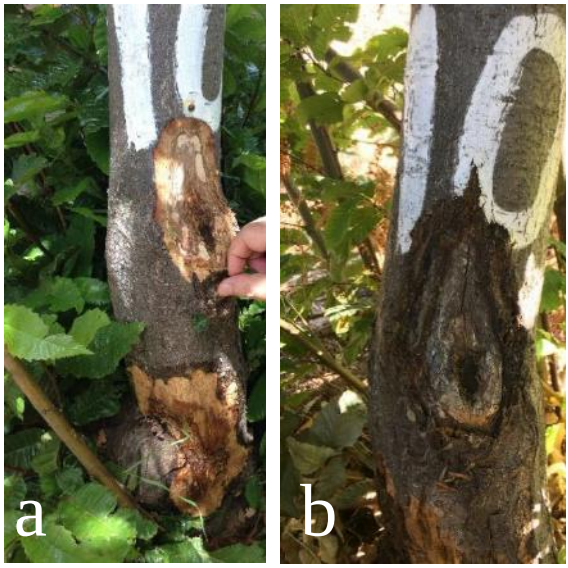

Figure 8. Hypovirulent paste application to the wells drilled around the cankers a) Application of the paste b) Healing a canker by new calli formation after 6 months

Canker development on six cankers treated by smearing the diluted paste with a brush also stopped and new calli formation occurred after 6 months of application, healing of the cankers observed after 18 months (**Table 3, Figure 9**).

Table 3. Status of the wounded cankers treated by hypovirulent diluted paste smeared by a brush

No of the trees	Status of the cankers treated by diluted hypovirulent smear					
	November, 2016			October, 2017		
	Calli formation		Condition of the cankers	Calli formation		Condition of the cankers
	+	-		+	-	
DP1*	X		Calli formation started, Goat moth damage started	X		Canker completely healed
DP2	X		Calli formation started, Goat	X		Canker completely healed

			moth damage started			
DP3	X		Calli formation started, Goat moth damage started	X		Canker completely healed
DP4	X		Calli formation started, further canker growth observed	X		Canker completely healed, Goat moth damage observed
DP5	X		Calli formation started.	X		Canker completely healed
DP6	X		Calli formation started, further canker growth observed	X		Canker completely healed, Goat moth damage observed

*DP; diluted paste

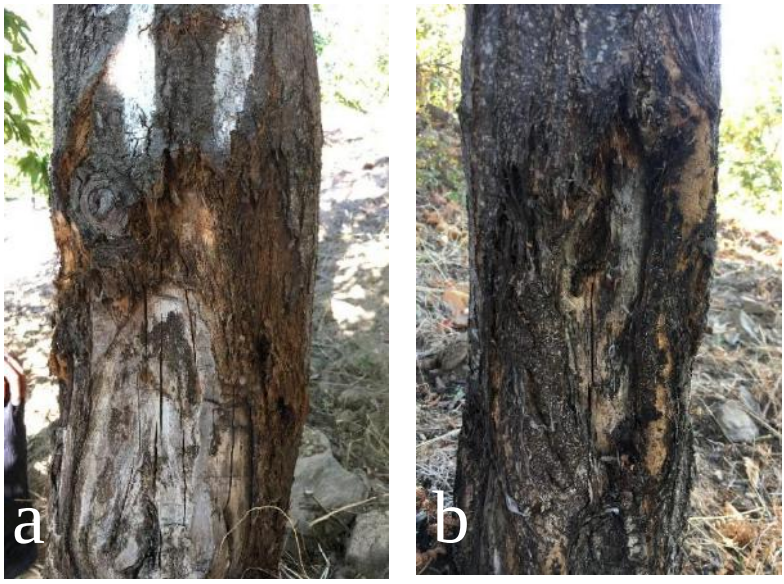

Figure 9. New calli formation on the cankers wounded by the instrument with nails after 6 months of treatment with diluted paste

Although new calli formation was observed on many of the third group unwounded cankers treated by diluted paste with a brush, some cankers escaped from the treatment (**Table 4, Figure 10)**. After 9 months, canker development also stopped on the escaped cankers and all of them healed.

Table 4. Status of the unwounded cankers treated by smearing the diluted paste with a brush

No of the trees	Status of the unwounded cankers treated by diluted hypovirulent paste					
	November, 2016			October, 2017		
	Calli formation		Condition of the cankers	Calli formation		Condition of the cankers
	+	-		+	-	
UDP* 1	X		Calli formation started, further canker growth observed	X		Calli formation and severe Goat moth damage present
UDP 2		X	No calli formation was observed on this big canker	X		Calli formation was observed
UDP 3	X		Calli formation started but also further growth observed. Goat moth damage present	X		Calli formation and severe Goat moth damage present
UDP 4	X		Healing started	X		Canker healed
UDP 5	X		Healing started	X		Canker healed
UDP 6	X		Healing started	X		Canker healed

*UDP; unwounded cankers treated by diluted paste

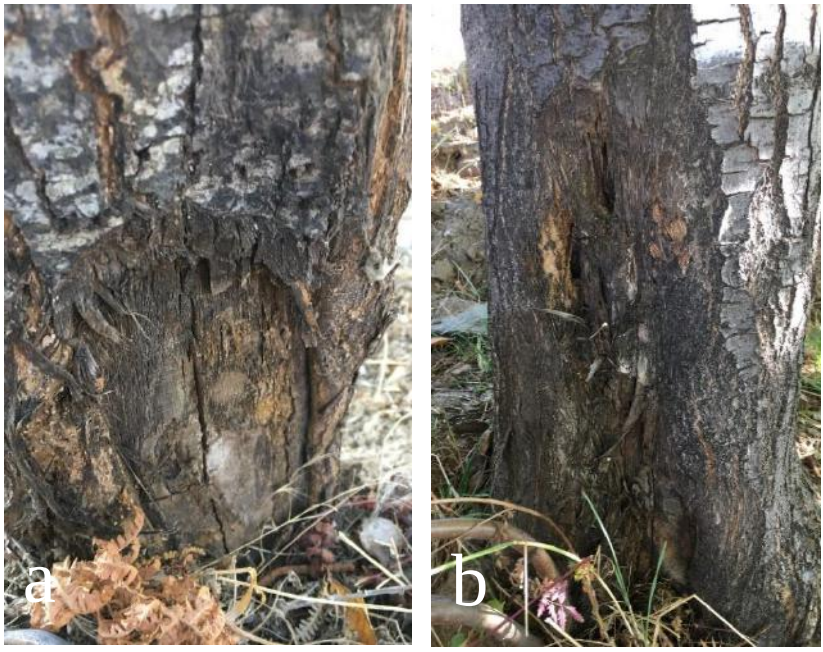

Figure 10. New calli formation on the unwounded cankers after 6 (a) and 18 months (b) of treatment with diluted paste

Healing apperared on all the fungicide treated cankers after 18 months (**Table 5, Figure 11**).

Table 5. Status of the cankers treated by Switch WG after wounded

No of the trees	Status of the cankers treated by Switch WG after wounded					
	November, 2016			October, 2017		
	Calli formation		Condition of the cankers	Calli formation		Condition of the cankers
	+	-		+	-	
F 1*	X		Calli formation started, no escape on the canker, Goat	X		Canker healed. Good calli formation. No further canker growth

			moth damage severe			
F 2		X	A little calli formation, no further canker growth	X		Good calli formation, healing good.
F 3		X	No further canker growth , calli formation started	X		Canker healed. Goat moth damage present.
F 4	X		Calli formation started, no escape on the canker.	X		Canker healed. Goat moth damage present.
F 5	X		Calli formation started, no escape on the canker.	X		Canker healed. Goat moth damage present.
F 6	X		Calli formation started, no escape on the canker.	X		Canker healed. Calli formation good. No Goat moth damage present.

*F; fungicide (Switch WG)

Figure 11. Effectiveness of fungicide treatment. a) A canker wounded and sprayed with Switch 62.5 WG, b) Completely healed canker after 18 monts from treatment

DISCUSSION

Chestnut canker caused by the fungus, *Cryphonectria parasitica*, has been present in Turkey since 1967 and has been causing serious dieback (Coşkun et al., 1999; Gürer et al., 2001). The most frequently applied control method against the disease is biological control by hypovirulent applications which is successfuly used in many countries in the world. In this study, a new application method of placing hypovirulent paste to the wells drilled around the cankers was used and found versatile.

In this study carried out in İzmir and Aydın provinces, no hypovirulence has been observed and all the samples taken from the cankers yielded orange colour growth on the isolation medium, which depicts active canker growth and also supports the previous findings (Erincik et al., 2011; FAO, 2014; Akıllı Şimşek et al., 2019). When the recovered vc types are considered, our results also match to the previous finding in this region, consequently two vc types Eu-12 and Eu-1 are the widespread ones. Since

almost all the chestnut trees in this region are grafted, introduction of new vc types is always possible with use of new scions. In addition, new vc types, mostly genetically similar to these but differentiating on one alles might be formed by natural mutations, which underlines the necessity of continuous biological studies. But when the general situation in the region is taken into consideration, biological control could be successful in this region because of occurrence of two vc types in the region.

In order to make the biocontrol application easier, two different hypovirulent application methods were also tested in this study. Traditional application method was applied both in İzmir and in Aydın and efficient calli formation was observed 18 months after the treatments in both of the provinces. With this application method, escape of the cankers from treatment was very low since hypovirulence was applied very close to each other.

When the cankers are wounded by the instrument with nails and, were treated with diluted paste by smearing with a brush, majority of the cankers showed healing while escapes from treatment was first observed but later on the canker growth stopped. Treatments of the unwounded cankers with diluted paste also showed similar results as above mentioned. Both of these application methods are more practical than the well treatment but before starting their use in larger areas, they should be tested in different ecological regions with higher repititions.

Treatment of the cankers with a systemic fungicide also yielded complete healing after 18 months. Although it is effective, its sustainability can be discussed since the treatment is needed every year. Hypovirulence treatment, on the other hand can be spread to the untreated cankers thus there would not be new efforts if it is naturally spread and settled.

In the treated cankers in both of the regions, extensive bark damage caused by Goat moth (*Cossus cossus*) was observed and, this impaired the healing process by preventing new calli formation. Goat moth laid its eggs into the bark crevices made by wounding or naturally occurring cracks on the stems. It is also attracted by the chestnut ooze made by drilling the wells. For this reason, hypovirulent treatments should not be done in the periods of maximum Goat moth flight which was determined as July and August in this region (Kaplan and Turanlı, 2017). Goat moth damage was more severe in Aydın treatments which was done in the end of July and İzmir treatments done in July, for this reason biological control treatments should be done early in the Spring in the places where Goat moth is present or an insecticide or a repellent should be sprayed onto the treated surfaces if the application is done later on.

Although it is more effective, the application of the traditional hypovirulent treatment to the large cankers or to the ones on the high upper places not easily reached is difficult and time consuming. For these type of cankers, alternative methods tested here can be used.

Although many of the treated cankers healed, the healing process of hypovirulent treatments could not be understood by some of the farmers and many cankers were cut down, while some of them found the treatment very promising and are going to treat their trees. For this reason, the farmers should be informed about the effects of hypovirulent treatment

Though spread of hypovirulence to the control cankers was not so many in this region, observation of completely healed cankers on some controls encouraged us to extend the treatment to various placaes. One of the farmers in İzmir found the treatment very promising and started to treat all the cankers in his orchard (Personel communication with Bilal Güngör). Natural spread of hypovirulence may be depended on various factors such as humidity, light and vector population and their investigation would be useful. Increase of hypovirulent treatments may increase natural spread.

Another approach for biocontrol of chestnut canker was tested by Meyer et al. (2019) and they inoculated chestnut branches with a hypovirulent strain and hanged them on the infected trees after they profusely sporulated. They traced the spread of the hypovirulent strain and found transmission of hypovirulence in the Swiss climatical conditions. This method also deserves to be tested in our region which is rather dry compared to Swiss conditions.

ACKNOWLEDGEMENT

We would like to thank The Ministry of Agriculture and Forestry/ General Directorate of Forestry, The Western Black Sea Forestry Research Institute Directorate. This study is also partly supported by Cankırı Karatekin University.

LITERATURE

ADAMCIKOVA, K., ONDRUSKOVA, E., KADASI-HORAKOVA, M., BOTU, M., KOBZA, M. AND ACHIM, G. 2015. “Distribution and population structure of the chesnut blight fungus in Romania”. *Plant Protect Science*, 51, 141-149.

AKILLI S., ULUBAŞ-SERÇE Ç., KATIRCIOĞLU YZ., MADEN S., RIGLING D. 2013. “Characterization of hypovirulent isolates of the chestnut blight fungus, *Cryphonectria parasitica* from the Marmara and Black Sea regions of Turkey”. *European Journal of Plant Pathology*. Volume 135, pages 323-334. DOI: 10.1007/s10658-012-0089-z.

AKILLI ŞİMŞEK S., KATIRCIOĞLU Y. Z., BORST N., ÇAKAR D., PROSPERO S., RİGLİNG D., MADEN S., 2019. "Identification and characterization of hypovirus-infected *Cryphonectria parasitica* isolates from biological control plots in Izmir, Kütahya and Sinop". *Turkish Journal of Agriculture and Forestry*. 43: doi:10.3906/tar-1901-82

ANAGNOSTAKIS S. 1977. "Vegetative incompatibility in *Endothia parasitica"*. *Exp. Mycol.* 1, 306–316.

ANAGNOSTAKİS SL. AND DAY PR. 1979. "Hypovirülence conversion in *Endothia parasitica"*. *Phytopathology* 69: 1226–1229.

ANAGNOSTAKIS SL. AND WAGGONER PE. 1981. "Hypovirulence, vegetative incompatibility and the growth of cankers of Chestnut blight". *Phytopathology* 71: 1198–1202.

ANAGNOSTAKIS SL., HAU B. AND KRANZ J. 1986. "Diversity of vegetative compatibility groups of *Cryphonectria parasitica* in Connecticut and Europe". *Plant Disease* 70: 536–538.

BISIACH M., DE MARTINO A., INTROPIDO M., MOLINARI M. 1991. "Nuove esperienze di protezione biologica contro il cancro della corteccia del castagno". *Frutticoltura* 12, 55–58.

BISIACH, M., CORTESI, P., DE MARTINO, A. AND INTROPIDO, M. 1995. "Biological control of chestnut blight fungus *Cryphonectria parasitica*. En: Proceedings of the International Congress "Microbial control agents in sustainable agriculture field experience, industrial production and registration". *Saint Vincent (Aosta)*, 167.

BISSEGGER M., RIGLING D. AND HEINIGER U. 1997. "Population structure and disease development of *Cryphonectria parasitica* in European Chestnut forest in the presence of natural hypovirülence". *Phytopathology* 87: 50–59.

BRAGANÇA, H., SIMOES, S., ONOFRE, N., TENREIRO, R. AND RIGLING, D. 2007. "*Cryphonectria parasitica* in Portugal: diversity of vegetative compatibility types, mating types, and occurrence of hypovirulence". *Forest Pathol*., 37, 391-402.

BRYNER, SF. AND RIGLING, D. 2011. "Temperature-dependent genotype-by-genotype interaction between a pathogenic fungus and its hyperparasitic virus". *The American Naturalist*, 177, 65-74.

CALZA CA. 1993. "Biological control of chestnut blight: large-scale application techniques". In: *Proc. Int. Congr. Chestnut, Spoleto, Italy. October, 20–23, 1993*. Ed. by Antognozzi, E., pp. 599–602.

CASTANO, C., BASSIE, L., OLIACH, D., GOMEZ, M., MEDINA, V., LIU, B. AND COLINAS, C. 2015. "*Cryphonectria hypovirus* I as inferred from gene genealogies and the coalescent". *Genetics*, 166, 1611-1629.

CHIRA, D., TEODORESCU, R., BOTU, M., ACHIM, G., SCUTELNICU, A. 2017. "Testing Chestnut Hybrids For Resistance To *Crypnonectria"*. *6. İnternational Chesnut Symposium*, October 9-13/2017, Samsun-Turkey.

CORTESI, P. AND MILGROOM, MG. 1998. "Genetics of vegetative incompatibility in Cryphonectria parasitica". *Appl. Environ. Microb*., 64, 2988-2994.

COŞKUN H., TURCHETTI T., MARESI G. AND SANTAGADA A. 1999. "Preliminary investigations into *Cryphonectria parasitica* (Murr) Barr isolates from Turkey". *Phytopathology Mediterranean* 38:101–110.

CORTESI, P., MCCULLOCH, CE., SONG, HY., LIN, HQ. AND MILGROOM, MG. 2001. "Genetic control of horizontal virus transmission in the chesnut blight fungus. *Cryphonectria parasitica"*. *Genetics*, 159, 107-118.

ÇELIKER NM. AND ONOĞUR E. 2009. "Biological control of chestnut blight and prospect for future: Turkey as a case study". International Workshop on Chestnut Management in Mediterranean Countries: Problems and Prospects pp 221-226, 23-25 October 2007 Bursa, Turkey. *Acta Hort*. 815.

ÇELIKER, NM., KAPLAN, C., ONOĞUR, E., ÇETINER, B., POYRAZ, D. AND UYSAL, A. 2017. "Natural dissemination of hypovirulent *Cryphonectria parasitica* strain used for biological control of chestnut blight". *Turk. J. Agric. For*., 41, 278-284

DIAMANDIS, S., PERLEROU, C., NAKOPOULOU, Z., CHRISTOPOULOS, E., TOPALIDOU, E. AND TZIROS, G. 2014. "Application of biological control of chesnut blight on a nationwid scale in Greece: Results and prospects". *Acta Horticulturae,* 1043, 23-34.

DÖKEN MT., AÇIKGÖZ S., ERINCIK Ö., ERTAN E. 2004. "Studies in the chestnut growing areas of AydınTurkey to determine the incidence of *Cryphonectria parasitica* (Murill) Barr infections (Chestnut Blight) and vegetative compatibility group diversity among the isolates". Türkiye 1. Bitki Koruma Kongresi 8-10 Eylül Samsun.

ERINCIK, Ö., DÖKEN, TM., AÇIKGÖZ, S. AND ERTAN, E. 2003. "Frist report for Aydın, Turkey: *Cryphonectria Parasitica* (Murrill.) Barr. Threatens The Chestnut Orchards". *J. Turk. Phytopath*., 32, 41-44.

ERINCIK, O., OZDEMIR, Z., DURDU, OF., DOKEN, MT. AND ACIKGOZ, S. 2011. "Diversity and spatial distribution of vegetative compatibility types and mating types of *Cryphonectria parasitica* in the Aydın Mountains, Turkey". *Eur. J. Plant. Pathol*., 129, 555-566.

FAO 2014. Management of chestnut blight and for improving forest health and vitality (2012-2014), Report, TCP/TUR/615676.

GÜRER M., TURCHETTI T., BIAGIONI P. AND MARESI G. 2001. "Assessment and characterisation of Turkish hypovirulent isolates of *Cryphonectria parasitica* (murr) Barr". *Phytopathology* 40: 265–275.

HEINIGER U. AND RIGLING D. 1994. "Biological control of chestnut blight in Europe". *Annu. Rev. Phytopathol*. 32: 581–599.

HEINIGER U. AND RIGLING D. 2009. "Application of the *Cryphonectria hypovirus* (Chv-1) to control the chestnut blight, experience from Switzerland". *Acta Horticulturae*, 815, pp. 233–245.

HOEGGER, PJ., RIGLING, D., HOLDENRIEDER, O. AND HEINIGER, U. 2000. "Genetic structure of newly established populations of *Cryphonectria parasitica". Mycol. Res*., 104, 1108-1116.

HOEGGER, PJ., HEINIGER, U., HOLDENRIEDER, O. AND RIGLING, D. 2003. "Differential transfer and dissemination of hypovirus and nuclear and nuclear and mitochondrial genomes of a hypovirus-infected *Cryphonectria parasitica* strain after introduction into a natural population". *Appl. Environ. Microb*., 69, 3767-3771.

JUHÁSOVÁ, G., ADAMCIKOVA, K. AND ROBIN, C. 2005. "Results of biological control of chesnut blight in Slovakia". *Phytoprotection*, 86, 19-23.

KAPLAN, C. AND TURANLI, T. 2017. "Monitoring of Seasonal Fluctuation of Goath Moth, *Cossus cossus* L. (Lepidoptera: *Cossidae*), In Chestnut Plantations In İzmir And Manisa, Turkey". *6. İnternational Chesnut Symposium*. October 9-13/2017- Samsun-Turkey.

KUNOVA, A., PIZZATTI, C., CEREA, M., GAZZANIGA, A. AND CORTESI, P. 2016. "New Formulation and Delivery method of *Cryphonectria parasitica* for biological control of chesnut blight". *Journal of Applied Microbiology*, 122, 180-187.

MACDONALD WL. AND FULBRIGHT DW. 1991. "Biological control of chestnut blight: Use and limitations of transmissible hypovirulence". *Plant Dis.* 75, 656–661.

MEYER JB., CHALMANDRİER, L., FASSLER F., SCHEFER C., RİGLİNG D. AND PROSPERO, S. 2019. "Role of Fresh Dead Wood in the Epidemiology and the Biological Control of the Chestnut Blight Fungus". *Plant Disease*.103:430-438

MILGROOM GM. AND CORTESI P. 2004. "Biological control of chestnut blight with hypovirulence; a critical analysis". *Ann. Rev. Phytopathol.* 42: 311–338.

RIGLING, D. AND PROSPERO, S. 2017. "*Cryphonectria parasitica*, the causal agent of chesnut blight: invasion history, population biology and disease control". *Aceppted Article*,1-50.

RISTESKI, M., MILEV, M., RIGLING, D., MILGROOM, MG., BRYNER, SF. AND SOTIROVSKI, K. 2013. "Distribution of chesnut

blight and diversity of *Cryphonectria parasitica* in chesnut forests in Bulgaria". *Forest Pathol.*, 43, 437-443.

ROBIN C., ANZIANI C., CORTESI P., 2000. "Relationship between biological control, incidence of hypovirulence, and diversity of vegetative compatibility types of *Cryphonectria parasitica* in France". *Phytopathology* 90, 730–737.

ROBIN, C. AND HEINIGER, U. 2001. "Chesnut blight in Europe: diversity of *Cryphonectria parasitica*, hypovirulence and biocontrol". *Forest Snow and Landscape Research*, 76, 361-367.

SOTIROVSKI, K., RIGLING, D., HEINGER, U. AND MILGROOM MG. 2011. "Variation in virulence of *Crphonectria hyphovirus* 1 in Macedonia". *For. Pathol*., 41, 59-65.

TURCHETTI, T. AND MARESI, G. 2008. "Biological control and management of chesnut diseases. In: Ciancio, A. and Mukerji, K. J. (eds) Integrated Management of Diseases Caused by Fungi, Phytoplasma and Bacteria (ıntegrated Management of Plant Pests and Diseases, Volume 3)". *Springer Science*, Dordrecht, The Netherlans, 85-118.

ZAMORA, P., MARTIN, A.B., RIGLING, D. AND DIEZ, JJ. 2012. "Diversity of *Cryphonectria parasitica* in western Spain and identification of hypovirus-infected isolates". *Forest Pathol*., 42, 412-419.

ZAMORA, P., MARTÍN, AB., SAN MARTÍN, R., MARTÍNEZ-ÁLVAREZ, P. AND DIEZ, J.J. 2014. "Control of chestnut blight by the use of hypovirulent strains of the fungus *Cryphonectria parasitica* in northwestern Spain". *Biological Control*, 79, 58–66.

AN INTRODUCTION TO THE STRUCTURAL AND FUNCTIONAL METHODOLOGY FOR FRAGMENT tRNA MOLECULES

Serap Çetinkaya*

1. INTRODUCTION

The introduction of the next-generation sequencing (NGS) technologies into the sequencing of small, defined sizes of RNA molecules has exposed a new picture of the transcriptome both in prokaryotic and in eukaryotic cells. These molecules are essentially made up of different non-coding RNAs (ncRNA), expressed by the genome (Djebali et al., 2012). The first practical implication of those ncRNA molecules having 20- to 31-nucleotides (nt) has been that they were able to bind Argonaute proteins (Farazi, 2008; Ghildiyal and Zamore, 2009; Kim and Han, 2009). Within this range of nucleotide lengths, 22 nt, there have been other RNA molecules which are called microRNAs (miRNAs). This RNA species have been much better characterised both in functional and in structural terms, and it appears that it negatively regulates the expression of a wide range of proteins via complementation to their specific mRNAs. Now the addition of functional ncRNA creates a massive pool of modulator RNA molecules involved in the regulation of the cellular processes. So far approximately 2,800 types of human miRNAs have been submitted in the miRBase database (Kozomara and Griffiths-Jones, 2014). These efforts have also revealed a new species of ncRNA molecules, mostly derived from the cleavage of a well-known RNA type, the tRNA (Shigematsu and Kirino, 2015).

* (Res. Ass. Dr.); Department of Molecular Biology and Genetics, Science Faculty, Sivas Cumhuriyet University, Sivas, Turkey.
e-mail: serapcetinkaya2012@gmail.com

As RNA molecules generally exist in the single-stranded state, they can assume various types of secondary structures by internal base-pairing. tRNAs, for example, by having a defined length and almost identical nucleotide content, are known to form a cloverleaf structure. It seems that this unique structure enables these molecules to faithfully serve in the translational apparatus. In a human cell as many as 500 different tRNA molecules can be encoded (Chan and Lowe, 2009). Together with their inherent stability, this species of RNA constitutes most of the cellular RNA fraction. In the beginning, fragments of tRNA have been excluded from the NGS results as experimental artefacts. Now, however, they have been specifically mapped in diverse representatives of the biological tree and the research aiming at the understanding of their biochemical implications has recently gained momentum (Anderson and Ivanov, 2014; Garcia-Silva, et al., 2012; Gebetsberger and Polacek, 2013; Shigematsu, et al., 2014; Sobala and Hutvagner, 2011).

Fragment tRNAs are mostly derived from tRNAs by the specific endonucleolytic cleavage at the anticodon region. This cleavage produces two types of fragment RNAs, as 5′- and 3′-arms, having lengths ranging from 30 to 35 (Anderson and Ivanov, 2014; Garcia-Silva, et al., 2012; Gebetsberger and Polacek, 2013; Shigematsu, et al., 2014; Sobala and Hutvagner, 2011). Apart from these, fragments that are shorter than the tRNA-halves are further classified into four subgroups: 5′-tRFs, 3′-CCA tRFs, 3′-U tRFs, and 5′-leader-exon tRFs. The 5′-tRFs and 3′-CCA tRFs include mature 5′- and 3′-CCA termini (Fig. 1). The 3′-U tRFs are specified with uridine repeats and generated from the precursor tRNAs (pre-tRNAs, Fig. 1). In turn, the 5′- tRFs include the 5′-leader sequence of pre-tRNAs and the 5′-section of mature tRNAs (Shigematsu and Kirino, 2015).

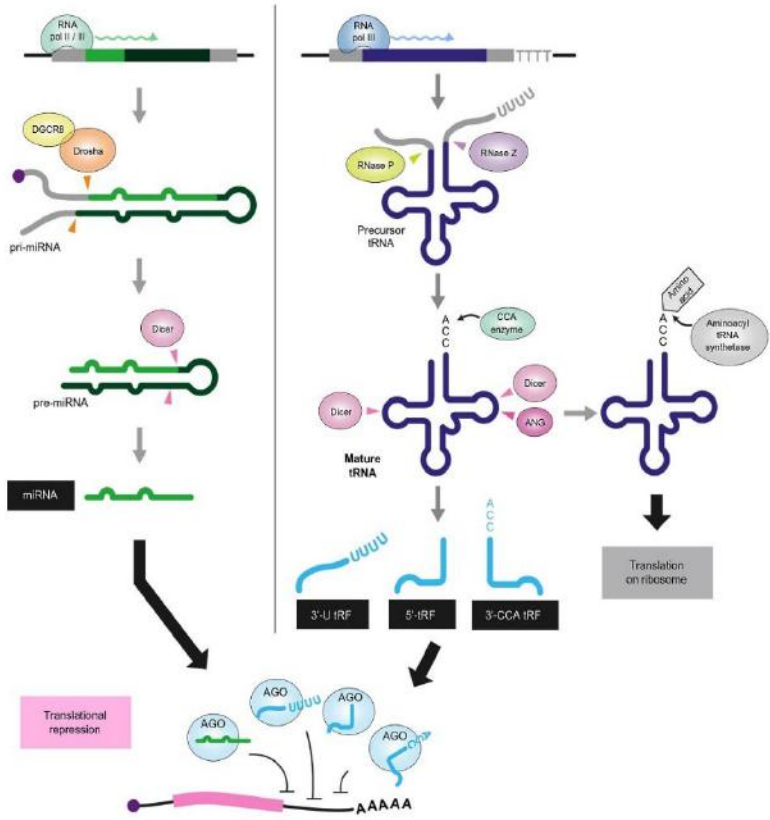

Figure 1. Schematic representation of the biogenesis of miRNAnas and tRFs associated with AGO proteins (Shigematsu and Kirino, 2015).

2. METHODS

2.1 Preparation of sRNA Libraries from a Prokaryotic Source, *Haloferax volcanii*

In the making of any cDNA library the first step involves the preparation of the starting material, the total RNA (Nieuwlandt et al., 1995). It can be achieved by following the usual cell lysis and organic solvent extraction procedures or simply by using a spin

column available in a commercial RNA extraction and purification kit. preparation kit. Much longer messenger and ribosomal RNAs are excluded by electrophoresis through a polyacrylamide gel, usually 8%. The RNA molecules residing in length between 106 and 450 bases are then eluted from the gel slices. Before converting into complementary DNA, the ends of these molecules are modified by adding two specific oligonucleotides. These are named as SMARTIV(5′AAGCAGTGGTATCAACGCAGAGTGGCCATTACGGCCGGG-3′,R2012-SMARTIV) and CDSIII (5′-ATTCTAGAGGCCGAGGCGGCCGACATG-d(T)$_{30}$-N-1N-3′. Complementary DNA is synthesized in a polymerase chain reaction (PCR), using again specified amplification protocols, and then cloned into a plasmid. Sequencing experiments use these plasmid clones for the determination of the nucleotide content of the individual tRNA fragments (Straub et al., 2009).

2.2 Verification of the tRNA Genes from the Raw Nucleotide Data

Physical structure of a given gene is made up of both regulatory- and coding regions. Regulatory sequences often reside 5′ to the coding sequences and are generally known as the putative promoter region. The characterising feature is given to this region by common nucleotide motifs. These short runs of specific nucleotides are also known as consensus elements. In *Escherichia coli* for example TTGACA and TATAAT sequence motifs are the putative promoter elements residing at -35 and -10 regions, respectively. Tranfer RNA genes also have such defined consensus motifs within their promoter regions. Such elements can also be mapped within the coding region or 3′ to the coding region of a gene. By looking at these motifs along the sequence data a given genomic library the interested genes can be identified theoretically. This procedure is now simplified by using specific computer software packages (Straub et al., 2009).

2.3 Identification of Specific RNA Molecules in a Total RNA Sample by Nucleotide Hybridisation

Prokaryotes are comparably easy to grow in the laboratory. Growth conditions can be altered to apply stress on the cells during incubation. Stress conditions include the use of increasing or decreasing amounts of ion (salt) concentrations, a range of low or high incubation temperatures. It has been known that specific tRNA fragments are produced upon stress. The ribonucleotide hybridisation technique, northern-blotting, is one of the common methods used in detecting the stress-induced tRNA fragments. Total RNA extracted from the cultures grown under each of the altered conditions is resolved by denaturing polyacrylamide gel electrophoresis. RNA banding patterns are then transferred onto nylon membranes, and hybridised with labelled DNA oligonucleotides. These are short and single-stranded DNA molecules that are complementary to a RNA gene of interest. Hybridisation patterns change in those RNA samples produced under stress conditions in comparison to those extracted from the cultures grown under optimum conditions. Thus a differential gene expression pattern can be visualised by this method after exposing the hybridised RNAs on the membrane to a sensitive film (Straub et al., 2009).

2.4 Mapping on the Genome

Transfer RNA genes are repetitive in the genome and thus the sequence data should be handled carefully by taking the following rules into consideration: (1) the sequence must include a large number of distinct genomic loci, (2) exact matches should be taken into account, (3) the whole genome has to be mapped, (4) signal sequences such as the 3′-CCA should be located, and (5) the presence of introns has to be noted (Telonis et al., 2015).

2.5 Construction of sRNA Deletion Mutants

Prokaryotes and up to a certain extent single celled eukaryotes are generally preferred in the deletion experiments by homologous recombination in order to see directly the consequences of the absence of a specific gene or locus on the chromosome. For the RNA gene loci, a new technology, named as the "Pop-In/Pop-Out" method, has been adopted. It involves two plasmid vectors, each harbouring either the 5′- or the 3′- region of an RNA gene of interest. The plasmids also carry marker genes for the selection of positive subclones. In the case of the archaeon *Haloferax volcanii* a specific plasmid vector, pMH101, carrying the upstream or the downstream of $sRNA_{30}$ and $sRNA_{63}$ has been used for the transformation. For the clones of deletion mutants, an uracil-based selection method has been developed. Deletion mutants have also been verified by nucleotide hybridisation and DNA amplification technology (Telonis et al., 2015).

2.6 Phenotypic Comparisons and Complementation of Mutant Strains

Deletion mutants might be complemented with vector plasmids into which the wild-type respective RNA gene or gene arrays are inserted. Resulting transformants are grown along with the control wild type strains under the same growth conditions (Wanner and Soppa, 2002). Cell densities are periodically read and calculated. Complementation of the deletion mutants can be evaluated by comparing the growth rates. Such experiments require basic spectroscopy and the use of various growth media. Cell densities of the cultures are periodically read at 600 nm and the values are plotted. Growth curves obtained are then compared (Straub et al., 2009).

2.7 Two – Dimensional (2-D) Gel Electrophoresis

This technique is specifically designed for obtaining a whole picture of the protein content of a cell, grown under defined

conditions. Each protein is represented by a dark spot in this picture. This image can be compared with the protein spots of the control samples. Different spots on the images can be accounted for by the changes taken place in the "original" proteome of the cell of interest. In the experiments purified total protein is used. Other biomolecules, nucleic acids, fats, and carbohydrates, are therefore removed. The first step is the precipitation of the cells grown in liquid media. Total protein extraction generally starts inflating the precipitated cells in a buffer containing high concentrations of urea. After determining the concentration, protein samples are sucked into the strips of immobilized pH gradient (IPG). Individual protein molecules are resolved as distinct spots through a liner voltage gradient between 300 V and 8,000 V for about 24 h. After an equilibration step, the second dimension electrophoresis is carried out at constant current for approximately 16 h. These steps are followed by the visualisation of protein molecules by silver staining, after which proteins are represented as distinct spots. Mass spectrometry can also be used to gain an insight into the primary structure of these proteins (Straub et al., 2009).

2.7.1 Gel Preparation

Two-dimensional (2-D) gel electrophoresis is a quite laborious task and requires the use of variety of buffers and acrylamide solutions (Table 1). Two letters, T and C, were specified for the concentration of solutions. Stock gel solutions should be kept at 4^{o}C in a light-proof bottle (SchaÈgger and von Jagow, 1987).

Table 1 Stock solutions for SDS-PAGE (SchaÈgger and von Jagow, 1987).

Buffer	Tris (m)	Tricine (m)	pH	SDS (%)
Anode buffer	0.2	-	8,9[a]	-
Cathode buffer	0.1	0.1	8,45[b]	0.1
Gel buffer	3.0	-	8.45[a]	0.3
Acrylamide-bisacrylamide mixture	Percentage Acrylamide (w/v)		Percentage bisacrylamide (w/v)	
49.5% T. 3% C	48		1.5	
49.5% T. 6% C	46.5		3.0	

[a]Adjusted with HCl.

[b]No correction 3f the pH, which is around 8.25.

Two-dimensional gel electrophoresis consists of quite a few types of gels: (1) the main separating gel (10% T, 3% C), (2) onto the separating gel, the stacking gel (4% T, 3% C) is formed. Other gels (Table 2) are made of a small-pore gel (16.5% T) which are overlaid with a 10% T, 3% C spacer- and again with the 4% T, 3% C stacking gel. In the polymerisation of gels, the usual reagents, ammonium persulfate and TEMED, are used (SchaÈgger and von Jagow, 1987).

Table 2 Composition of Separating, “spacer" and stacking gels (SchaÈgger and von Jagow, 1987).

			Separating gels			
	Stacking gel 4% T, 3% C	"Spacer" gel 10% T, 3% C	10% T, 3% C	16.5% T, 3% C	16.5% T, 6% C	16.5% T, 6% C with 6 M urea
49.5% T, 3% C Solution	1 ml	6.1 ml	6.1 ml	10 ml	-	-
49.5% T, 6% C Solution	-	-	-	-	10 ml	10 ml
Gel buffer	3.1	10 ml	10 ml	10 ml	10 ml	10 ml
Glycerol	-	-	4g	4g		-
Urea	-	-	-	-	-	10.8 g
Add water to a final volume of	12.5 ml	30 ml	30 ml	30 ml	30 ml	30 ml

2.7.2 Sample Application

Protein samples are incubated for 30 min at 40°C in 4% SDS, 12% glycerol (w/v), 50 mM Tris, 2% β-mercaptoethanol (v/v), 0.01% Serva blue G, whose pH is adjusted to 6.8 with HCl. Serva blue G is a dye, used for the tracking of migration during electrophoresis. This dye runs faster than usual bromophenol blue and thus the running off of the small proteins from the gel is somewhat prevented. The filling height of the sample is usually 2.5-10 mm. The sample, 0.5-2 µg per protein band, is laid under the cathode buffer using a 1 µl syringe. In the case of small proteins (l-3 kDa), an amount of 2-5 µg is loaded for the compensation of losses during further manipulations such as staining and destaining procedures. For large proteins usually 1 or 2 mg is required (SchaÈgger and von Jagow, 1987).

2.7.3 Electrophoresis Conditions

Electrophoresis involves the vertical running of slab gels at room temperature. Other conditions are outlined (Table 3).

Table 3 Electrophoresis conditions for different gel types (SchaÈgger and von Jagow, 1987).

Gel Type	Small-pore-gel dimensions (cm)	Voltage Start	Voltage End	Current at Start	Current at End	Time (h)
10% T, 3% C	11.5 x 14 x 0.07	150 V const.		(70 mA	30 mA)	4
	11.5 x 14 X 0.16	110 V const.		(90 mA	45 mA)	5
	24 x 15.5 x 0.07	140 V const.		(40 mA	12 mA)	16
	24 x 15.5 x 0.16	130 V const.		(80 mA	25 mA)	16
16.5% T, 3% C	24 x 15.5 X 0.32	120 V const.		(115 mA	40 mA)	20
	I0 x 14 x 0.07	90 V const.		(30 mA	8 mA)	16
	10 x 14 x 0.16	85 V const.		(45 mA	15 mA)	16
	22 x 15.5 x 0.07	(120V	380 V)	30 mA const.		16
16.5% T, 6% C	22 x 15.5 X 0.16	(80 V	250 V)	50 mA const.		23
	I0 x 14 x 0.07	105 V const.		(38 mA	10 mA)	16
	10 x 14 x 0.16	95 V const.		(55 mA	13 mA)	16
	22 x 15.5 x 0.07	(130V	440 V)	30 mA const.		19

Note. Underlined values for voltage or current were held constant. As a result the corresponding values given in parentheses could be measured. All electrophoresis runs started at 30 V constant for about I h. Voltage or current was only raised to the values given in the table when the sample had completely left the sample pocket.

2.7.4 Fixing, Staining, and Destaining

Proteins in the gel are fixed after the completion of the electrophoresis with a solution containing methanol (50%) and acetic acid (10%). Fixation time ranges from 30 min to 1 h, depending on the thickness of the gel. Fixation is followed by the usual coomassie-brilliant blue staining procedure. Destainig involves only the use of 10% acetic acid (SchaÈgger and von Jagow, 1987).

2.8 Metabolic Labelling

Metabolic studies are usually performed with the "youngest cell state" at which the cell division rate becomes maximum and the demand for the structural molecules reaches its highest point (Allers, et al., 2004; Cline et al., 1989). The specific metabolic labelling experiment designed for the prokaryote *H. volcanii*, requires a culture preparation with 0.6 cell density at 600 nm. Second step involves the preparation of spheroplasts. Pelleted cells are transferred into a spheroplasting solution: 1 M NaCl, 27 mM KCl, 50 mM Tris/HCl (pH 8.5), and sucrose (15%, w/v). Re-pelleted cells are re-suspended in fresh spheroplasting buffer (600 µl) and then divided into three aliquots. Onto each of the aliquots, 20 ml EDTA (0.5 M, pH 8.0) are added and the samples are incubated for 10 min at room temperature. Occasional mixing of the sample content is effected by manual inversion of the tubes. Onto the180 µl final sample volume 30 µl of the following buffer mixture is added: (15 µl; 1 M NaCl, 27 mM KCl, 15% (w/v) sucrose) and (15 µl; 5 µl EDTA (0.5 M pH 8.0), 1 µl ^{35}S-methionine (1,000 Ci/mmol, 10 mCi/ml), RNA (200 pmol). The final mixtures are further incubated for 5 min (Gebetsberger et al., 2017).

In the transformation of the spheroplasts three RNA oligomers used are Val(GAC)-tRF: 5′-GGGUUGGUGGUCUAGUCUGGUUAUGA-3′, Ile-tRF:5′-GGGCCAAUAGCUCAGUCAGGUU GAGC-3′, and Val-tDF: 5′-GGGTTGGTGGTCTAGTCTGGTTATGA-3′. Transformation is achieved using a polyethylene glycol (PEG_{600}) solution prepared in 1 M NaCl, 27 mM KCl, and 15% (w/v) sucrose. Transformed spheroplasts are diluted in a 1 ml spheroplast dilution solution [15% sucrose (w/v), 3.2 M NaCl, 109 mM $MgSO_4$, $7H_2O$, 112mM $MgCl_2$ $6H_2O$, 71mM KCl, 4mM$CaCl_2$, 15mM Tris/HCl (pH 7.2)]. Onto the re-pelleted speheroplast, a 500µl regeneration solution [2.5 M NaCl, 85 mM $MgSO_4$, 7H2O, 88 mM $MgCl_2$, $6H_2O$, 56 mM KCl, 4 mM $CaCl_2$, and 12 mM Tris/HCl (pH 7.20), 0.45% (w/v) tryptone,

0.275% (w/v) yeast extract, 0.1% (w/v) casamino acids, and 15% (w/v) sucrose], is added without re-suspension. The spheroplasts are incubated for 20 min at 42°C, and then re-suspended. Pelleted spheroplasts are lysed in 50 µl for 2 min H_2O at 95°C. After passing the lysate through a G25-Sepadex spin column, total protein content is resolved by electrophoresis through 11% Tricine-SDS-PAGE. The images of the novel proteins are obtained by reading and quantifying their radioactivity content by using special instruments, such as densitometers and phosphor imagers (Gebetsberger et al., 2017).

2.9 Fragment RNA Tetramers

It has recently been reported that fragment RNA molecules can form tetramers, RNA G-quadruplex (RG4), *in vitro*, through the 5′-guanine motif of a monomeric tRNA fragment with the help of a monovalent cation (Fig. 2a). The existence of many putative RNA tetramers has been evidenced through transcriptome studies. While monomeric tRNA fragments are mainly involved in the repression of translation, in tetrameric form they lead to the formation of stress granules in eukaryotic cell. Below some of the experimental procedures involved in the manipulations of RG4s are introduced (Lyons et al., 2017).

2.9.1 Stress Granule Induction and Quantification

Confluent cultures of U2OS cells (ATCC, USA), obtained in multi-well plates, are used for transfection with RNA (~250 pmol). Transfected cells are fixed in 4% paraformaldehyde for 15 min and permeabilised with ice-cold 100% methanol for 10 min. Immunofluorescence technology is used for the visualisation of the granules under a fluorescent microscope (Emara et al., 2010). Stress granules are monitored by co-localization of foci positive for G3BP1 (Ras-GAP SH3 domain binding protein-1), 4 eIF4G (eukaryotic initiation factor 4G), and TIAR (T cell intracellular antigen-1 related protein). RNA is extracted from parallel transfection samples and its

stability is checked by 15% denaturing polyacrylamide gel electrophoresis. Resolved RNA bands are visualized by staining with SYBR gold. This is followed by the transfer of RNA onto a membrane and by the specific detection of the RNA of interest with biotinylated DNA probes. A horse radish peroxidase-conjugated streptavidin binds to biotin on the hybridised DNA probe and allows the detection of a specific RNA molecule (Aulas et al., 2017; Kedersha and Anderson, 2007; Lyons et al., 2017).

2.9.2 RNA Affinity Chromatography

Transfer-RNA derived stress-induced RNA (tiRNA) binding proteins can be obtained by affinity chromatograph. Recently this has been demonstrated on a human osteosarcoma, U2OS, cell line. A confluent cell culture is first lysed by the common procedure involving the use of NP-40 detergent. Particulate material is removed by centrifugation and biotinylated RNA oligonucleotides (250 pmol) are added onto the aliquots of culture supernatant. The lysate and RNA mixture is incubated on a rotary shaker at 4 ^{o}C. Streptavidin is added after the two hours of incubation and the final samples are further incubated for two hours. Unbound material is removed by washing with NP-40 containing lysis buffer. The samples are now expected to contain only the RNA-bound proteins which are ready for further manipulations (Ivanov et al., 2011; Lyons et al., 2016; Lyons et al., 2017).

2.9.3 Heterogeneous tRNA Tetramer Capture

Streptavidin-biotin coupling is also used in capturing RNA G-quadruplex (RG4) structures (Fig. 2b). In such experiments biotinylated arms of a tRNA, prepared from a tRNA specific to an amino acid, is used as the probe and is expected to take part in the formation of tetramers with non-biotinylated other RNA arms. Tetramer form is constituted in the presence of 150mM NaCl. Streptavidin agarose beads are used for the adsorption of biotinylated RNA in the tetramer. The adsorption requires two hours

of incubation at 4 °C on a rotary shaker. RNA tetramers on the agarose beads are washed in 150mM NaCl, in water, and in 150mM LiCl, respectively. RNA tetramers on the agarose beads are then eluted by heating at 100 °C in 150mM LiCl. Eluted material is resolved in denaturing acrylamide gels (15%) and the RNA bands are visualized by staining with SYBR Gold (Lyons et al., 2017).

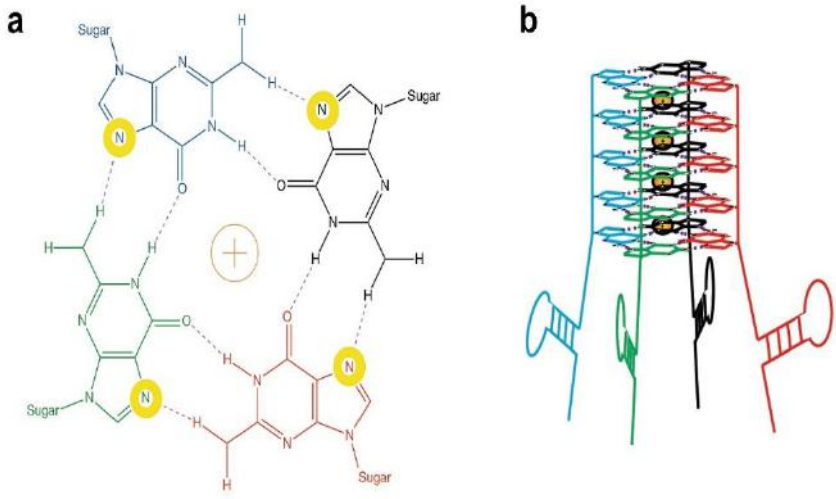

Figure 2. a Tetramer formation through guanines, **b** An RG4 model for alanine 5′-tiRNA (Lyons et al., 2017).

3. CONCLUSION: FUTURE IMPLICATIONS

Accumulating evidence suggests that the arms of both mature and precursor tRNAs are involved globally in the regulation of translation in the stressed cell. In certain types of cancer, in breast and prostate cancers for example, functional fragment tRNAs could be found in a sex hormone-dependent manner and acting in the direction of cell proliferation (Honda et al., 2015; Shigematsu and Kirino, 2015).

It has generally been accepted that working with tRNA fragments is not as straight forward as other short RNA species, such as

miRNA, because tRNA molecules undergo hundreds of posttranscriptional modifications that interfere with the classical Watson-Crick base-pairing. These modifications are on the other hand also responsible for the structural diversity of tRNA that play a crucial role in the specificity of codon recognition (Kellner et al., 2010; Shigematsu and Kirino, 2015).

Transfer RNAs are generally transcribed as identical- or slightly modified copies. Some fragments of tRNA are the products of the genomic regions residing outside canonical tRNA loci. Moreover, some other fragments that are generated from the internal regions of mature tRNA can be loaded onto Argonaute, AGO, proteins, which are involved in the inhibition of translation (Shigematsu and Kirino, 2015).

Clinical findings suggest that quantitative assessment of transfer RNA-derived small RNAs (tsRNAs) can serve as a diagnostic tool in neurological diseases. Here, such measurements can also include the simultaneous quantification of miRNAs in order to question whether biological activities of these two distinct RNA species are sometimes interrelated. Some of tsRNAs are detected more often than miRNAs in the exosomes of body fluid. A therapeutic potential for tsRNAs has also been implicated in some studies. The establishment of such a possibility requires experiments both on animals and in clinical trials (Qin et al., 2020).

Extracellularly tsRNAs survive in extracellular vesicles. They appear to be stabilised by divalent cations in the extracellular fluid. This might imply the involvement of metalloproteins in the stability of tsRNAs in the extracellular environment because EDTA treatment of the plasma appears to lead to their destabilisation. The proteins involved in this protection remain to be identified (Tosar and Cayota, 2020).

It has been shown that certain 5′ tRNA halves can re-programme gene expression when they are transferred into the cells of a mouse

embryo. Such a dramatic effect might involve the epigenetic regulation pathways of embryonic gene expression, where the fragment tRNAs might act as intercellular messengers. Further attempts in this direction might open up a new and fruitful research area in the near future (Tosar and Cayota, 2020).

References

Allers, T., Ngo, H. P., Mevarech, M., Lloyd, R. G. (2004), "Development of additional selectable markers for the halophilic archaeon Haloferax volcanii based on the leuB and trpA genes", *Applied Environ Microbiol.*, 70:943-53.

Anderson, P. and Ivanov, P. (2014), "tRNA fragments in human health and disease", *FEBS Lett*., 588(23): 4297–304.

Aulas, A., Fay, M. M., Lyons, S. M., Achorn, C. A., Kedersha, N., Anderson, P., Ivanov, P**.** (2017), "Stress-specific differences in assembly and composition of stress granules and related foci", *J. Cell Sci.*, 130, 927–937.

Chan, P. P. and Lowe, T. M**.** (2009), "GtRNAdb: a database of transfer RNA genes detected in genomic sequence", *Nucleic Acids Res*., 37 (Database issue): D93–7.

Cline, S. W., Lam, W. L., Charlebois, R. L., Schalkwyk, L. C., Doolittle, W. F. (1989), "Transformation methods for halophilic archaebacteria", *Canadian J Microbiol.,* 35:148-52.

Djebali S, Davis C. A, Merkel A., *et al*. (2012), "Landscape of transcription in human cells", *Nature*., 489 (7414): 101–8.

Emara, M. M., Ivanov, P., Hickman, T., Dawra, N., Tisdale, S., Kedersha, N., Hu, G. F, Anderson, P. (2010), "Angiogenin-induced tRNA-derived stress-induced RNAs promote stress-induced stress granule assembly", *J. Biol. Chem.*, 285, 10959–10968.

Farazi, T.A., Juranek, S. A., Tuschl, T. (2008), "The growing catalog of small RNAs and their association with distinct Argonaute/Piwi family members", *Development*, 135(7):1201–14.

Garcia-Silva, M. R., Cabrera-Cabrera, F., Guida, M. C., Cayota, A. (2012), "Hints of tRNA-derived small RNAs role in RNA silencing mechanisms", *Genes (Basel)*, 3(4):603–14.

Gebetsberger, J., Polacek, N. (2013), "Slicing tRNAs to boost functional ncRNA diversity" *RNA Biol*., 10(12):1798–806.

Gebetsberger, J., Wyss, L., Mleczko, A. M., Reuther, J., Polacek, N. (2017), "A tRNA-derived fragment competes with mRNA for ribosome binding and regulates translation during stress", *RNA Biol.*, 14, 1364–1373.

Ghildiyal, M. and Zamore, P. D. (2009), "Small silencing RNAs: an expanding universe", *Nat Rev Genet*., 10(2):94–108.

Honda, S., Loher, P., Shigematsu, M., Palazzo, J. P., Suzuki, R., Imota, I., Rigoutsos, I., Kirino, Y**.** (2015), "Sex hormone-dependent tRNA halves enhance cell proliferation in breast and prostate cancers", *Proc Natl Acad Sci USA*, 112(29):E3816–25.

Ivanov, P., Emara, M. M., Villen, J., Gygi, S. P., Anderson, P**.** (2011), "Angiogenininduced tRNA fragments inhibit translation initiation", *Mol. Cell*, 43, 613–623.

Kedersha, N. and Anderson, P**.** (2007), "Mammalian stress granules and processing bodies", *Methods Enzymol.*, 431, 61–81.

Kellner, S., Burhenne, J., Helm, M. (2010) "Detection of RNA modifications", *RNA Biol*., 7(2):237–47.

Kim, V.N. and Han, J**.** (2009), "Siomi MC. Biogenesis of small RNAs in animals", *Nat Rev Mol Cell Biol*., 10(2):126–39.

Kozomara, A. and Griffiths-Jones, S. (2014), "miRBase: annotating high confidence microRNAs using deep sequencing data", *Nucleic Acids Res*., 2014;42 (Database issue): D68–73.

Lyons, S. M., Achorn, C., Kedersha, N. L., Anderson, P. J., Ivanov, P. (2016), "YB-1 regulates tiRNA-induced Stress Granule

formation but not translational repression", *Nucleic Acids Res.,* 44, 6949–6960.

Lyons, S.M., Gudanis, D., Coyne, S.M., Gdaniec, Z., Ivanov, P. (2017), "Identification of functional tetramolecular RNA G-quadruplexes derived from transfer RNAs", *Nat Commun*., 8(1):1127.

Nieuwlandt, D. T., Palmer, J. R., Armbruster, D. T., Kuo, Y. P., Oda, W., Daniels, C. J. (1995), "A rapid procedure for the isolation of RNA from *Haloferax volcanii*", In: Robb FT, Place AR, Sowers KR, Schreier HJ, DasSarma S, Fleischmann EM, eds. Archaea: *A laboratory manual. New York: Cold Spring Harbour Press.* 161.

Qin, C., Xu, P. P., Zhang, X., Zhang, C., Liu, C. B., Yang, D. G., Gao, F., Yang, M. L., Du, L. J., L,, J. J. (2020), "Pathological significance of tRNA-derived small RNAs in neurological disorders", *Neural Regeneration Research.,* 15, 212-221.

SchaÈgger, H. and von Jagow, G. (1987), "Tricine-sodium dodecyl sulfate-polyacrylamide gel electrophoresis for the separation of proteins in the range from 1 to 100 kDA", *Anal. Biochem.,* 166, 368-379.

Shigematsu, M., Honda, S., Kirino, Y. (2014), "Transfer RNA as a source of small functional RNA", *J Mol Biol Mol Imaging*., 1(2):1–8.

Shigematsu, M. and Kirino, Y. (2015), "tRNA-derived short non-coding RNA as interacting partners of argonaute proteins", *Gene Regul Syst Bio*., 9:27–33.

Sobala, A. and Hutvagner, G. (2011), "Transfer RNA-derived fragments: origins, processing, and functions", *Wiley Interdiscip Rev RNA.*, 2(6):853–62.

Straub, J., Brenneis, M., Jellen-Ritter, A., Heyer, R., Soppa, J., Marchfelder, A. (2009), "Small RNAs in haloarchaea: Identification, differential expression and biological function", *RNA Biol.,* 6: 281–292.

Telonis, A. G., Loher, P., Honda, S., Jing, Y., Palazzo, J., Kirino, Y., Rigoutsos, I. (2015), "Dissecting tRNA-derived fragment

complexities using personalized transcriptomes reveals novel fragment classes and unexpected dependencies", *Oncotarget,* 22, 24797–24822.

Tosar, J. P. and Cayota, A. (2020), "Extracellular tRNAs and tRNA-derived fragments", *RNA Biol.,* 1-19.

Wanner, C. and Soppa, J. (2002), "Functional role for a 2-oxo acid dehydrogenase in the halophilic archaeon *Haloferax volcanii*", *J Bacteriol.,* 184:3114-21.

ANTIFUNGAL ACTIVITY OF BORIC ACID AND CITRIC ACID MIXTURE AS A SANITIZER AGENT

Elif Ayşe Erdoğan Eliuz*

1. INTRODUCTION

Over the past decade the chemistry of boric acid and citric acid has undergone a rapid development. This growing interest is mainly due to their combined with their environmentally benign character and commercial availability. Boric acid also known as boracic acid or orthoboric acid is a weak inorganic acid and white crystalline solid having the H_3BO_3 ($B(OH)_3$) chemical formula. It can soluble in water, lower alcohols, pyridine and acetone. It is also used as an antiseptic agent, preservative, insecticide, as swimming pool chemical and a precursor to many useful chemicals (Pal, 2018: 1-26). Colourless and odourless citric acid (tricarboxylic acid ($C_6H_8O_7$) is slightly hygroscopic and highly soluble in water (62.07% at 25 °C) and slightly hygroscopic. The code of citric acid is E330 as food ingredient in European Union (E331 and E332, respectively, for sodium and potassium citrate) and has been Generally Recognized as Safe (GRAS) in the US. Citric acid's popularity has increased even more in household detergents and home hygiene because of restrictions on the use of phosphate in dishwasher detergents in the US (since 2010), EU (2017), (Ciriminna, et al. 2017: 1-9)., and Turkey (RG, 2018).

Many yeast species and mycotoxin-producing fungi are classified as food-borne pathogens that are responsible for food poisoning or infection besides bacteria, viruses and parasites (Jacques and Casaregola, 2008:321-326; Loureiro and Malfeito-Ferreira, 2003:23-50). Some species of *Candida* genus among yeasts such as *Candida glabrata*, *Candida parapsilosis*, and *Candida tropicalis* with those species cause nosocomial bloodstream infections with high morbidity and mortality rates (Wisplinghoff et al. 2004:309-317; Yapar, 2014: 95-105; Pappas et al. 2016: 1-50). In the past two decades, infections have been observed to increase in the past two decades due to non-albicans species (Fidel et al. 1999: 80-96; Miguel et al. 2005: 548-52). More species from *Candida*

* (Dr. Öğr. Üye.); Mersin University, Vocational School of Technical Sciences, Department of Food technology, Mersin, TURKEY,
e-mail: eliferdogan81@gmail.com.

glabrata, *C. parapsilosis* and *C. tropicalis* were determined in silage, fodders, olive brine, olive products because of yeast's rapid degradation of lactic or acetic acids under aerobic conditions and reported that they were very harmful when present. This can lead to loss of nutritional value, an increase in foodborne infections and various diseases (Middelhoven and Van Baalen, 1988: 199-207; Middelhoven, 2002: 279-292). Among them, vulvovaginal candida infections are an important health problem for women and over 75% of women affected at least once throughout their lifetime. When these symptoms are due to *Candida glabrata*, boric acid was commonly described as an alternative treatment, although the exact mechanism of action is unknown (Guaschino et al. 2001: 598-602; Ray et al. 2007: 312–317; De Seta et al. 2009: 325-336). Similarly, ketoconazolegarlic tablets, including citric acid, are used in the treatment of such diseases against *C. albicans* (Powar et al. 2017: 1-10). The other emerging human pathogen is *Candida parapsilosis* and, it is now one of the leading causes of invasive candidal disease (Trofa et al. 2008: 606-625). *C. tropicalis* is a species that occurs with more detailed screening methods with the increase of diseases related to candida pathogen and it causes serious infections with other *Candida* pathogens (Silva et al. 2012: 288-305). Therefore, disinfection of surfaces should be not only bacteria, but also substances that can control the presence of yeast.

Insufficient sanitation on food processing materials or surfaces causes long-term trapping of microorganisms and irreversible contamination of food (Carpentier and Cherf, 1993: 499-511). In addition microorganisms' gaining resistance against sanitizer over time makes difficult achieve adequate hygiene (Notermans et al. 1991: 21-36). So that, the production of effective sanitizers for the inhibition of pathogens in agricultural and food products is important for the hazard identification and critic control point (HACCP) system of the food industry (Issa-Zacharia et al. 2010: 740-5).

In the present study, it is firstly evaluated that antimicrobial activity of boric acid and citric acid mixture in terms of a natural sanitizer agent and the tolerance or persistence levels in *C. albicans, C. glabrata, C. parapsilosis* and *C. tropicalis* exposed to this mixture based on the modified Kirby–Bauer disk diffusion method.

2. MATERIALS AND METHODS

2.1.Materials and Instruments

Mueller Hinton Agar (MHA), Mueller Hinton Broth (MHB), Sabouraud Dextrose Broth (SDB), Triptic Soy Broth (TSB) were supplied from Merck (Darmstadt, Germany). *C. albicans, C. glabrata, C.*

parapsilosis and *C. tropicalis* were taken from Refik Saydam Hıfzıssıhha Centre (Ankara/Turkey). Eliza spectrophotometer (Thermo Scientific, MULTISKAN GO) was used for antimicrobial measurements. Citric acid and boric acid was purchased from Sigma.

2.2.Preparing of Boric acid and Citric Acid Solution

To prepare boric acid and citric acid, 1 g citric acid and 1 g boric acid were weighed and added to 60 mL of previously sterilized distilled water. It was then homogenized in the magnetic stirrer for 1 hour and stored at 4ºC. The pH value of each two organic acids in water was determined using Ph meters.

2.3.Antifungal Screening

The inoculums of *C. albicans, C. glabrata, C. parapsilosis* and *C. tropicalis* were prepared in 4 mL SDB and incubated at 37 ºC, overnight. After 24 hours, the yeast suspensions were adjusted to 0.5 McFarland Standard Turbidity and stored at +4 °C until experiments.

2.3.1.Spectrophotometric Broth Microdilution Method

The 50 µL of MHB medium were added into 96-well microtiter plates and two-fold serial dilutions of 50 µL boric acid and citric acid was made x-axis along from 2nd to 10th columns and used columns 11 and 12 as negative control (only MHB and microbe). Then, 5 µL culture of yeast were inoculated on all wells except negative control. Finally, all plates were incubated at 37ºC for 24 hours and the growth (turbidity) was measured at 415 nm. MIC (Minimum Inhibitory Concentration) was determined as the lowest concentration where no visible turbidity was observed in the each row of the 96-well plate (Sicak and Erdoğan Eliuz, 2019: 928-934) .

2.3.2.Modified TDtest

To evaluate tolerance or persistence levels in *C. albicans, C. glabrata, C. parapsilosis* and *C. tropicalis* against boric acid and citric acid mixture were used by TDtest (Kirby–Bauer disk diffusion method modified). This method consists of two steps: First, the MIC values of the mixture were used for well difusion method. For this, the cultures at stationary phase were spread onto MHA plates and 6mm diameter wells were drilled into the middle of them. The 50 µL (0.1g/mL) of the mixture was placed in the wells and incubated at 37°C for 24 hrs. Second: 50 µL glucose (10%) was placed in the well which discharged because of the diffusion of the extract into the agar. The alteration in the zone regions of the petri dishes re-incubated during 37°C for 24 hrs were measured and compared with the

clear zone in the primary step. TDtest, which the mixture was replaced with the glucose, allows re-growth and detection of the surviving microorganisms on agar surface. According to the method, it is interpreted as susceptible strain if inhibition zone were found around the well after glucose addition and tolerant strain if colonies inside the clear zone after glucose (Figure 1) (Bauer et al. 1959: 208-216; Gefen et al. 2017: 41284).

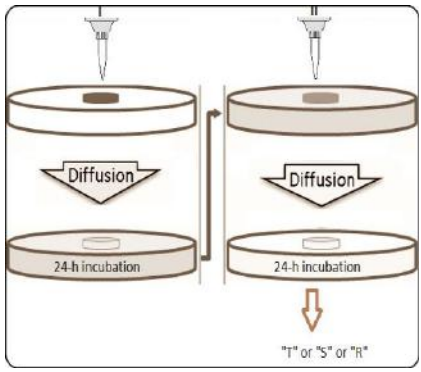

Figure 1: The diagram of modified TDtest. Application of boric-citric acid solution on the agar well (I), Replacing the boric-citric acid solution with glucose solution (II). "T", "S", "R" Susceptible strain (S): no colonies in the inhibition zone around well after glucose addition. Tolerant strain (T): Colony observation in inhibition zone after glucose

2.4.Surface Disinfection Test

Surface sanitizer tests were performed using the EN 13697:2015 standard "Chemical disinfectants and antiseptics. Quantitative non-porous surface test for the evaluation of fungicidal activity of chemical disinfectants used in many industries such as food, cosmetic and agricultural. Test method and requirements without mechanical action". The fungicidal activity of boric acid and citric acid as sanitizer (Bo-Ci-SAN) was evaluated on glass lam. Lams were sterilized at 121^{o}C for 15 min in autoclave before each assay. Briefly, yeast suspensions were diluted (ratio 1:1) with 0.3 and 3 g/l bovine serum albumin (BSA) to mimic dirty and clean working conditions (as in EN 13697:2015), respectively. Then 50 µl of resulting inocula (8 log CFU/ml) were spotted into sterile lams and dried at RT for 15 min. Later, 50 µl of 10% Bo-Ci-SAN aprepared on hard water as diluent according to EN 13697:2015 and 50 µl mixture was transferred to 96-elisa plates by mixing with a pipette and 50 µl TTC (2,3,5- triphenyl tetrazolium chloride) was added. Plates were incubated at 37^{o}C to be visualized by staining with TTC and after 4 hours,

spectrophotometric measurements were made at 485 nm. Although there were no Bo-Ci-SAN agents studied in the negative control well, other conditions were the same.

For percent of inhibition was calculated according to following formule (1);

$$\text{Percent of Inhibition (\%)} = \left[1 - \frac{OD_{test\ well}}{OD_{corresponding\ control\ well}}\right] \times 100 \quad (1)$$

2.5.Statistical analysis

Statistical analyses and significance were measured by Tukey test in one way analysis of variance for MICs and IZ using SPSS 25. Differences were considered significant at $p \leq 0.05$.

3. RESULTS AND DISCUSSION

3.1.Antimicrobial Activity and Response of Yeasts According to TDTest

The results showed that boric acid and citric acid solution was effective against *C. albicans, C. glabrata, C. parapsilosis* and *C. tropicalis* by spectrophotometric broth microdilution and agar well diffusion method (Table 2). There was statistically significant difference between the MICs of boric acid and citric acid mixture against the pathogens. While MIC of the solution on *C. albicans* was 0.06 g/mL, it was 0.03 g/mL for *C. glabrata, C. parapsilosis* and *C. tropicalis.*

Although, it wasn't seen any statistically significant difference between inhibition zones at the end of the 24-h incubation, there was a significant difference in among 48-h IZs ($p<0.05$). The highest inhibition zone was found with 5.53 mm on *C. albicans* while the lowest IZ with 2.87 mm *C. glabrata* and also it was 5.1 mm on *C. parapsilosis* and 3.6 mm on *C. tropicalis* at the end of the 24-h incubation by well diffusion agar test ($p<0.05$) Table 2.

Table 2: Minimal Inhibition Concentration and Inhibition zone (mm) of boric acid and citric acid mixture against *C. albicans, C. glabrata, C. parapsilosis* and *C. tropicalis.* Res: Response of microorganisms in step 2 according to TDTest, S: Susceptible strain; T: Tolerant strain.

boric acid and citric acid (pH: 3.39)

	MIC (g/mL)	IZ (24 h)	IZ (48 h)-Res
Ca	0.06^{a}±0.01	5.53^{a} ±0.03	5.20^{a}±0.08-**T**
Cg	0.03^{b}±0.02	2.87^{a} ±0.02	2.36^{ab} ±0.02-**S**
Cp	0.03^{b}±0.1	5.1^{a} ±0.01	3.7^{a}±0.03-**T**
Ct	0.03^{b}±0.1	3.6^{a} ±0.01	1.5^{b}±0.03-**S**

The average MICs were expressed with the standard deviation (±) and significance level (ANOVA, 25; 0.05, Tukey test). Values on the same column with different superscript letters differ statistically at the 0.05 level.

Boric acid and citric acid are known to have separately antifungal activity. Since citric acid is a stronger acid than boric acid, its effectiveness is also higher. In the study which examined the fungistatic effect of boric acid, MICs were changed between 1562 and 3125 mg/L on clinical *C. albicans* isolates including *C. glabrata* (De Seta, 2009: 325-336). Citric acid was active with MIC of 2-10 mg/mL against *C. albicans* and some fungi species (Shokri, 2011: 543-545). Organic acids inhibit microorganisms through a process which hydrogenes become released through order to preserve intracellular pH and the acid pH within the cell induces deformation and harm to enzymatic activity, proteins and DNA structure or affect the electron transport system thereby destroying the extracellular membrane (Kong et al. 2001:178–183; Mani-López et al. 2011: 713-721). No previous study has been carried out on antifungal activities of these acids mixture which pH is 3.39.

The disc-diffusion test used in antimicrobial activities assesses only the concentration at which microorganism inhibits proliferation, namely the degree of resistance. This test was expanded with a few simple techniques to state the tolerance of microorganisms against antimicrobial agents and their persistence. This method, the "TDtest (Tolerance Disc Test)", has made it possible to detect tolerant and persistent microorganisms by encouraging the growth of the surviving microorganisms in the inhibition zone after the antimicrobial agent has spread (Gefen et al. 2017: 41284). In present study, it was applied the TDtest with boric-citric acid solution and discriminate by tolerance levels (T) of *C. albicans* and *C. parapsilosis* at the end of the 48-h incubation. At the end of the 48-h incubation, the inhibition zones were found as 5.20 mm, 2.36 mm, 3.7 mm, 1.5 mm for *C. albicans, C. glabrata, C. parapsilosis* and *C. tropicalis*, respectively. In

addition, the IZ (1.5 mm) on *C. tropicalis* was significantly different from the others ($p<0.05$) (Table 2).

It is clear that the solution had a strong and persistent antifungal against *C. glabrata* and *C. tropicalis.* Finally, it was determined that *C. albicans* and *C. parapsilosis* were tolerance to boric-citric acid solution because of many colonies in the inhibition region. But, *C. parapsilosis* has been shown to be more tolerant than *C. albicans*. (Figure 2).

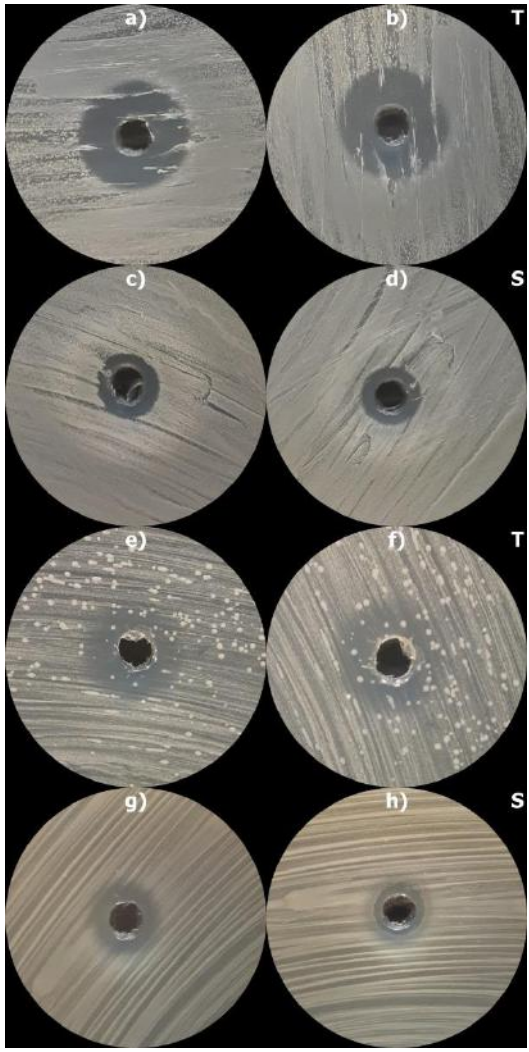

Figure 2: The images of tolerance and sensitivity levels of *C. albicans*(a,b), *C. glabrata* (c,d), *C. parapsilosis*(e,f) and *C. tropicalis* (g,h) in exposure to boric acid and citric acid

solution. The first (a, c, e, g) and second (b, d, f, h) step of TDtest, S: Susceptible strain; T: Tolerant strain.

In this study, unlike the previous TDtest method, well diffusion method was used instead of disk and *C. glabrata* and *C. tropicalis* were very sensitive to the mixture and no colony was found even in the 48-h incubation. In addition, it was seen an almost 50 percent reduction in the zone of inhibition on *C. tropicalis*.

3.2.Evaluation of inhibition activity of Bo-Ci-SAN

Survival of *C. albicans, C. glabrata, C. parapsilosis* and *C. tropicalis* were investigated by surface disinfection test exposure to Bo-Ci-SAN. The percentages of inhibition were used to assess number of cells that died after 4 hours compared with negative control (live of 100% : 8 log). There was no statistically significant difference between yeasts in terms of the number of cells inhibited. In glass surface which was mimiced dirty working conditions (3 g/mL BSA), while the inhibition order is presented: *C. glabrata* (48.1%) > *C. tropicalis* (43.5%) > *C. parapsilosis* (37.0%) > *C. albicans* (36.0%) ; *C. glabrata* (49.6%) > *C. tropicalis* (46.9%) > *C. parapsilosis* (46.60%) > *C. albicans* (39.8%) in clean working conditions (0.3 g/mL BSA) (Figure 3).

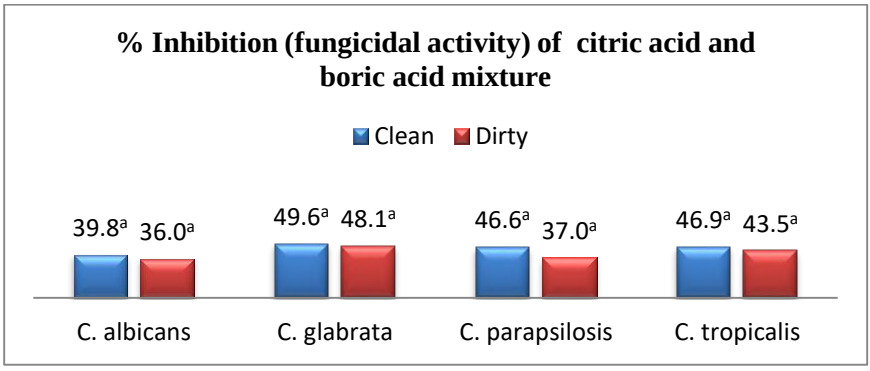

Figure 3: Fungicidal activity (%) of Bo-Ci-SAN against *C. albicans, C. glabrata, C. parapsilosis* and *C. tropicalis* on a glass surface clean (0.3 g/mL BSA) and dirty (3 g/mL BSA) conditions at 4-h contact times according to EN 13697:2015. Values with same superscript letters doesn't differ statistically at the 0.05 level.

In literature, no any surface sanitation studies have been found regarding Bo-Ci-SAN. However in some studies, Boric acid and citric acid are known to have separately inhibition effect on fungi. Hassan et al. (2015) reported that citric acid (10%) had inhibitory effect as 17.71% and

20.16% on *Aspergilus flavus* and *Penicillium purpurogenum*, respectively, at the end of the day of 8 (Hassan et al. 2015: 1-11). In a study which examined the fungistatic effect of boric acid, 96.2% were inhibited by 3125 mg/L and 39.7% of strains were inhibited by MIC of 1563 mg/L; all fluconazole-resistant isolates were inhibited by MIC of 3125 mg/L of boric acid on clinical *C. albicans* isolates including *C. glabrata* (De Seta et al. 2009: 325-336). When compared with these studies, it was observed that a mixture of boric acid and citric acid killed half of the yeasts in a short time.

It is reported that at even high concentrations organic acids can used as decontaminants of food products or surface to improve food safety and hygiene (Virto et al. 2006: 865-870). In this study where the permanence effect is evaluated, the prepared boric acid and citric acid mixture was effective for Candida species. This effect is lowest for *C. parapsilosis* and high for *C. albicans, Candida glabrata* and *C. tropicalis*. This mixture can prevent the spread by stopping *C. glabrata* and *C. tropicalis* contamination. It is an alternative to many chemicals that may be toxic to the human cell especially in household disinfectants.

4. CONCLUSION

In this study, the antifungal effect of boric acid and citric acid mixture on *C. albicans, C. glabrata, C. parapsilosis* and *C. tropicalis* pathogens was investigated and it was checked whether this effect was permanent or tolerant according to TDTest method. In present paper, all yeasts were sentisitive against boric acid and citric acid mixture but it was determined that *C. glabrata* and *C. tropicalis* showed permanent sensitivity to the solution. At the same time, the modified surface sanitizer test was measured at the 4th hour, when viable microorganisms can be stained with TTC dye, and at the end of this period, approximately half of the microorganisms were inhibited. As a result, it is an antifungal agent that can be used in place of hazardous chemicals that may be toxic to the human cell on all surfaces where yeast pathogen has a risk of contamination.

REFERENCES

BAUER, Alfred W., PERRY, David M., AND KIRBY, William M.M., (1959), "Single-Disk Antibiotic-Sensitivity Testing of Staphylococci: An Analysis of Technique and Results", *Archives of Internal Medicine*, Volume 104/2, p. 208-216.

CARPENTIER, Brigitte and CERF, O, (1993), "Biofilms and their consequences, with particular reference to hygiene in the food industry", *Journal of Applied Bacteriology*, Volume 75/6, p. 499-511.

CIRIMINNA, Rosaria, MENEGUZZO, Francesco, DELISI, Riccardo, PAGLIARO, Mario, (2017), "Citric acid: Emerging applications of key biotechnology industrial product", *Chemistry Central Journal*, Volume 11/22, p. 1-9.

DE SETA, Francesco, SCHMIDT, Martin, VU, Bau, ESSMANN, Michael, LARSEN, Bryan, (2009), "Antifungal mechanisms supporting boric acid therapy of *Candida vaginitis"*. *Journal of Antimicrobial Chemotherapy*, Volume 63/2, p. 325-336.

FIDEL, Paul L., VAZQUEZ, Jose A., SOBEL, Jack D., (1999), "Candida glabrata: Review of epidemiology, pathogenesis, and clinical disease with comparison to *C. albicans"*, *Clinical Microbiology Reviews*, Volume 12/1, p. 80-96.

GEFEN, Orit, CHEKOL, Betty, STRAHILEVITZ, Jacob. and BALABAN, Nathalie Q., (2017), "TDtest: Easy detection of bacterial tolerance and persistence in clinical isolates by a modified disk-diffusion assay", *Scientific Reports*, Volume 7, 41284.

GUASCHINO, Secondo., DE SETA, Francesco, SARTORE, Andrea, RICCI, Giuseppe, DE SANTO, Davide, PICCOLI, Monica, and ALBERICO, Salvatore. (2001). "Efficacy of maintenance therapy with topical boric acid in comparison with oral itraconazole in the treatment of recurrent vulvovaginal candidiasis", *American Journal of Obstetrics and Gynecology*, Volume 184/4, p. 598-602.

HASSAN, Ramadan, EL-KADI, Sherif, SAND, Mostafa. (2015). "Effects of Some Organic Acids on Some Fungal Growth and Their Toxins Production", *International Journal of Advances in Biology*, Volume 2/1, 1-11.

ISSA-ZACHARIA, Abdulsudi, KAMITANI, Yoshinori, MORITA, Kazuo and IWASAKI, Koichi. (2010). "Sanitization potency of slightly acidic electrolyzed water against pure cultures of *Escherichia coli* and *Staphylococcus aureus*, in comparison with that of other food sanitizers", *Food Control*, Volume 21/5, 740-5.

JACQUES, Noemie, and CASAREGOLA, Serge. (2008). "Safety assessment of dairy microorganisms: The hemiascomycetous yeasts", *International Journal of Food Microbiology*, Volume 126, 321–326.

KONG, Young-Jun, PARK, Boo-Kil, OH, Deog-Hwan. 2001, "Antimicrobialactivity of Quercus mongolica leaf ethanol extract and organicacids against food-borne microorganisms", *Korean Journal of Food Science and Technology*, Volume 33, 178–183.

LOUREIRO, V., MALFEITO-FERREIRA, M. (2003), "Spoilage yeasts in the wine industry", *International Journal of Food Microbiology*, Volume 86/1-2, 23-50.

MANI-LÓPEZ, E., GARCÍA, H. S., LÓPEZ-MALO, A, (2012), "Organic acids as antimicrobials to control Salmonella in meat and poultry products", *Food Research International*, Volume 45/2, 713-721.

MIDDELHOVEN, Wouter J., (2002), "Identification of yeasts present in sour fermented foods and fodders", *Applied Biochemistry and Biotechnology - Part B Molecular Biotechnology*, Volume 21, 279-292.

MIDDELHOVEN, Wouter. J., and VAN BAALEN, Anja H. M., (1988), "Development of the yeast flora of whole-crop maize during ensiling and during subsequent aerobiosis", *Journal of the Science of Food and Agriculture*, Volume 42/3, 199-207.

MIGUEL, Lucia Garcia San, COBO, Javier, OTHEO, Enrique, SÁNCHEZ-SOUSA, Aurora, ABRAIRA, Victor, MORENO, Santiago, (2005), "Secular Trends of Candidemia in a Large Tertiary-Care Hospital From 1988 to 2000: Emergence of *Candida parapsilosis*", *Infection Control and Hospital Epidemiology*, Volume 26/6, 548-52.

NOTERMANS, S., DORMANS, J. A. M. A. AND MEAD, G. C, (1991), "Contribution of surface attachment to the establishment of microorganisms in food processing plants: A review", *Biofouling*, Volume 5/(1-2), 21-36.

PAL, Rammohan, (2018),"Boric acid in organic synthesis: Scope and recent developments", *The Free Internet Journal for Organic Chemistry*, Volume 346, 1-26.

PAPPAS, Peter, G., KAUFFMAN, Carol, A., ANDES, David, R., CLANCY, Cornecilus, J., MARR, Kieren, A., OSTROSKY-ZEICHNER, Luis, REBOLI, Annette C., SCHUSTER, Mindy, G., VAZQUEZ, Jose, A., WALSH, Thomas, J., ZAOUTIS, Theoklis, E., SOBEL, Jack, D, (2015) "Clinical Practice Guideline for the Management of Candidiasis: 2016 Update by the Infectious Diseases Society of America", *Clinical Infectious Diseases*, Volume 62/4, 1-50.

POWAR, Trupti, A., HAJARE, Ashok, A., PATIL-VIBHUTE, Preeti, B., NADAF, Sameer, J., JARAG, Ravinda, J., (2017), "Bioadhesive garlic and ketoconazole vaginal tablets for treatment of candidiasis". *Indian Journal of Pharmaceutical Education and Research*, Volume 51/2, 1-10.

RAY, Debarti, GOSWAMI, Ravinder, BANERJEE, Uma, DADHWAL, Vatsla, GOSWAMI, Deepti, MANDAL, Piyali, SREENIVAS, Vishnubhatla, KOCHUPILLAI, Narayana, (2007), "Prevalence of *Candida glabrata* and its response to boric acid vaginal suppositories in comparison with oral fluconazole in patients with diabetes and vulvovaginal candidiasis", *Diabetes Care*, Volume 30/2, 312–7.

RG. (RESMI GAZETE), (2018). https://www.resmigazete.gov.tr/eskiler/2017/09/20170922-4.htm.

Erişim tarihi: 14.05.2020.

SHOKRI, Hojjatollah, (2011), "Evaluation of inhibitory effects of citric and tartaric acids and their combination on the growth of *Trichophyton mentagrophytes*, *Aspergillus fumigatus*, *Candida albicans*, and *Malassezia furfur*, *Comparative Clinical Pathology*, Volume 20, 543-545.

SICAK, Yusuf, and ERDOĞAN ELIUZ, Elif, A., (2019), "Chemical content and biological activity spectrum of *Nigella sativa* seed oil", *Kahramanmaraş Sütçü İmam Üniversitesi Tarım ve Doğa Dergisi*, Volume 22/6, 928-934.

SILVA, Sonia, NEGRI, Melyssa, HENRIQUES, Mariana, OLIVEIRA, Rosario, WILLIAMS, David, W., AZEREDO, Joana, (2012), "*Candida glabrata*, *Candida parapsilosis* and *Candida tropicalis*: Biology, epidemiology, pathogenicity and antifungal resistance", *FEMS Microbiology Reviews*, Volume 36/2, 288-305.

TROFA, David, GÁCSER, Attila, NOSANCHUK, Joshua, D, (2008), "*Candida parapsilosis*, an emerging fungal pathogen". *Clinical Microbiology Reviews*, Volume 21/4, 606-625.

VIRTO, R., SANZ, D., ÁLVAREZ, I., CONDÓN, S., RASO, J, (2006), "Application of the Weibull model to describe inactivation of *Listeria monocytogenes* and *Escherichia coli* by citric and lactic acid at different temperatures", *Journal of the Science of Food and Agriculture*, Volume 86/6, 865-870.

WISPLINGHOFF, Hilmar, BISCHOFF, Tammy, TALLENT, Sandra, M., SEIFERT, Harald, WENZEL, Richard, P., EDMOND, Michael, B., (2004), "Nosocomial Bloodstream Infections in US Hospitals: Analysis of 24,179 Cases from a Prospective Nationwide Surveillance Study", *Clinical Infectious Diseases*, Volume 39/3, 309-317.

YAPAR, Nur, (2014), "Epidemiology and risk factors for invasive candidiasis", *Therapeutics and Clinical Risk Management*, Volume 10, 95-105.

USE OF SONOGASHIRA CARBON-CARBON COUPLING TO GIVE WAY TO NEW PHTHALOCYANINE MACROCYCLES

Altuğ Mert Sevim[*] *& Barbaros Akkurt*[†]

Incorporating triphenylimidazole into a phthalonitrile

A research group from India has completed a reaction in which an alkyne-containing triphenylimidazole to a phthalonitrile, which was then turned into a phthalocyanine with a well-known reaction referred to as cyclotetramerization. In the reaction, they used 2-(4-ethynylphenyl)-1,4,5-triphenyl-1*H*-imidazole, 4-iodophthalonitrile, tris(dibenzylideneacetone) dipalladium(0), and triphenylarsine (see Figure 1). The solvent was tetrahydrofuran and the base was triethylamine. They refluxed the contents for four hours and finished the reaction (Bhattacharya *et al*., 2019).

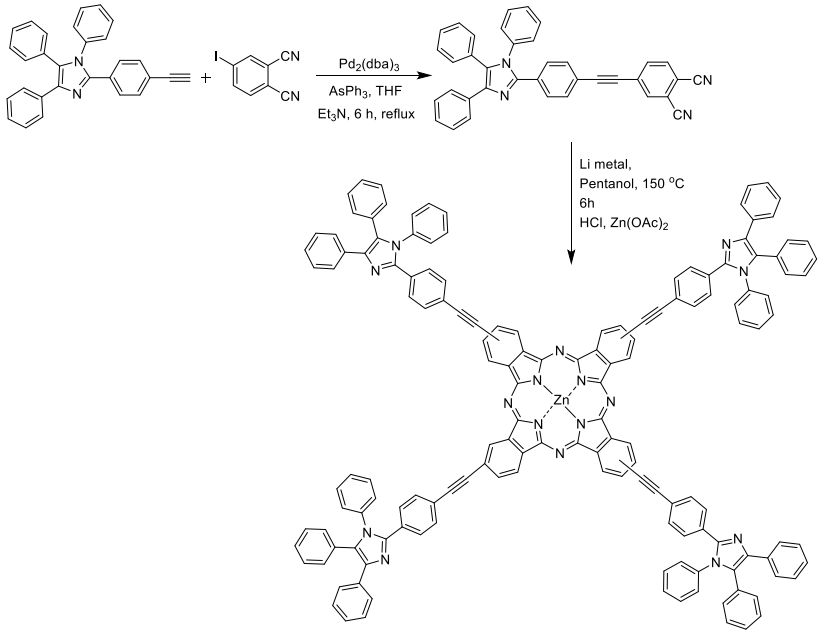

Figure 1. Synthetic route utilized for the preparation of the zinc phthalocyanine.

[*] (Assoc. Prof. Dr.). Istanbul Technical University, Faculty of Science and Letters, Department of Chemistry, 34469 Maslak, İstanbul – TURKEY. E-mail: sevim@itu.edu.tr.
[†] (Lecturer, PhD). Istanbul Technical University, Mustafa İnan Central Library, 34469 Maslak, İstanbul – TURKEY. E-mail: akkurtb@itu.edu.tr.

Coupling BODIPY to a phthalocyanine

Bizet and co-workers have studied a BODIPY-conjugated phthalocyanine. In their Sonogashira reaction, they reacted tetraiodophthalocyanine, alkyne-BODIPY, copper iodide, and tetrakis(triphenylphosphine)palladium(0) in tetrahydrofuran and triethylamine as the solvent/base pair (see Figure 2).

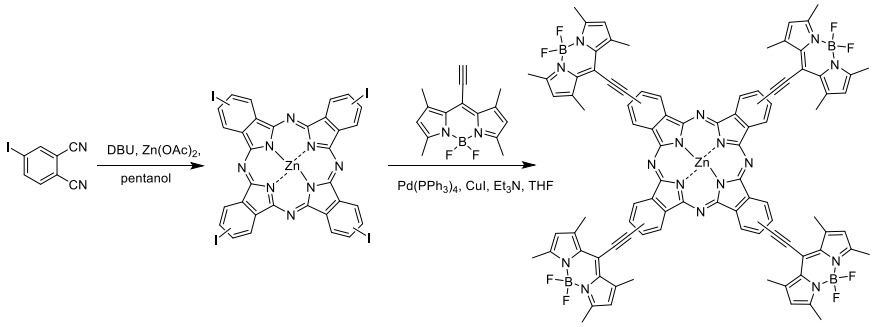

Figure 2. Synthesis of BODIPY-Pc conjugate via Sonogashira coupling between iodinated zinc(II)phthalocyanine and alkynyl-BODIPY.

Coupling a phthalocyanine to ethylene and devising a use in quantum dots (QD)

Blas-Ferrando and colleagues have devised a system in which they coupled iodotri-*tert*-butylphthalocyaninatozinc(II) to acetylthiophenylethyne, and the catalyst was bis(triphenylphosphine)palladium(II) chloride, with copper(I) iodide as the co-catalyst in the reaction. They reported a reaction yield of 41%, which is extraordinarily good for non-symmetrical phthalocyanines (Blas-Ferrando et al., 2015).

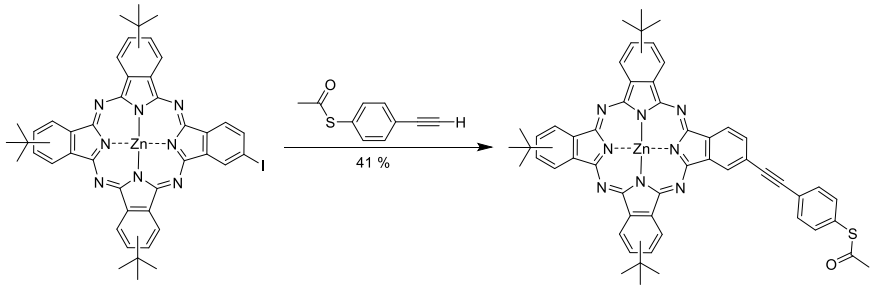

Figure 3. 23-[4-(acetylthio)phenylethynyl]-2,9,16-tri-tert-butylphthalocyaninatozinc (II).

Coupling of a phthalocyanine and buckminsterfullerene via an ethynyl bridge

Bottari and Torres have completed a synthetic scheme in which a non-symmetric tris(*tert*-butyl)iodophthalocyaninatozinc(II) and 4-ethynylbenzaldehyde were coupled in the presence of copper iodide, bis(triphenylphosphine)palladium(II) chloride as catalysts and triethylamine as the base and toluene as the solvent (see Figure 4). After coupling the ethynyl group to the phthalocyanine, it was then connected to the C_{60} in the presence of N-methylglycine in refluxing toluene (Bottari & Torres, 2010).

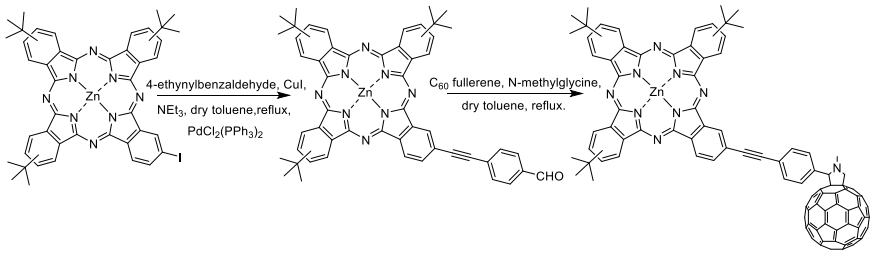

Figure 4. Synthesis of the structurally rigid Pc-C60 conjugate.

Deoxyribonucleotides coupled to phthalocyanines

Das and co-workers published a reaction in which they coupled deoxyribonucleosides to phthalocyanine molecules (see Figure 5). In a typical reaction, the deoxyribonucleoside, bis(triphenylphosphine)palladium(II) chloride, copper(I) iodide in THF, and trimethylamine as the base were reacted with 87% of yield (Das *et al.*, 2010).

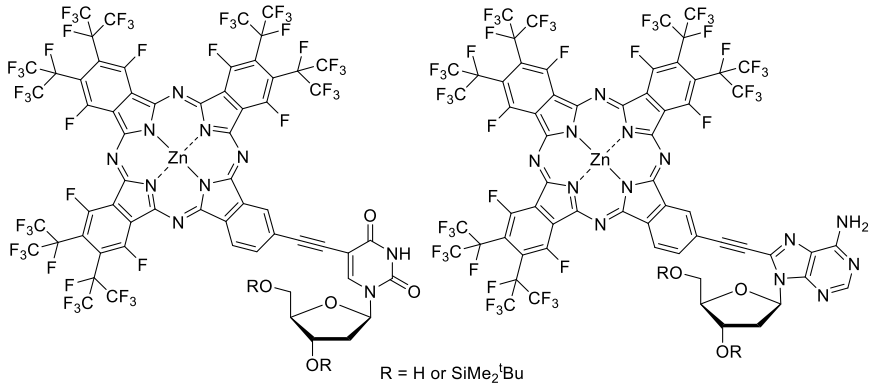

Figure 5. Structures of perfluoroisopropyl-Pc-deoxyribonucleoside conjugates.

A biotinylated phthalocyanine

Ghazal and co-workers reported a biotinylated phthalocyanine and its quaternized counterpart. Sonogashira reaction was performed by starting from 5-((3aR,6S,6aS)-hexahydro-2-oxo-1*H*-thieno[3,4-d] imidazole-6-yl)-*N*-(prop-2-ynyl)pentanamide and iodophthalocyanine. As the catalyst and co-catalyst, they used bis(triphenylphosphine)palladium(II) chloride and copper(I) iodide, respectively (Ghazal *et al.*, 2019).

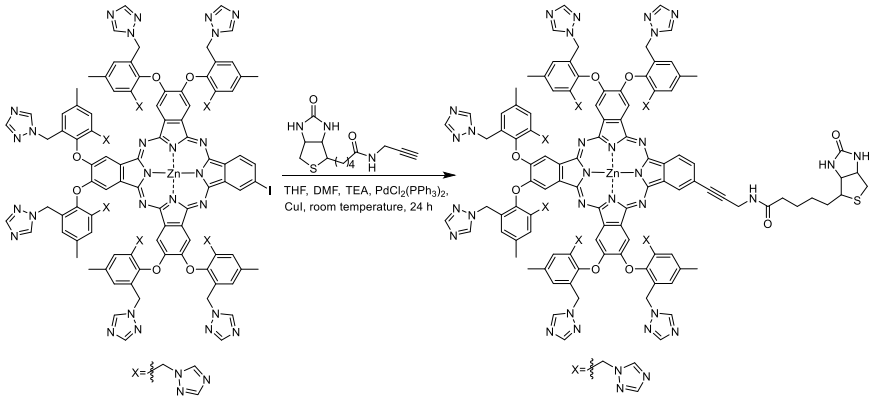

Figure 6. The synthetic route of the biotinylated zinc(II) phthalocyanine.

A reaction between propargyl alcohol and iodophthalocyanine

Langmar and colleagues prepared a propargylated phthalocyanine with a reaction between iodophthalocyanine and propargyl alcohol. The other groups on the phthalocyanine were 2-ethylhexyl. The alcohol group was oxidized to aldehyde with 2-iodoxybenzoic acid in the presence of DMSO/THF, and then the aldehyde group was reacted with H_3NSO_3 / H_2O then $NaClO_2$ to yield the carboxylic acid (Langmar *et al.*, 2015).

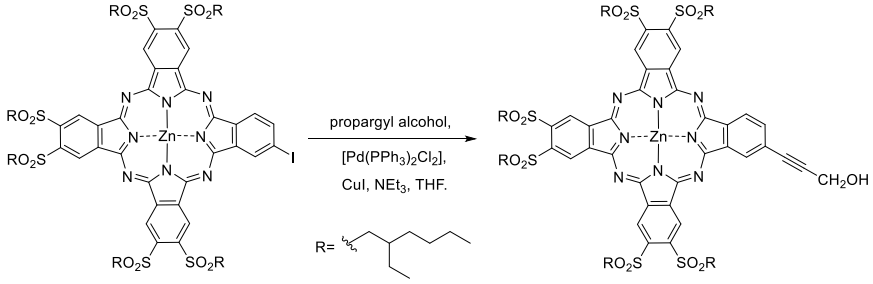

Figure 7. Synthesis of the zinc(II)phthalocyanine.

Electron-accepting dye-sensitized solar cells (DSSCs)

In the search for new electron-accepting dye-sensitized solar cells, Langmar and co-workers reported the syntheses of two compounds (see Figure 8). Being almost the same, the catalyst in the Sonogashira chemistry was tetrakis(triphenylphosphine)palladium(0), and the co-catalyst was copper(I) iodide as usual (Langmar *et al.*, 2019).

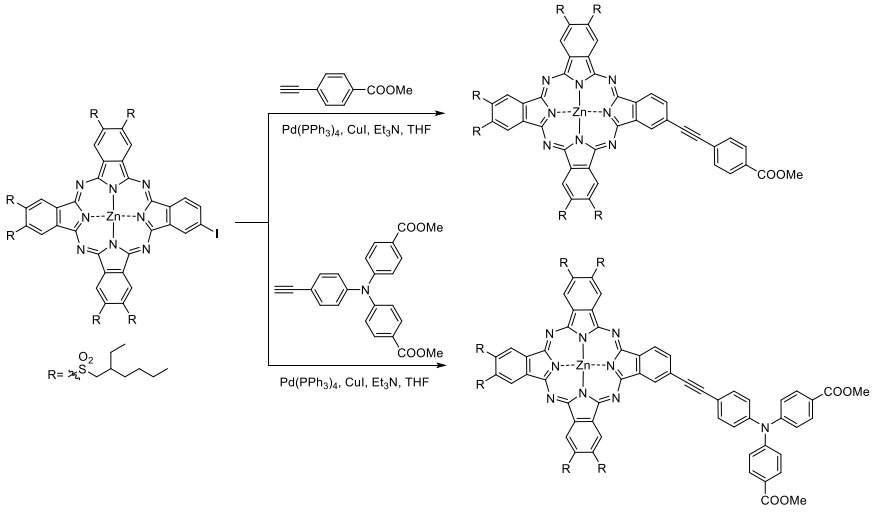

Figure 8. Synthesis of the zinc(II)phthalocyanines.

Ferrocenylcarborane-containing phthalocyanines

Nar and his colleagues prepared ferrocenylcarborane from a Sonogashira reaction of diiodobenzene and ethynylferrocene in trimethylamine and toluene, the catalysts being bis(triphenylphosphine)palladium(II) chloride and copper(I) iodide (see Figure 9). As a result, new carboranes on phthalocyanines were reported and they might find use in boron neutron capture therapy (Nar *et al.*, 2018).

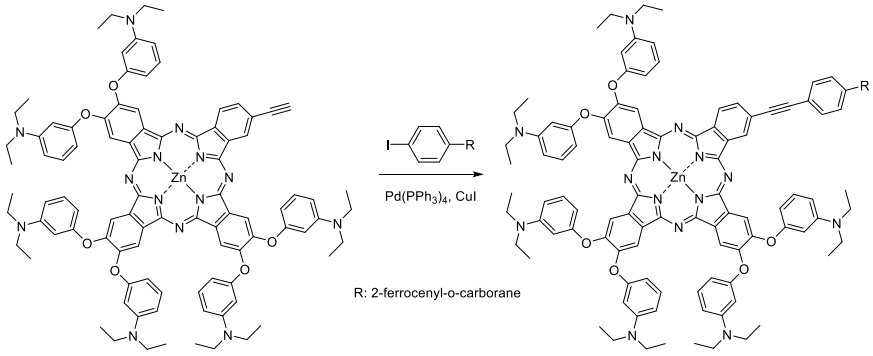

Figure 9. Synthetic route of the ferrocenylcarborane-substituted phthalocyanine.

Thiophene-containing phthalocyanines with an ethynyl linkage

Özçeşmeci and co-workers synthesized an octasubstituted phthalocyanine in which the alkynyl moiety contained a thiophene substitution. In the reaction, they reacted 3-alkynylthiophene and dichlorophthalonitrile in the presence of bis(triphenylphosphine)palladium(II) chloride, copper(I) iodide, triethylamine and the reaction time was 48 hours and the reaction temperature was 363 K. As stated before, chlorine groups are not reactive enough to induce ipso-type substitution of the alkyne and therefore, long reaction times and high temperatures were needed (see Figure 10). The reaction yield is not very high; 35% was reported (Özçeşmeci *et al.*, 2013).

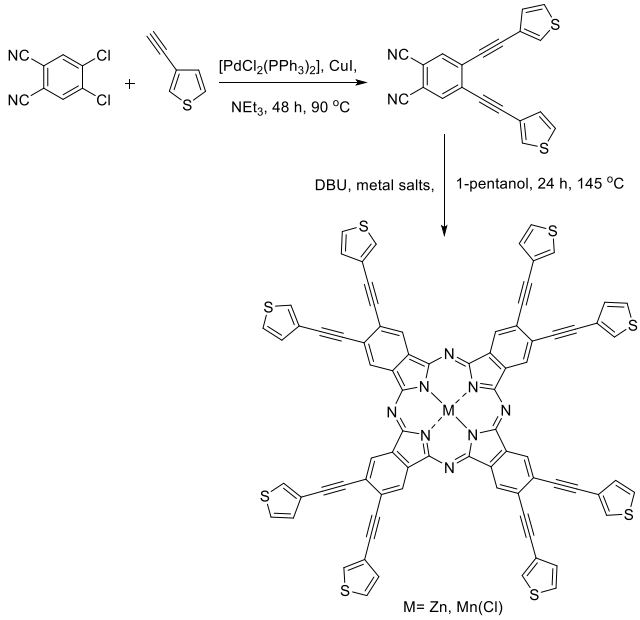

Figure 10. Synthesis of metallophthalocyanines.

Ethynyl-containing phthalocyanines

Pekbelgin *et al.* reported the synthesis, characterization, and related investigations of ethynyl-containing phthalocyanines (see Figure 11). They prepared the alkyne via the Corey-Fuchs synthesis and reacted with dibromophthalonitrile derivative with a Sonogashira reaction. In the reaction, the main and co-catalysts were bis(triphenylphosphine)palladium(II) chloride and copper(I) iodide, respectively. The base/solvent system was trimethylamine and tetrahydrofuran (Pekbelgin Karaoğlu *et al.*, 2019).

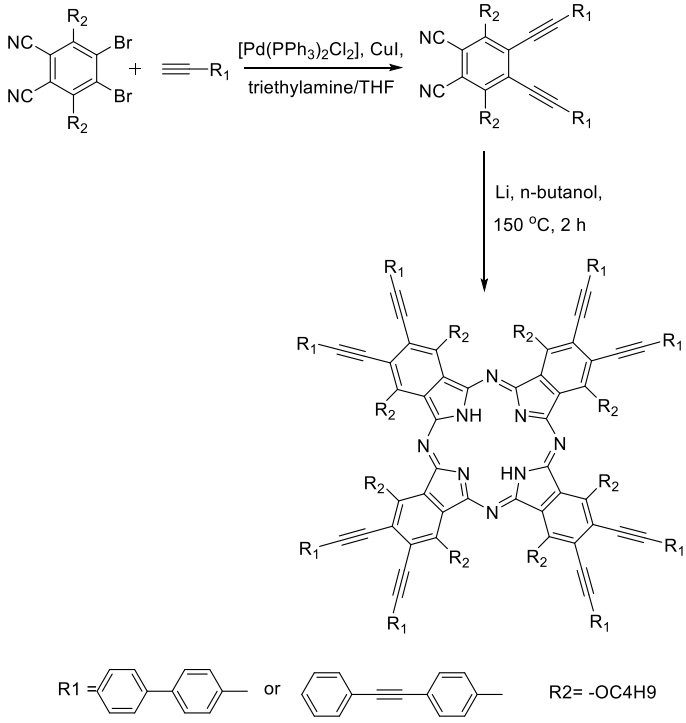

Figure 11. Synthesis of metal-free phthalocyanines.

Another study of our research group included a bis(trifluoromethyl)phenylethynyl-containing phthalocyanine. Sevim and co-workers first tried the Sonogashira reaction from 4-iodophthalonitrile and the alkyne to obtain the substituted phthalonitrile, but this compound failed to yield a phthalocyanine. As an alternative route, they reacted peripherally substituted tetraiodophthalocyanine with the alkyne and successfully prepared the alkyne-substituted phthalocyanine (see Figure 12). The reaction conditions are as follows: bis(triphenylphosphine)palladium(II) chloride, copper(I) iodide, trimethylamine, room temperature for 24 hours under nitrogen. The reaction yield was found to be 71% (Sevim *et al.*, 2013).

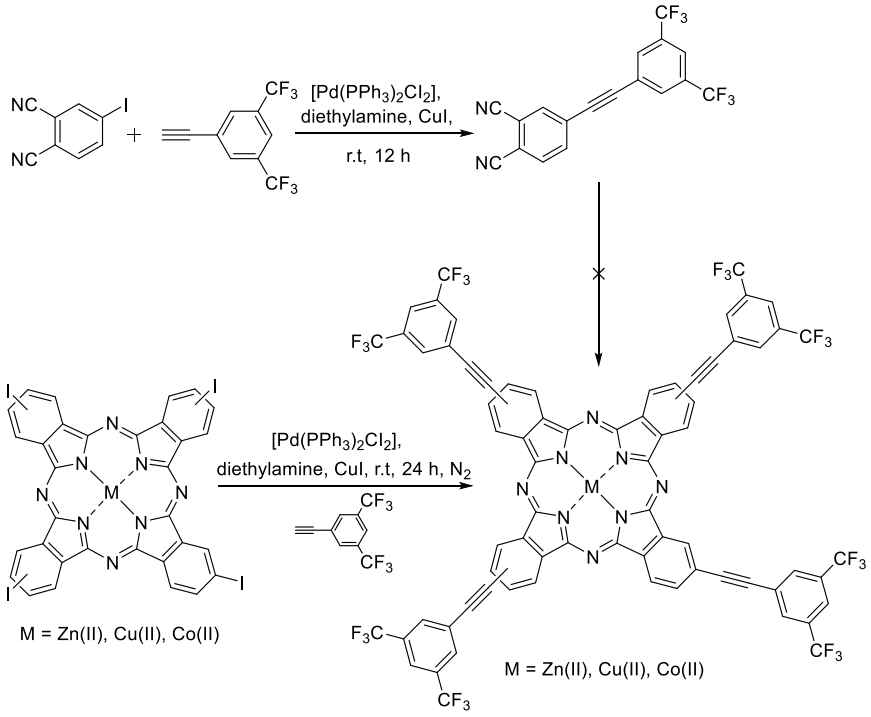

Figure 12. Synthesis route of targeted metallophthalocyanines.

Phthalocyanines for imaging purposes

Ranyuk and colleagues prepared DOTA and NOTA-containing zinc phthalocyanine conjugates for imaging purposes. In the synthetic part, they prepared tris(sodium sulfonate) iodophthalocyanine and reacted with an alkyne derivative. An interesting part in the synthesis is that they did not use the copper co-catalyst. They used palladium(II) acetate along with tris(o-tolyl)phosphine as the catalytic entity, diisopropyl ethylamine as the base, N,N-dimethylformamide as the solvent, at 343 K for 2 hours (see Figure 13). They then prepared the ^{68}Ga and ^{64}Cu-containing conjugates for imaging (Ranyuk *et al.*, 2013).

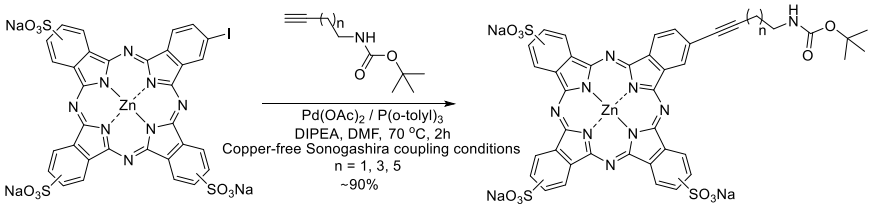

Figure 13. Synthesis of zinc(II)phthalocyanines.

Binaphthyl-bridged chiral phthalocyanines

Revuelta-Maza and co-authors synthesized binaphthyl-bridged chiral phthalocyanines from a series of phthalonitriles. To prepare the BINOL-type compound, the dibromo-BINOL was reacted with *tert*-butyl dimethylsilylacetylene in the presence of bis(triphenylphosphine)palladium(II) and copper(I) iodide as catalysts and triethylamine as the base. The reaction was conducted at 333 K for 4 hours (see Figure 14). (Revuelta-Maza *et al.*, 2019)

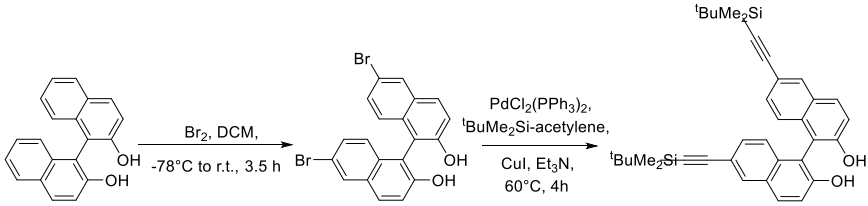

Figure 14. Functionalization of BINOL-type molecule with an alkyne fragment.

A reaction between tetraiodophthalocyaninatozinc(II) and ethynylpyridine

A research group from Spain worked on a zinc(II) phthalocyanine and its synthesis proceeded by the reaction of tetraiodophthalocyanine, 4-ethynylpyridine, and bis(triphenylphosphine)palladium(II) chloride and copper(I) iodide as the main catalyst and co-catalyst, respectively, and diisopropylamine was used as the solvent and the reaction content was stirred at 343 K overnight under Ar (see Figure 15) (Revuelta-Maza *et al.*, 2020).

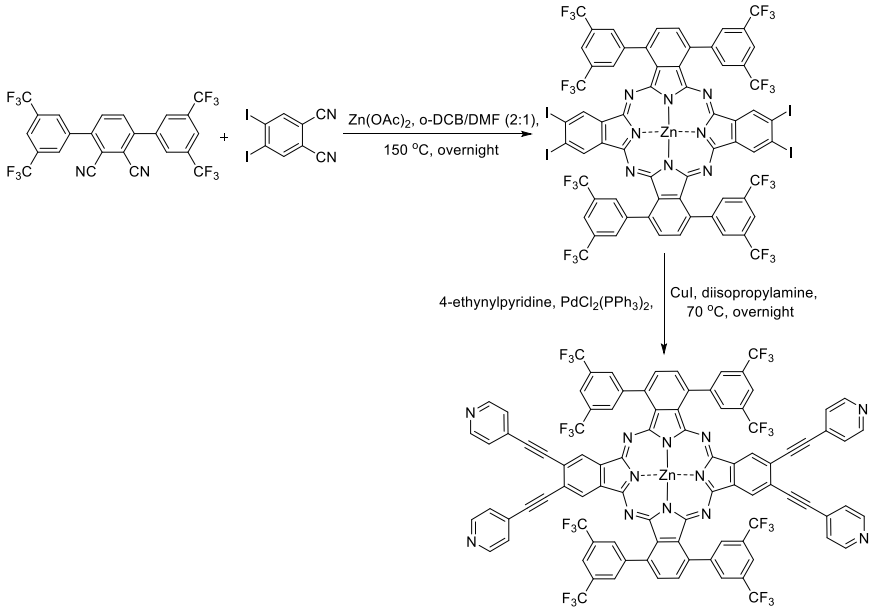

Figure 15. The synthesis of pyridyl-substituted ZnPcs.

Another ethynyl-bridged phthalocyanine

Schierl *et al.* prepared a phthalocyanine with ethynyl bridges, starting from tris(*tert*-butyl)iodo-substituted zinc(II) phthalocyanine and bis-sethynyl cyclopenta[hi]aceanthrylene structures (see Figure 16). The synthesis was performed with the phthalocyanine as the substrate, bis(triphenylphosphine)palladium(II) chloride, copper(I) iodide as catalysts, potassium carbonate and pyridine as the bases, then bis(trimethylsilylethynyl)cyclopenta[hi]aceanthrylene was introduced and the reaction was continued for 24 h at room temperature, yielding a green-colored solid at 61% yield (Schierl *et al.*, 2019).

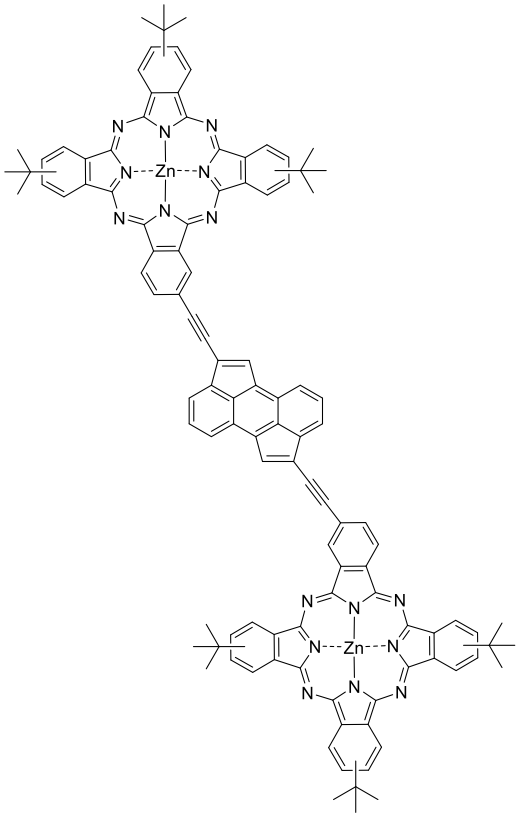

Figure 16. Molecular structure of the cyclopenta[hi]aceanthrylene -based phthalocyanine derivative.

Melamine-containing phthalocyanines

In an attempt to furnish melaminyl-containing phthalocyanines, 2,4-bis(octylamino)-6-ethynyl-1,3,5-triazine was reacted with tris(*tert*-butyl)iodophthalocyanine (substituents at peripheral positions) and as a catalyst, tetrakis(triphenylphosphine)palladium(II), as a co-catalyst, copper(I) iodide and as a base, trimethylamine was used (see Figure 17). The solvent was tetrahydrofuran (Seitz *et al.*, 2010).

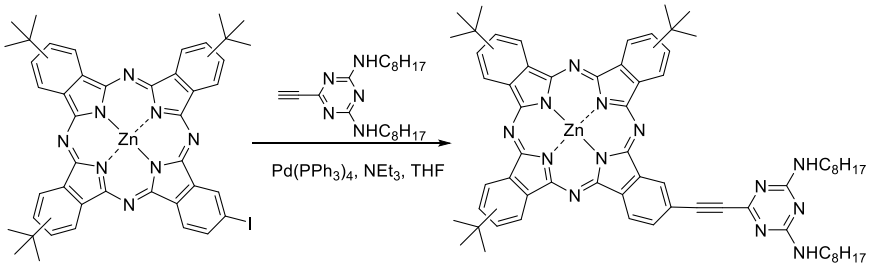

Figure 17. Synthesis of the melamine-functionalized phthalocyanine.

Carboxyl and alkynyl-containing phthalocyanines

Tejerina and her co-workers synthesized triiodohydroxymethylphthalocyanine at peripheral positions, and oxidized the hydroxymethyl group to aldehyde with 90% yield, 2-iodoxybenzene was the oxidant. Then, they carried out Sonogashira chemistry with bis(triphenylphosphine)palladium(II) chloride as the main catalyst, copper(I) iodide as the co-catalyst, and tetrahydrofuran/triethylamine as the solvent/base system. The alkyne was 2,6-bis(4-biphenyl)-4-methylethynylbenzene and the reaction proceeded with 70% yield (see Figure 18). The resulting structure was tested as a potential dye sensitized solar cell material (Tejerina *et al.*, 2016).

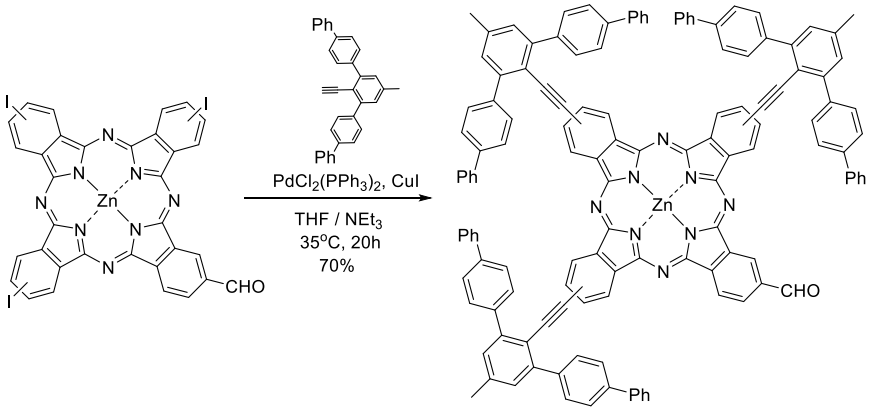

Figure 18. Convergent synthesis of β-triarylalkynyl-substituted ZnPc by triple Sonogashira coupling reaction.

Phthalocyanines containing propargyl-PEGME-2000

Uslan and her colleagues performed a synthesis in which they reacted tetraiodophthalocyaninatozinc (II), propargyl PEGME-2000, bis(triphenylphosphine)palladium(II) chloride, and copper(I) iodide to give the Sonogashira-coupled zinc(II) phthalocyanine in 84% yield (see Figure 19).

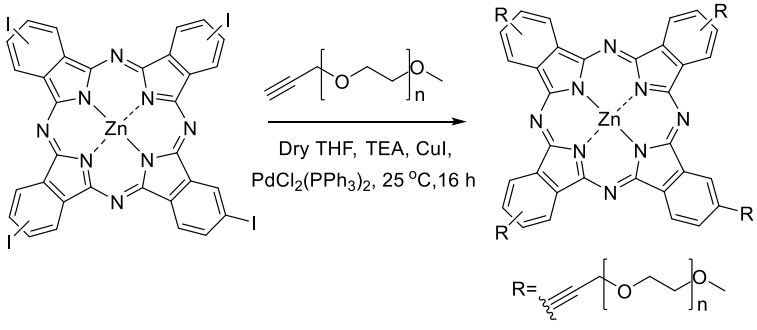

Figure 19. Synthetic pathway of the zinc(II)phthalocyanine substituted with PEGME-2000 block.

A series of BODIPY-containing zinc(II) phthalocyanines

Yanık and her co-workers synthesized a series of BODIPY-containing zinc(II) phthalocyanines. The Sonogashira conditions were the same, they used bis(triphenylphosphine)palladium(II) chloride as 5 mol% per halide moiety in tetraiodophthalocyaninatozinc(II), tetrahydrofuran/triethylamine (3:1) as the solvent/base pair, at 343 K to give BODIPY-containing phthalocyanines around 50-70% yields (see Figure 20). The photophysical and photochemical investigations were reported (Yanık *et al.*, 2016).

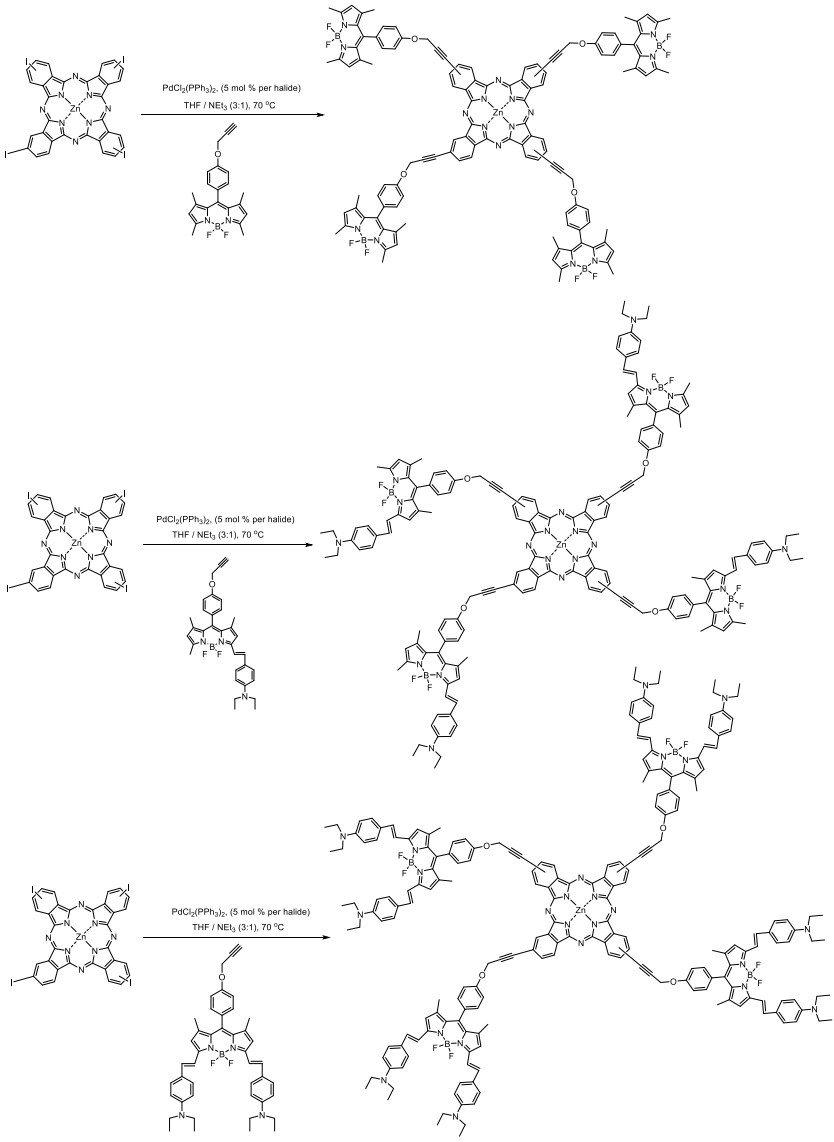

Figure 20. Synthetic route of phthalocyanine–BODIPY conjugates.

Palladium(II) phthalocyanine and porphyrin complexes as substitute catalysts in Sonogashira reaction

A very interesting example was published by Platonova and her coworkers, in which they prepared a palladium phthalocyanine as a substitute for palladium phosphine complexes in the Sonogashira reaction. Octamethoxy, octaethoxy, octabutoxy, and octaphenoxy phthalonitriles substituted at the peripheral positions led to Pd(II) phthalocyanines which were

tested in example Sonogashira reactions, they reacted bromobenzene with ethynylbenzene in a series of Pd catalysts including palladium(II) acetate, bis(acetonitrile)palladium(II) chloride, bis(triphenylphosphine)palladium(II) chloride, octasubstituted Pd(II) phthalocyanine, and tetraphenylporphyrin Pd(II) complex. With triethylamine as the base, the conversion was 68% and the yield was 65%, whereas *i*-dipropyl ethylamine as the base, the conversion was 71% and the yield was 66% (see Figure 21). It can be theorized that the bulkiness of the base increased the conversion, but almost no change was observed in the reaction yield (Platonova *et al.*, 2019).

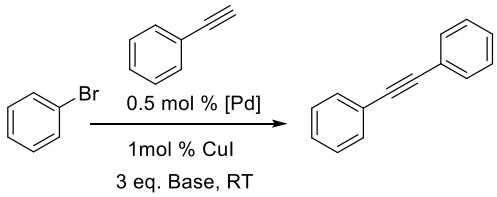

Figure 21. Reaction parameters for Sonogashira reaction catalyzed by PcPd or PdTPP.

In another trial, substituted bromobenzenes were reacted with ethynylbenzene, in the presence of 0.5 mol% octaphenoxyphthalocyaninatopalladium(II), 1 mol% copper(I) iodide, 3 equivalents of base in tetrahydrofuran, room temperature for 8 hours. The reaction yields were in the range of 64-72% (Platonova *et al.*, 2019).

Conclusion

To sum up, when researchers wish to include alkynyl bridges to their structures, they first prepare an iodine-derivative of their molecules. They react this iodine-containing molecule with an alkynyl derivative in the presence of a palladium complex like bis(triphenylphosphine)palladium(II) chloride or a simple palladium compound like palladium(II) acetate as the main catalytic entity. Copper(I) iodide is used as the auxiliary catalyst to speed up the reaction (in some cases, it was not used if the reaction was already quite fast). There was a base like triethylamine and/or potassium carbonate to capture the mineral acid (HI for most of the cases; when aryl bromides are used, HBr is produced, when, rarely indeed, aryl chlorides are used, HCl is produced). The reaction yields are often very promising, around 60-90%. Fourier transform infrared spectroscopy is used as an indispensable tool to check if the targeted molecule has alkynyl bridges, a peak around 2200 cm^{-1} tells us that the alkynyl moiety has successfully been introduced onto the main framework. There are rare studies in which a different strategy was used in place of the main catalyst, metallophthalocyanines and metalloporphyrins were employed. We consider

that this kind of studies should increase, because there might be very promising phthalocyanine and porphyrin catalysts waiting for use. It is hoped that we will see more of these examples we covered here in the future.

Acknowledgments

The authors are indebted to Prof. Dr. Mehmet ALTUN for his kind help in reading the drafts.

References

BHATTACHARYA, S., BISWAS, C., RAAVI, S. S. K., VENKATA SUMAN KRISHNA, J., KOTESHWAR, D., GIRIBABU, L., & VENUGOPAL RAO, S. (2019). "Optoelectronic, femtosecond nonlinear optical properties and excited state dynamics of a triphenyl imidazole induced phthalocyanine derivative". *RSC Advances*, 9(63), pp. 36726–36741. https://doi.org/10.1039/C9RA07758H

BLAS-FERRANDO, V. M., ORTIZ, J., GONZÁLEZ-PEDRO, V., SÁNCHEZ, R. S., MORA-SERÓ, I., FERNÁNDEZ-LÁZARO, F., & SASTRE-SANTOS, Á. (2015). "Synergistic interaction of dyes and semiconductor quantum dots for advanced cascade cosensitized solar cells". *Advanced Functional Materials*, 25(21), pp. 3220–3226. https://doi.org/10.1002/adfm.201500553

BOTTARI, G., & TORRES, T. (2010). "Towards Collective Physical Properties in Supramolecular Organized Phthalocyanine-C60 Fullerene Conjugates". *Macroheterocycles*, 3(1), pp. 16–18.

CHINCHILLA, R., & NÁJERA, C. (2007). "The Sonogashira Reaction: A Booming Methodology in Synthetic Organic Chemistry". *Chemical Reviews*, 107(3), pp. 874–922. https://doi.org/10.1021/cr050992x

DAS, B., TOKUNAGA, E., TANAKA, M., SASAKI, T., & SHIBATA, N. (2010). "Perfluoroisopropyl Zinc Phthalocyanines Conjugated with Deoxyribonucleosides: Synthesis, Photophysical Properties and In Vitro Photodynamic Activities". *European Journal of Organic Chemistry*, 2010(15), pp. 2878–2884. https://doi.org/10.1002/ejoc.201000179

GHAZAL, B., KAYA, E. N., HUSAIN, A., GANESAN, A., DURMUŞ, M., & MAKHSEED, S. (2019). "Biotinylated-cationic zinc(II) phthalocyanine towards photodynamic therapy". *Journal of Porphyrins and Phthalocyanines*, 23(01n02), pp. 46–55. https://doi.org/10.1142/S1088424618501158

LANGMAR, O., FAZIO, E., SCHOL, P., de la TORRE, G., COSTA, R. D., TORRES, T., & GULDI, D. M. (2019). "Controlling Interfacial Charge Transfer and Fill Factors in CuO-based Tandem Dye-Sensitized

Solar Cells". *Angewandte Chemie International Edition*, 58(12), pp. 4056–4060. https://doi.org/10.1002/anie.201812397

LANGMAR, O., GANIVET, C. R., LENNERT, A., COSTA, R. D., de la TORRE, G., TORRES, T., & GULDI, D. M. (2015). "Combining Electron-Accepting Phthalocyanines and Nanorod-like CuO Electrodes for p-Type Dye-Sensitized Solar Cells". *Angewandte Chemie International Edition*, 54(26), pp. 7688–7692. https://doi.org/10.1002/anie.201501550

NAR, I., ATSAY, A., ALTINDAL, A., & HAMURYUDAN, E. (2018). "*O* -Carborane, Ferrocene, and Phthalocyanine Triad for High-Mobility Organic Field-Effect Transistors". *Inorganic Chemistry*, 57(4), pp. 2199–2208. https://doi.org/10.1021/acs.inorgchem.7b03097

ÖZÇEŞMECİ, İ., KALKAN BURAT, A., İPEK, Y., KOCA, A., & ALTUNTAŞ BAYIR, Z. (2013). "Synthesis, electrochemical and spectroelect-rochemical properties of phthalocyanines having extended π-electrons conjugation". *Electrochimica Acta*, 89, pp. 270–277. https://doi.org/10.1016/j.electacta.2012.11.015

PEKBELGİN KARAOĞLU, H., ATSAY, A., NAR, I., MCKEE, V., KOÇAK, M. B., HAMURYUDAN, E., & GÜL, A. (2019). "Near-infrared absorbing π-extended hexadeca substituted phthalocyanines". *Journal of Molecular Structure*, 1197, pp. 736–741. https://doi.org/10.1016/j.molstruc.2019.07.086

PLATONOVA, Y. B., VOLOV, A. N., & TOMILOVA, L. G. (2019). "Palladium(II) octaalkoxy- and octaphenoxyphthalocyanines: Synthesis and evaluation as catalysts in the Sonogashira reaction". *Journal of Catalysis*, 373, pp. 222–227. https://doi.org/10.1016/j.jcat.2019.04.003

RANYUK, E., LEBEL, R., BÉRUBÉ-LAUZIÈRE, Y., KLARSKOV, K., LECOMTE, R., van LIER, J. E., & GUÉRIN, B. (2013). "^{68} Ga/DOTA- and ^{64} Cu/NOTA-Phthalocyanine Conjugates as Fluorescent/PET Bimodal Imaging Probes". *Bioconjugate Chemistry*, 24(9), pp. 1624–1633. https://doi.org/10.1021/bc400257u

REVUELTA-MAZA, M. Á., GONZÁLEZ-JIMÉNEZ, P., HALLY, C., AGUT, M., NONELL, S., de la TORRE, G., & TORRES, T. (2020). "Fluorine-substituted tetracationic ABAB-phthalocyanines for efficient photodynamic inactivation of Gram-positive and Gram-negative bacteria". *European Journal of Medicinal Chemistry*, 187, 111957. https://doi.org/10.1016/j.ejmech.2019.111957

REVUELTA-MAZA, M. Á., TORRES, T., & TORRE, G. de la. (2019). "Synthesis and Aggregation Studies of Functional Binaphthyl-Bridged

Chiral Phthalocyanines". *Organic Letters*, 21(20), pp. 8183–8186. https://doi.org/10.1021/acs.orglett.9b02718

SCHIERL, C., ALEX, W., MATEO, L. M., BALLESTEROS, B., SHIMIZU, D., OSUKA, A., TORRES, T., GULDI, D. M., & BOTTARI, G. (2019). "Quadrupolar Cyclopenta[*hi*]aceanthrylene-Based Electron Donor-Acceptor-Donor Conjugates: Charge Transfer versus Charge Separation". *Angewandte Chemie International Edition*, 58(41), pp. 14644–14652. https://doi.org/10.1002/anie.201906206

SEITZ, W., JIMÉNEZ, Á. J., CARBONELL, E., GRIMM, B., RODRÍGUEZ-MORGADE, M. S., GULDI, D. M., & TORRES, T. (2010). "Synthesis and photophysical properties of a hydrogen-bonded phthalocyanine–perylenediimide assembly". *Chem. Commun.*, 46(1), pp. 127–129. https://doi.org/10.1039/B921363E

SEVİM, A. M., YENİLMEZ, H. Y., & ALTUNTAŞ BAYIR, Z. (2013). "Synthesis and photophysical properties of novel (trifluoromethyl)phenylethynyl-substituted metallophthalocyanines". Polyhedron, 62, pp. 120–125. https://doi.org/10.1016/j.poly.2013.06.037

TEJERINA, L., CABALLERO, E., MARTÍNEZ-DÍAZ, M. V., NAZEERUDDIN, M. K., GRÄTZEL, M., & TORRES, T. (2016). "Introducing rigid π-conjugated peripheral substituents in phthalocyanines for DSSCs". *Journal of Porphyrins and Phthalocyanines*, 20(08n11), pp. 1361–1367. https://doi.org/10.1142/S1088424616501121

YANIK, H., GÖKSEL, M., YEŞİLOT, S., & DURMUŞ, M. (2016). "Novel phthalocyanine–BODIPY conjugates and their photophysical and photochemical properties". *Tetrahedron Letters*, 57(26), pp. 2922–2926. https://doi.org/10.1016/j.tetlet.2016.05.080

ON THE HECK REACTION: A LITERATURE SURVEY WITH SOME ARTICLES IN 2020

Altuğ Mert Sevim [*] ***& Barbaros Akkurt*** [†]

Heck reaction is a universal coupling reaction, allowing carbon-carbon coupling, a hard to achieve thing otherwise. It uses palladium complexes as catalysts and some base and high temperature, resulting with high reaction yields. In this study, we introduce the readers to the concept of Heck chemistry, founded by Dr. Richard Fred Heck in 1972 (passed away in 2015), a Nobel Laureate in 2010. There have appeared many variations of this coupling, along with the original one (see Figure 1), and we tried to summarize them. Due to space limitations, we selected some important publications that appeared in 2020.

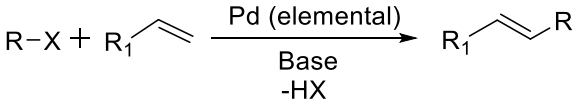

Figure 1. A simplified version of Heck (or Mizoroki-Heck) reaction (Anonymous, 2020).

Decarboxylative Heck-type reaction

Benzoic acids that are rich in electrons are found to undergo a decarboxylation catalyzed by Pd(II). The authors studied a group of electron-rich benzoic acids with ethyl-2-methoxyacrylate. The authors also reported that high steric hindrance and a high coordination of palladium with oxygen reduced the overall performance of this Heck coupling type (see Figure 2; Hachem et al., 2020).

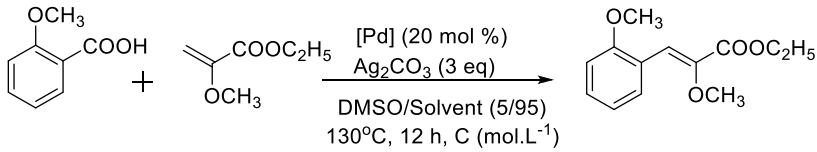

Figure 2. 2-Methoxyacrylate undergoes a decarboxylative Heck reaction; an optimization of conditions are given in the figure.

[*] (Assoc. Prof. Dr.); İstanbul Technical University, Faculty of Science and Letters, Department of Chemistry, Laboratory of Inorganic Chemistry 34469 Maslak, İstanbul-TURKEY, e-mail: sevim@itu.edu.tr

[†] (Lecturer, PhD.); İstanbul Technical University, Mustafa İnan Central Library, 34469 Maslak, İstanbul, TURKEY. akkurtb@itu.edu.tr

Dienedioic acid has been found to serve as an excellent alternative to the preparation of dienes for polyenes. According to mechanistic studies, a Heck-decarboxylate coupling occurs, and the carboxylic group is a director; the reaction is promoted and regioselectivity is controlled (see Figure 3; Ke & Chen, 2020).

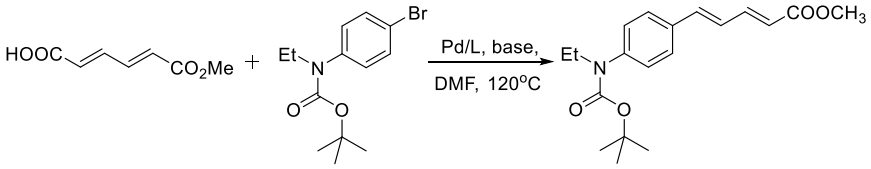

Figure 3. Optimization of the conditions for the reaction between 2,4-dienedioic acid and 4-bromophenyl ethyl *tert*-butyloxycarbonylamine.

Preparation of a reusable heterogeneous catalyst

Attapulgite, a natural clay, was used in a series of simple and green steps to form ATP-APTES-Pd heterogeneous catalysts. The prepared catalyst proved excellent for many instances of Suzuki and Heck cross-coupling reactions and the system did not contain any phosphine ligand. The removal of the catalyst is easy, it is stable, and without a deterioration of performance, it can be used several times (see Figure 4; Yang *et al.*, 2020).

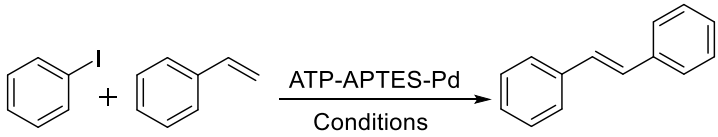

Figure 4. Optimization of the conditions of the reaction between iodobenzene and styrene.

A research group from Iran has shown that a cobalt-containing porous organic polymer (POP), which is high in nitrogen, was synthesized by the immobilization of cobalt onto the polymer. The resulting catalyst was effective in Heck and Sonogashira cross-coupling reactions, with the use of green media, and the reaction conditions are pretty mild. The catalyst is free from classical Heck phosphine ligands, copper, and the chief metal ion palladium, and is stable under the conditions tested, and could be re-used for at least eight runs without fouling (see Figure 5; Abdol R. Hajipour & Khorsandi, 2020).

A Chinese research group conducted a synthesis between magnetite and bis(triphenylphosphinomethyl)aminopropyl trimethylsilane and managed to anchor the organic molecule onto magnetite, leading to a magnetic

catalyst, then reacting with $PdCl_2$. As homogeneous catalysis has some disadvantages, the researchers decided to prepare a heterogeneous one. They conducted the main palladium-catalyzed couplings used in the polycondensations for conjugated polymers (see Figure 6; Zou *et al.*, 2020).

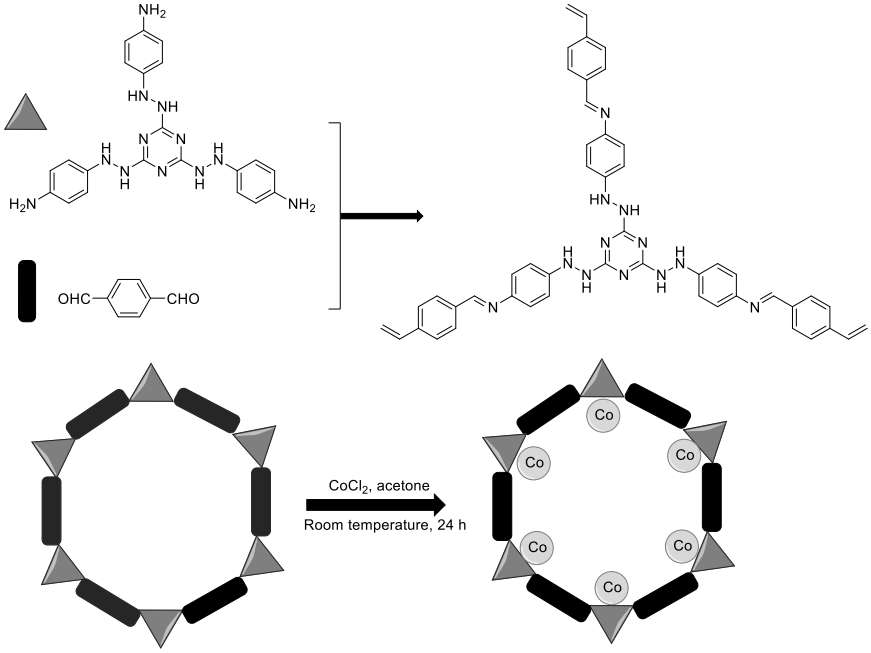

Figure 5. Syntheses of imine-POP and Co@imine-POP. POP stands for "porous organic polymer".

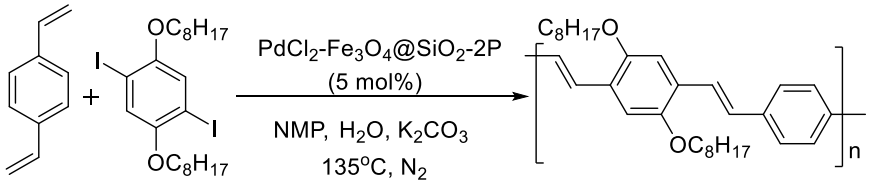

Figure 6. Synthesis of the polymer via C-C coupling with $PdCl_2$-Fe_3O_4@SiO_2-2P catalyst.

An Indian group of researchers started with TiO_2 powder, urea, and palladium acetate to obtain a Pd-C_3N_4@titanate nanotube to serve as a catalyst that is green, for Mizoroki-Heck and Suzuki-Miyaura C-C reactions in aqueous media, along with very high efficiency (> 99% product yield). The catalysts are usable for at least five repeating cycles. The process is green as water is used, with no leaching or agglomeration,

and fair recyclability, and reusability (see Figure 7 and 8; Velpula *et al.*, 2020).

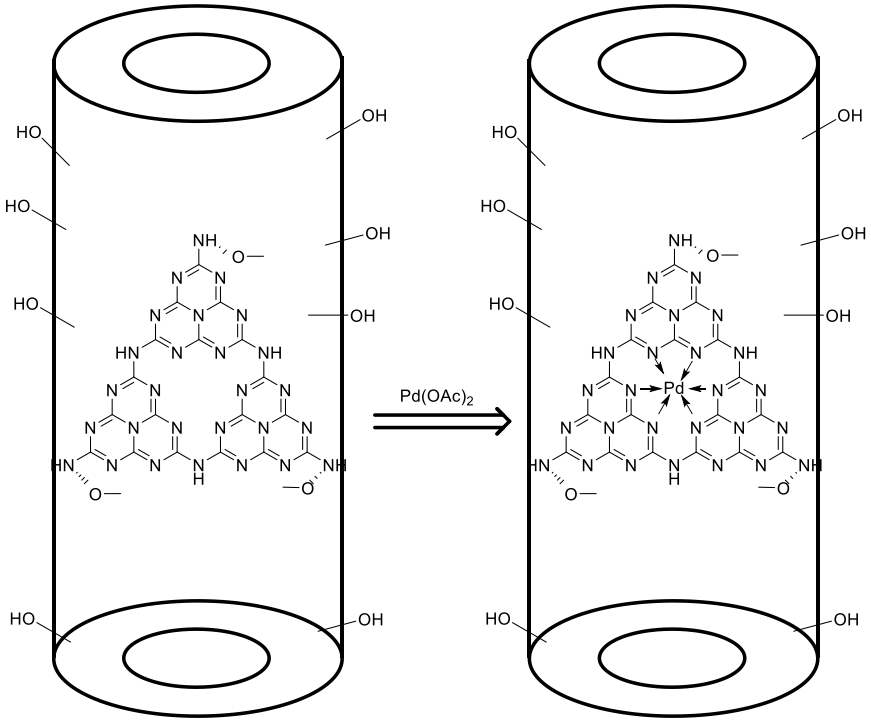

Figure 7. Schematic representation of Pd-C_3N_4@TNT structure.

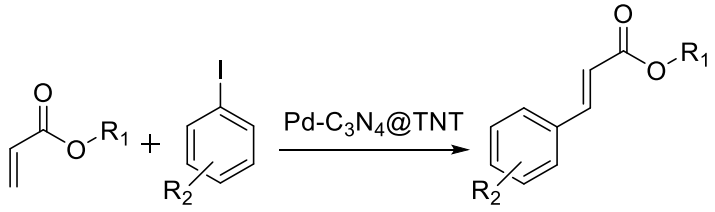

Figure 8. Heck reaction in which Pd–C_3N_4@TNT served as a catalyst.

Magnetite nanoparticles were coated and chemically modified to anchor hexamethylenetetramine to host Pd ions or Pd nanoparticles. The authors tried this catalyst for the reaction between 3-acrylomorpholine and iodobenzene, and the important parameters in catalysis (turnover number and turnover frequency) are better than those reported in the literature (see Figure 9; Rathod *et al.*, 2020).

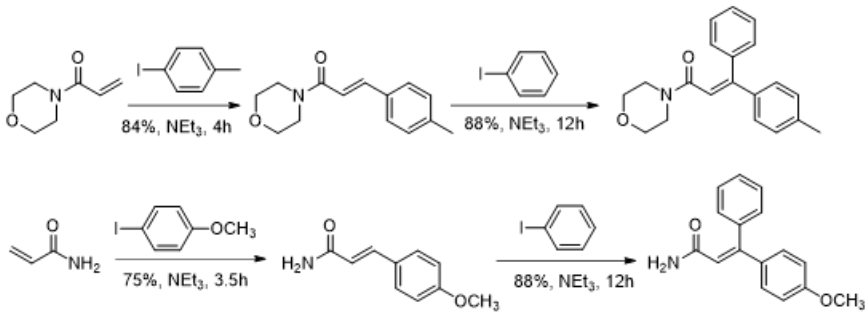

Figure 9. In the reaction, 1 mmol of aryl halide, 1 mmol of acrylate, 3 mmol of triethylamine, and 10 mg of Fe_3O_4@HMTA-(Pd^0) as catalyst were used at the temperature of 100 °C.

A group from India has realized to synthesize palladium on nanosilica over microsilica (Pd/SOS) spheres and used this as a scaffold to obtain ultra-small (about 2 nm) Pd NPs on these spheres. This material was used as a new catalyst for domino one-pot intramolecular Heck and intermolecular Sonogashira couplings. The heterogeneous catalyst was used up to five cycles with no marginal loss (see Figure 10; Lakshminarayana *et al.*, 2020).

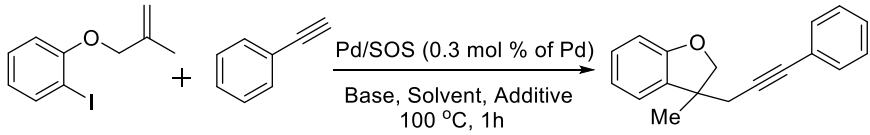

Figure 10. Formation of the Heck product.

A group of researchers from China has succeeded to prepare a heterogeneous catalyst of palladium produced from porous chitosan/reduced graphene oxide (RGO) microspheres. The performance of the catalyst is excellent in Heck coupling reactions (see Figure 11; X. Zheng *et al.*, 2020).

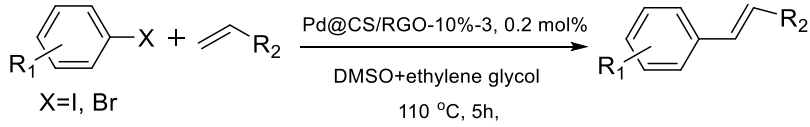

Figure 8. Heck reaction performance of aromatic halides and alkenes in the presence of the catalyst.

A group from Iran has conducted a method in which RGO was treated with H_2N-$(CH_2)_2$-NH-$(CH_2)_2$-NH_2 and then loaded with $H_2[PdCl_4]$ with a sonochemical procedure. The so-obtained heterogeneous catalyst's

performance was quite successful for the Mizoroki-Heck coupling, in which different alkenes were reacted with several aryl iodides. The reaction yields were moderate to excellent. Without a loss in catalytic activity, the obtained catalyst could serve for about six successive runs (see Figure 12; Mirza-Aghayan *et al.*, 2020).

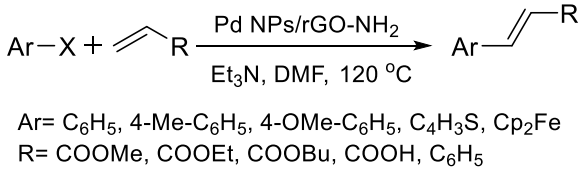

Figure 9. Iodo and bromo compounds and different alkenes catalyzed by heterogeneous PdNPs/rGO-NH_2 nanocomposite underwent Mizoroki-Heck coupling.

N-heterocyclic carbene-based catalyst in Heck-type reaction

A Turkish research group has prepared N-heterocyclic carbenes (NHC) from the reaction between (NHC)PdI_2(Py) with triphenylphosphine; an exchange occurred between pyridine and triphenylphosphine. The catalysts were used in the coupling of aryl bromides with styrene, and 80-100% catalytic conversions were achieved (see Figure 13; Erdemir *et al.*, 2020).

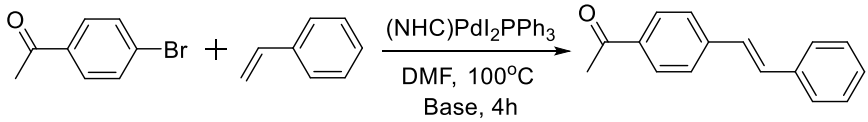

Figure 10. Use of an NHC-Pd as a catalyst in the Heck coupling.

Preparation of alkyl carboxylic acid derivatives

Organohalides were reacted with internal and terminal alkenes, aliphatic and unactivated, in high yield and the selectivities were completely of the anti-Markovnikov fashion. The process was applicable to drug synthesis and the directing group was removable. The structures were efficient hydride sources. Easily found starting materials led to more than one hundred remote carbo-functionalized alkyl carboxylic acid derivatives (see Figure 14; K. Zheng *et al.*, 2020).

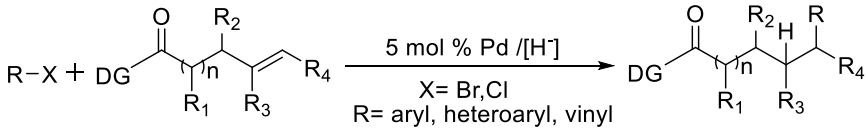

Figure 11. The reaction between organohalides and terminal and unactivated aliphatic alkenes.

Cyclization of an aldimine and subsequent Heck coupling

A cyclization followed by Heck C-C coupling was attempted by the authors (see Figure 15; Malunavar *et al.*, 2020). The authors provided a two-step procedure in a one-pot reaction scheme, starting from the aldimines, and they also showed the recycling or reuse of the ionic liquid.

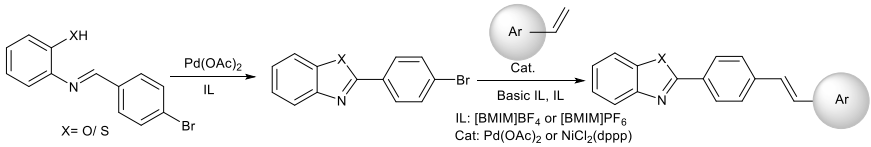

Figure 12. Heck coupling using palladium acetate or dichloro(dppp)nickel(II) chloride as catalyst.

An unexpected development

Under palladium-norbornene (Pd/NBE) catalysis, authors expected a Catellani product to form; however, as an unexpected development, an ortho-Heck product did occur. Also, a nonbornyl group was introduced into the ipso position. According to the observations, the authors proposed the 1,4-palladium migration followed by an intramolecular H-transfer pathway (see Figure 16; Rago & Dong, 2020).

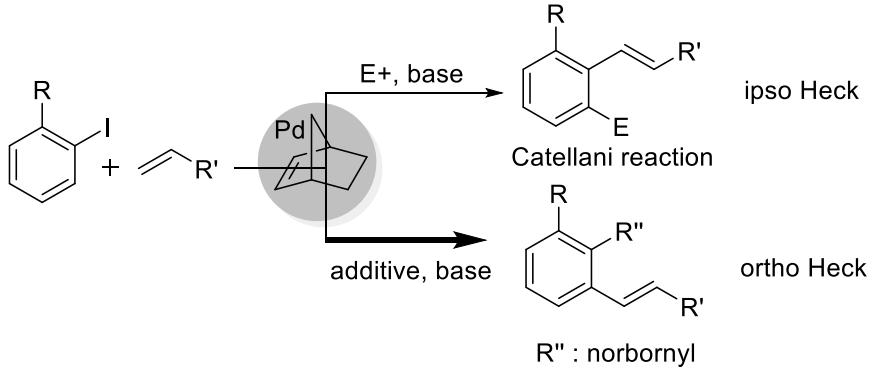

Figure 13. Unexpected formation of ortho-Heck product in which the catalyst is Pd-nonbornene complex.

A research group from Germany tested the Heck-conditions of (hetero)aryl bromides and several unsaturated molecules. The reaction was found to be a consecutive three- and *pseudo*-four-component synthesis (see Figure 17; Stephan *et al.*, 2020).

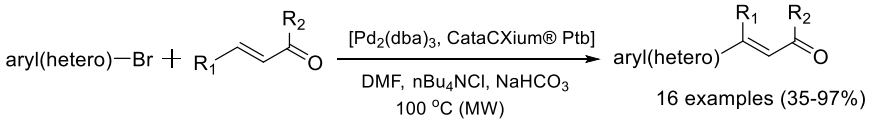

Figure 14. The Heck reaction between (hetero)aryl bromides and acrolein or vinyl ketones.

Polymerization studies

A Chinese research group has reported a stepwise Heck-type polymerization with the aid of visible light at ambient temperature. In the presence of light, the reaction proceeded well, indicating that blue light was necessary to promote the reaction between PEG and TBAB, and a larger molecular weight of polymer product was obtained (see Figure 18; He *et al.*, 2020).

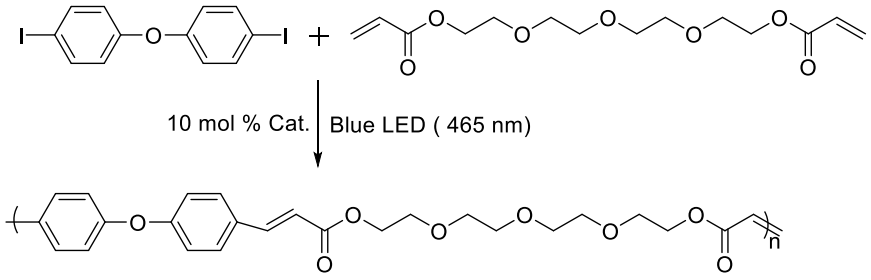

Figure 15. The monomers and polymer obtained with Mizoroki-Heck reaction in the presence of light.

Polymer-containing nitrogen-based ligand

Another Iranian group has created a polymer containing nitrogen-based ligand, in which they immobilized palladium nanoparticles, and tested the polymeric catalyst in some C-C coupling reactions (see Figure 19; Targhan *et al.*, 2020).

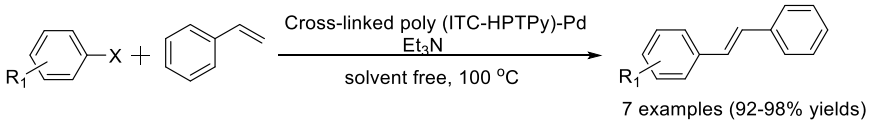

Figure 16. The cross-linked Mizoroki-Heck coupling reaction by using a polymer-Pd complex.

Dendrimeric cobalt-based catalyst

A research group from Bangladesh has investigated the Heck coupling reactions by a dendrimeric cobalt nanoparticle as the catalytic entity. They studied the catalytic reactions in tetrabutylammonium bromide solution to see excellent catalytic reactivity in a very short time of 45 minutes. It was also stated that the polymeric catalyst could be reused (see Figure 20; Islam & Mia, 2020).

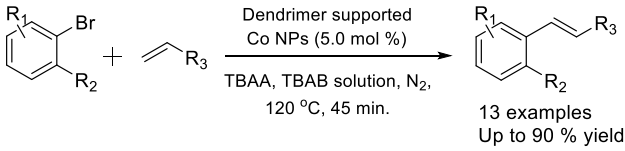

R_1 = H, o-CH_3, p-OCH_3, m-OCH_3, m-F, m-CH_3, m-NH_2, m-Cl, R_2 = H, OH, R_3 = Ph, CO_2Me, CO_2Bu, CO_2Et

TBAA= tetrabutylammonium acetate, TBAB= tetrabutylammonium bromide

Figure 20. A cobalt-based dendrimeric ligand used in Heck-type reaction.

An Iranian research group studied on magnetic chitosan as the base and cyanuric chloride/melamine as functionalizing material, and finally 5-bromo-2-hydroxybenzaldehyde/cyanuric chloride as another functionalizing material. They were able to host cobalt nanoparticles to work in Heck and C-N coupling reactions (only the former will be shown here) under mild reaction conditions and they were applied to a comparison of these two. The products were free of palladium/copper and phosphines and could be used for several times without experiencing a decline in activity (see Figure 21; Abdol Reza Hajipour *et al.*, 2020).

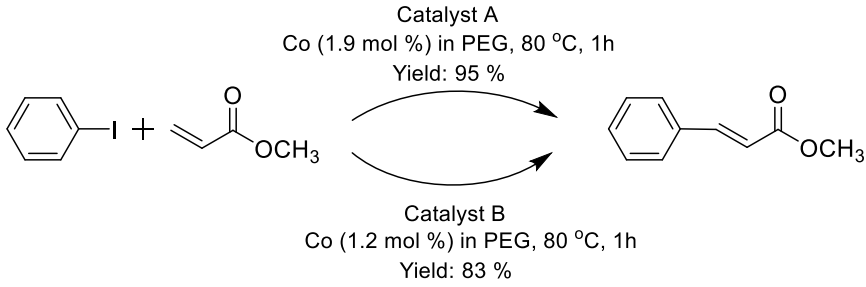

Figure 17. Catalytic activities of the tested catalyst (tri-s-triazine functionalized MNPs-chitosan, containing cobalt) for a Heck reaction.

A group from India has published a use of a polymer-palladium complex as the catalyst in Heck reaction. The reaction yield was around 96% and they used some activated alkenes and aryl halides. The catalyst

was easily removed, after the reaction, from the solution by simple filtration and was stable for about 5 runs (see Figure 22; Sruthi *et al.*, 2020).

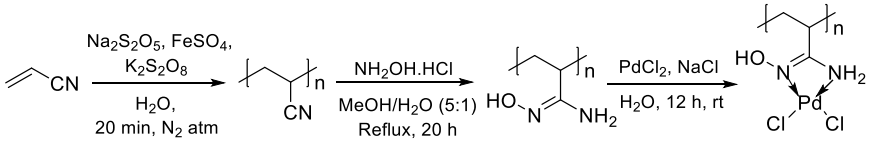

Figure 18. Synthesis of a m-PAN-Pd catalyst for Heck coupling.

A collaboration between Nigeria and Germany produced a fruitful work, in which a series of azo-palladium complexes were obtained for use in Heck coupling (see Figure 23; Oloyede *et al.*, 2020).

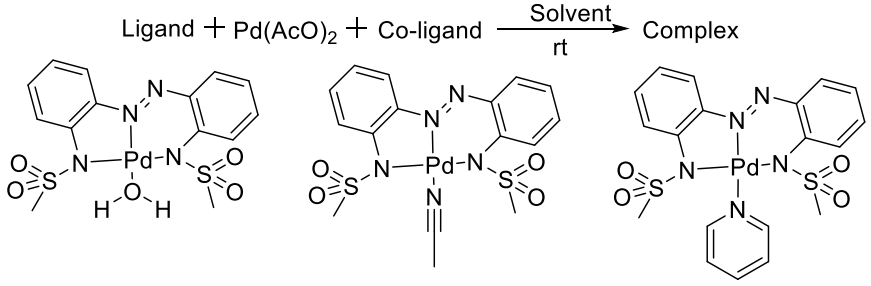

Figure 19. Preparation of the palladium complexes for Heck coupling.

Tang and coworkers have reported about the preparation of polycinnamamides through the reaction of aryl diiodides and bis(acrylamides), in DMF at 373 K and the catalyst was a bidentate phosphine-palladium complex anchored on magnetic nanoparticles (see Figure 24; Tang *et al.*, 2020). Due to the magnetic features, the catalyst could easily be separated from the medium and be used at least eight times without a decay in the catalytic activity.

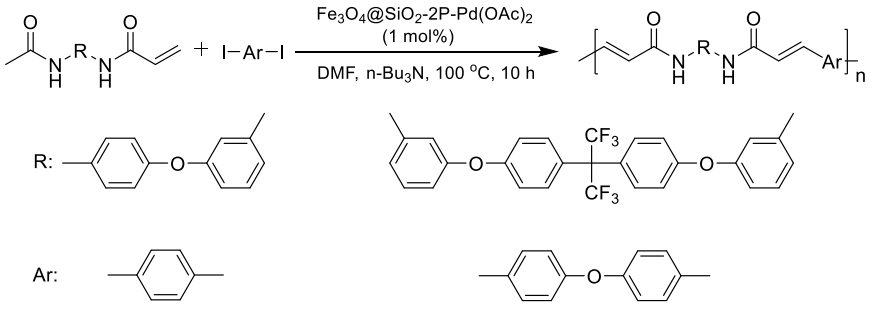

Figure 20. Reaction of bis(acrylamides) and aryl diiodidies.

A Hungarian group of researchers investigated the heterogenization of tetraamminepalladium(II) chloride complex on hydrophilic graphite oxide (GO) and prepared two different (2% and 5%) palladium contents of the catalyst. Tetrabutylammonium chloride (TBAC) yielded the highest conversions. They investigated the model reaction between styrene and bromobenzene. The conversions were around 96%. Both catalysts were usable around five times without a decay (see Figure 25; Mastalir *et al.*, 2020).

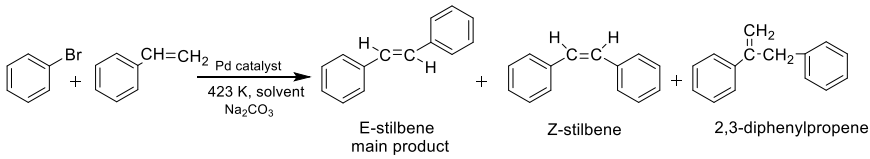

Figure 21. The Heck reaction of styrene with bromobenzene and the products obtained.

An Iranian research group has prepared a catalytic system with the reaction of melamine, formaldehyde and iron(III) chloride and then reacting with Pd(II). A model Heck reaction was investigated with this new catalyst (see Figure 26; Shahamat *et al.*, 2020). Computational methods were also employed to bring out the optimization of the reaction.

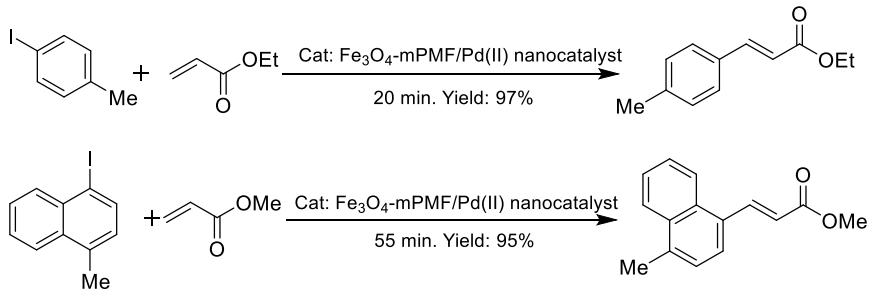

Figure 22. The use of the newly prepared catalyst in a classical Heck reaction.

Nuri and co-workers examined Mizoroki-Heck cross-coupling with a Pd(II)-supported, amino functionalized magnetic catalyst (see Figure 27; Nuri et al., 2020).

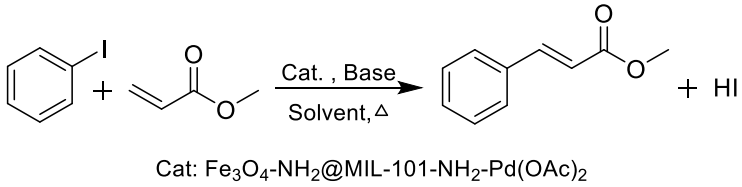

Figure 23. The reaction between methyl prop-2-enoate and iodobenzene in the presence of a catalyst in Heck conditions.

Boztepe and co-workers have reported PEPPSI[‡] and vinylimidazole (VI) based Pd-NHCs[§] and they also reported the presence of catalytic activity of these compounds in homogeneous Heck reaction. The novel complexes were converted into heterogeneous catalysts, in a reaction between acrylamide and 2-acrylamido-2-methylpropanesulfonic acid with free-radical polymerization (see Figure 28; Boztepe *et al.*, 2020).

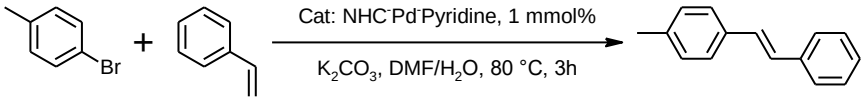

Figure 24. A model Heck reaction between aryl bromides and styrene, in the presence of the new catalyst.

An Iranian group of researchers has prepared a polymeric nanocatalyst to use in the Heck cross-coupling reaction. The new catalyst was phosphine-free, and the reaction times were extremely short (20 to 30 minutes), and the yields were excellent (75-93%). The catalysts were usable around ten cycles without the loss of catalytic activity (see Figure 29; Barazandehdoust *et al.*, 2020).

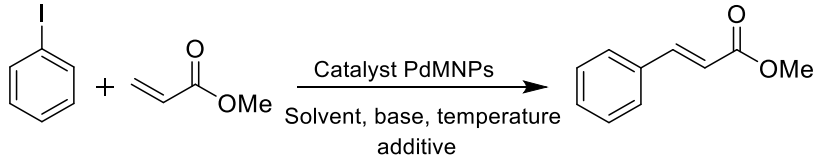

Figure 25. Reaction of iodobenzene and methyl 2-prop-2-enoate in Heck conditions.

[‡] pyridine-enhanced precatalyst preparation, stabilization, and initiation.
[§] palladium complexes of N-heterocyclic carbenes.

Hong and co-workers have reported about palladium nanoparticles on carbon nanospheres and their use in Heck coupling reaction (see Figure 30; Hong *et al.*, 2020).

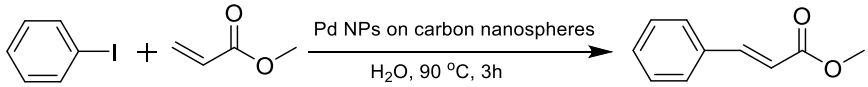

Figure 26. Heck reaction between methyl acrylate and aryl iodides.

Hong and co-workers devised a catalytic coupling reaction in which the catalyst was a heterogeneous Pd/N-doped CNT (see Figure 31; Hong *et al.*, 2020).

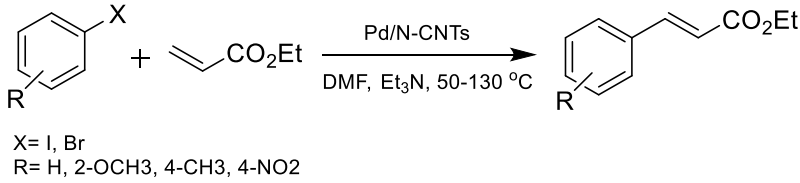

Figure 31. Use of the new Pd catalyst in the classical Heck reaction between ethyl acrylate with a series of aryl halides.

Lima and co-workers have shed light on thiosemicarbazone-containing Ni, Pd, and Pt complexes as potent catalysts in Heck reaction (see Figure 32; Lima *et al.*, 2020).

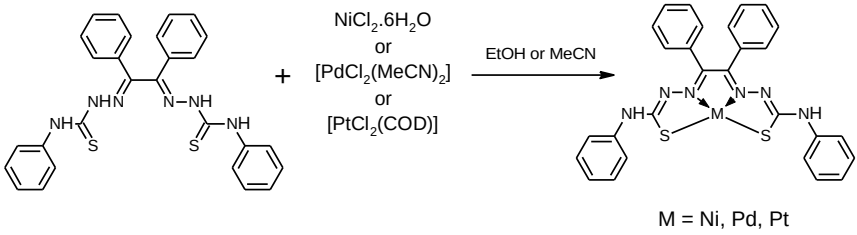

Figure 27. Synthesis of the thiosemicarbazone-based complexes.

Discussion

Heck reaction is a very versatile C-C bond formation which is being used for more than forty years. In time, researchers broadened their scope by including different reagents, ligands, and reaction conditions. Researchers also proved it possible to include polymeric materials to act as heterogeneous catalysts, which are very easy to isolate from the medium and reused many times. Sometimes, Heck chemistry is used tandem with other palladium-catalyzed couplings like Suzuki or Sonogashira reactions.

This possibility allows the researchers to use more reagents and more different conditions than ever before. We hope that this piece of work becomes useful for readers.

Acknowledgments

The authors thank Prof. Dr. Mehmet ALTUN for carefully proofreading and commenting on the paper.

References

ANONYMOUS. (2020, April 18). Heck Reaction. https://en.wikipedia.org/wiki/Heck_reaction.

BARAZANDEHDOUST, M., MAMAGHANI, M., & KEFAYATI, H. (2020). "A novel phosphine-free and recyclable palladium organic–inorganic hybrid magnetic nanocatalyst for Heck cross-coupling reactions". *Reaction Kinetics, Mechanisms and Catalysis*, *129*(2), pp. 1007–1026. https://doi.org/10.1007/s11144-020-01744-5

BOZTEPE, C., KÜNKÜL, A., & GÜRBÜZ, N. (2020). "Hydrogel supported vinylimidazole based PEPPSI-Pd-NHC catalysts: The catalytic activities in Heck and Suzuki-Miyaura coupling reactions". *Journal of Molecular Structure*, 1209, p. 127948. https://doi.org/10.1016/j.molstruc.2020.127948

ERDEMİR, F., AKTAŞ, A., BARUT CELEPCİ, D., & GÖK, Y. (2020). "New (NHC)Pd(II)(PPh_3) complexes: Synthesis, characterization, crystal structure and its application on Sonogashira and Mizoroki–Heck cross-coupling reactions". *Chemical Papers*, 74(1), pp. 99–112. https://doi.org/10.1007/s11696-019-00859-x

HACHEM, M., SCHNEIDER, C., & HOARAU, C. (2020). "Direct Stereoselective β-arylation of enol ethers by a decarboxylative Heck-Type reaction: Direct stereoselective β-arylation of enol ethers by a decarboxylative Heck-Type reaction". *European Journal of Organic Chemistry*, 2020(14), pp. 2052–2061. https://doi.org/10.1002/ejoc.201901877

HAJIPOUR, Abdol R., & KHORSANDI, Z. (2020). "Pd/Cu-free Heck and Sonogashira coupling reactions applying cobalt nanoparticles supported on multifunctional porous organic hybrid". *Applied Organometallic Chemistry*, 34(4), e5398, pp.1-8. https://doi.org/10.1002/aoc.5398

HAJIPOUR, Abdol Reza, KHORSANDI, Z., ABESHTIANI, Z., & ZAKERI, S. (2020). "Pd/Cu-free Heck and C–N coupling

reactions using two modified magnetic chitosan cobalt catalysts: Efficient, inexpensive and green heterogeneous catalysts". *Journal of Inorganic and Organometallic Polymers and Materials*. pp. 2163-2171. https://doi.org/10.1007/s10904-019-01397-5

HE, L., JIA, C., ZHANG, Y., & HE, J. (2020). "Visible light catalyzed step-growth polymerization through Mizoroki–Heck coupling reaction". *Macromolecular Rapid Communications*, 41(7), 1900640.pp. 1-6. https://doi.org/10.1002/marc.201900640

HONG, K., SAJJADI, M., SUH, J. M., ZHANG, K., NASROLLAHZADEH, M., JANG, H. W., VARMA, R. S., & SHOKOUHIMEHR, M. (2020). "Palladium nanoparticles on assorted nanostructured supports: Applications for Suzuki, Heck, and Sonogashira cross-coupling reactions". *ACS Applied Nano Materials*, 3(3), 2070–2103. https://doi.org/10.1021/acsanm.9b02017

ISLAM, M. S., & MIA, M. A. S. (2020). "Synthesis of dendrimer assisted cobalt nanoparticles and catalytic application in Heck coupling reactions in ionic liquid". *SN Applied Sciences*, 2(4), 679. pp. 1-13. https://doi.org/10.1007/s42452-020-2448-2

KE, L., & CHEN, Z. (2020). "Dienedioic acid as a useful diene building block via directed Heck-decarboxylate coupling". *Communications Chemistry*, 3(1), 48. pp. 1-12. https://doi.org/10.1038/s42004-020-0295-0

LAKSHMINARAYANA, B., VINODKUMAR, T., SATYANARAYANA, G., & SUBRAHMANYAM, Ch. (2020). "Novel ultra-small Pd NPs on SOS spheres: A new catalyst for domino intramolecular Heck and intermolecular Sonogashira couplings". *RSC Advances*, 10(8), 4568–4578. https://doi.org/10.1039/C9RA09429F

LIMA, J. C., NASCIMENTO, R. D., VILARINHO, L. M., BORGES, A. P., SILVA, L. H. F., SOUZA, J. R., DINELLI, L. R., DEFLON, V. M., da HORA MACHADO, A. E., BOGADO, A. L., & MAIA, P. I. S. (2020). "Group 10 metal complexes with a tetradentate thiosemicarbazonate ligand: Synthesis, crystal structures and computational insights into the catalysis for C–C coupling via Mizoroki-Heck reaction". *Journal of Molecular Structure*, 1199, 126997. https://doi.org/10.1016/j.molstruc.2019.126997

MALUNAVAR, S. S., SUTAR, S. M., SAVANUR, H. M., KALKHAMBKAR, R. G., & LAALI, K. K. (2020). "Facile access

to libraries of diversely substituted 2-aryl-benzoxazoles/benzothiazoles from readily accessible aldimines via cyclization/cross coupling in imidazolium-ILs with $Pd(OAc)_2$ or $NiCl_2$ (dppp) as catalyst". *Tetrahedron Letters*, 61(6), 151509. https://doi.org/10.1016/j.tetlet.2019.151509

MASTALIR, Á., HANCSÁRIK, M., & SZABÓ, T. (2020). "Immobilization of a Pd(II) complex on hydrophilic graphite oxide and its catalytic investigation in the Heck coupling reaction". *Applied Organometallic Chemistry*, 34(4). e5565. pp. 1-9. https://doi.org/10.1002/aoc.5565

MIRZA-AGHAYAN, M., MOHAMMADI, M., ADDAD, A., & BOUKHERROUB, R. (2020). "Pd nanoparticles supported on reduced graphene oxide as an effective and reusable heterogeneous catalyst for the Mizoroki–Heck coupling reaction". *Applied Organometallic Chemistry*, 34(4). e5524. pp. 1-12. https://doi.org/10.1002/aoc.5524

NURI, A., VUCETIC, N., SMÅTT, J.-H., MANSOORI, Y., MIKKOLA, J.-P., & MURZIN, D. Yu. (2020). "Synthesis and characterization of palladium supported amino functionalized magnetic-MOF-MIL-101 as an efficient and recoverable catalyst for Mizoroki–Heck cross-coupling". *Catalysis Letters*. pp. 1-13. https://doi.org/10.1007/s10562-020-03151-w

OLOYEDE, H. O., ORIGHOMISAN WOODS, J. A., GÖRLS, H., PLASS, W., & ESEOLA, A. O. (2020). "N-donor-stabilized Pd(II) species supported by sulphonamide-azo ligands: Ligand architecture, solvent co-ligands, C–C coupling". *Journal of Molecular Structure*, 1199, 127030. https://doi.org/10.1016/j.molstruc.2019.127030

RAGO, A. J., & DONG, G. (2020). "Unexpected *ortho*-Heck Reaction under the Catellani Conditions". *Organic Letters*, acs.orglett.0c00952. https://doi.org/10.1021/acs.orglett.0c00952

RATHOD, P. B., KUMAR, K. S. A., KUMAR, M., DEBNATH, A. K., PANDEY, A. K., & ATHAWALE, A. A. (2020). "Palladium acetate and Pd nanoparticles loaded hexamethylenetetramine anchored magnetically retrievable assemblies for catalyzing Mizoroki-Heck type mono and *gem*-Dicoupling reactions". *ChemistrySelect*, 5(6), pp. 1961–1971. https://doi.org/10.1002/slct.201903498

SHAHAMAT, Z., NEMATI, F., & ELHAMPOUR, A. (2020). “Palladium (II) anchored on a magnetic mesoporous polymelamine–formaldehyde as new catalyst for Heck coupling reaction: Optimization of reaction using response surface methodology”. *Journal of Porous Materials*, 27(1), pp. 107–122. https://doi.org/10.1007/s10934-019-00795-x

SRUTHI, P. R., SARIKA, V., SUKU, A., KRISHNAN, A., & ANAS, S. (2020). “Amidoxime modified PAN supported palladium complex: A greener and efficient heterogeneous catalyst for Heck reaction”. *Inorganica Chimica Acta*, 502, 119305. https://doi.org/10.1016/j.ica.2019.119305

STEPHAN, M., PANTHER, J., WILBERT, F., OZOG, P., & MÜLLER, T. J. J. (2020). “Heck reactions of acrolein or enones and aryl bromides - synthesis of 3-Aryl propenals or propenones and consecutive application in multicomponent pyrazole syntheses: Heck reactions of acrolein or enones and aryl bromides - synthesis of 3-Aryl propenals or propenones and consecutive application in multicomponent pyrazole syntheses”. *European Journal of Organic Chemistry*, 2020(14), pp. 2086–2092. https://doi.org/10.1002/ejoc.202000066

TANG, H., YAO, F., LIU, L., & CAI, M. (2020). “Recyclable heterogeneous palladium-catalyzed Heck coupling polycondensation of bis(acrylamide)s with aromatic diiodides towards polycinnamamides”. *Journal of Macromolecular Science, Part A*, 57(3), pp. 198–206. https://doi.org/10.1080/10601325.2019.1680256

TARGHAN, H., HASSANPOUR, A., SOHRABNEZHAD, S., & BAHRAMI, K. (2020). “Palladium nanoparticles immobilized with polymer containing nitrogen-based ligand: A highly efficient catalyst for Suzuki–Miyaura and Mizoroki–Heck coupling reactions”. *Catalysis Letters*, 150 (3), pp. 660–673. https://doi.org/10.1007/s10562-019-02981-7

VELPULA, V. R. K., KETIKE, T., PALETI, G., KAMARAJU, S. R. R., & BURRI, D. R. (2020). “A facile synthesis of Pd–C3N4@Titanate nanotube catalyst: Highly efficient in Mizoroki–Heck, Suzuki–Miyaura C–C couplings”. *Catalysis Letters*, 150(1), pp. 95–105. https://doi.org/10.1007/s10562-019-02955-9

YANG, Q., WU, H., ZHAN, H., HOU, J., GAO, M., SU, Q., & WU, S. (2020). “Attapulgite-anchored Pd complex catalyst: A highly active and reusable catalyst for C–C coupling reactions”. *Reaction*

Kinetics, Mechanisms and Catalysis, 129(1), pp. 283–295. https://doi.org/10.1007/s11144-019-01698-3

ZHENG, K., XIAO, G., GUO, T., DING, Y., WANG, C., LOH, T.-P., & WU, X. (2020). "Intermolecular reductive Heck reaction of unactivated aliphatic alkenes with organohalides". *Organic Letters*, 22(2), pp. 694–699. https://doi.org/10.1021/acs.orglett.9b04474

ZHENG, X., ZHAO, J., XU, M., & ZENG, M. (2020). "Preparation of porous chitosan/reduced graphene oxide microspheres supported Pd nanoparticles catalysts for Heck coupling reactions". *Carbohydrate Polymers*, 230, 115583. https://doi.org/10.1016/j.carbpol.2019.115583

ZOU, F., YAO, F., LIU, L., & CAI, M. (2020). "Recyclable heterogeneous palladium-catalyzed carbon–carbon coupling polycondensations toward highly purified conjugated polymers". *Journal of Polymer Research*, 27(1), 1. https://doi.org/10.1007/s10965-019-1979-y

DETERMINATION OF FATTY ACID COMPONENTS OF SOME TROPICAL FRUITS BY MICROWAVE ASSISTED ANALYSIS METHOD AND COMPARISON WITH TRADITIONAL METHOD

Mustafa Biriken & Rifat Battaloğlu**

1. Introduction

Many tropical fruits can be considered a reservoir of bioactive substances with a special interest due to their possible health-promoting properties [1]. *Citrus aurantifolia* is an important food and medicinal which is plant widely cultivated in many areas of the world. It is valuable because of its nutritional qualities and various health benefits. The plant is widely used in traditional medicine as antiviral, antiseptic, anthelmintic, antifungal, astringent, diuretic, mosquito bite repellent, for the treatment of stomach ailments, constipation, headache, arthritis, colds, coughs, sore throats and used as appetite stimulant [2]. *Fortunella margarita*, belonging to the genus *Fortunella*, is a relative of *Citrus* and also included in the Rutaceae family. The fruits and leaves of *Fortunella* species are used in folk medicine in China [3]. *Passiflora edulis* is a wide spread plant cultivated around all tropical countries of the world. The *Passiflora edulis* is commonly known as yellow passion fruit [4]. A large variety of methods are available for extraction of medicinal plants and choice of suitable method depends on the nature of the analyzed plant. Recently, microwave assisted extraction has drawn significant research attention in medicinal plant research due to its inherent advantages [5].

2. Materials and Methods

2.1 Plant Materials

Citrus aurantifolia, Fortunella matgarita Swingle. *Passiflora edulis* samples were freshly purchased from the market. Samples were dried and ready to be analyzed. Dried fruit samples were grinded prior to analysis.

2.2 Oil Extraction

The oils were extracted from three fruits by Soxhlet extraction according to method [6] given below with some modifications. Shortly, 10 g sample of each fruits was ground in a ball mill and extracted with acetone-hexane (1/1) for 6 hrs. The solvents were removed with a rotary evaporator. Microwave oven was modified instead of classic heating devices for the

* (Dr. Öğr. Üyesi); Niğde Ömer Halisdemir University, Science and Art Faculty, Department of Chemistry, 51245, Niğde, Turkey, e-mail: rbattaloglu@ohu.edu.tr

comparison aimed studies, and microwave supported Soxhlet extraction (MSE) was used.

2.3 Analysis of Fatty acid

The methyl esters of the fatty acids were prepared according to the International Union of Pure and Applied Chemistry (IUPAC) [7]. The fatty acid composition was analysed by GC_MS(Shimadzu QP2010 Ultra) equipped with a fused silica capillary Rxi-5ms column (60 mm × 0.32 mm i.d., 0.25 μm film thickness). Injector, column and detector temperatures were 230, 195 and 240 °C, respectively. The split ratio was 80:1. The carrier gas was helium at1.0 mL/min ratio.

3. Results and Discussion

3.1 Oil yields of fruits samples

Heating mantle was used for SE analysis of the fruits and the temperature measures changed Between 70-90ºC. Power indicator of the microwave oven remained constant at 600 Watt. The analysis took 360 minutes for the Soxhlet Extraction (SE) and 60 minutes for the microwave supported Soxhlet extraction (MSE). Saving of time was nearly 91.67 % for the Microwave supported Soxhlet Extraction (MSE). It is known that time has been saved for the thermal operations included thermal operation of eatibles during the application of microwave heating method.

Table 1.Oil yields of fruits samples

Fruits	**SE Yield (%)**	**MSE Yield (%)**
Citrus aurantifolia	18.15	20.02
Fortunella matgarita Swingle	19.74	24.95
Passiflora edulis	23.38	29.02

3.2 Fatty acid composition of Citrus aurantifolia fruit

Table 2 shows the dominant fatty acids' compontents of Citrus Aurantifolia fruit obtained by raw oils given to gas chromotography after methyl esters were obtained by both MSE and SE methods.

Table 2. Fatty acids' compontents of *Citrus aurantifolia* fruit

Fatty acid		SE		MSE	
		RT*	%	RT	%
Palmitic acid	C16:0	36.33	21.05	37.21	20.92
Stearic acid	C18:0	41.40	10.81	44.24	11.12
Oleic acid	C18:1	40.19	30.57	43.01	31.65
Linoleic acid	C18:2	40.06	12.19	42.35	13.09
Linolenic acid	C18:3	52.43	9.61	52.15	10.03
Total			**84.23**		**86.81**

*: RT: Retention Time.

While citrus aurantifolia fruit's fatty acid components was examined, the observation was that while dominant fatty acids were %84.23 at SE technique, it increased to %86.81 at MSE method. Dominant fatty acids' components were appeared as same components at both methods.

Each C16:00 (Palmitic acid) and C18:00 (Stearic acid) from these components is a saturated fatty acid. It is determined that sum of the saturated fatty acids at SE method is %31.86, sum of the unsaturated fatty acids at SE methods is %52.37. Moreover; sum of the saturated fatty acids at MSE method is 32.04 %, sum of the unsaturated fatty acids at MSE methods is 54.57 %. It can be seen that sum of the unsaturated fatty acids are at the higher rates at both methods. However, there is no change, even a little decrease at percent component of MSE method only for C16:0.

3.3 Fatty acid composition of Fortunella matgarita Swingle fruit

Table 3 shows the dominant fatty acids' compontents of *Fortunella matarita* Swingle fruit obtained by raw oils given to gas chromotography after methyl esters were obtained by both MSE and SE methods.

Table 3. Fatty acids' compontents of *Fortunella matgarita* Swingle

Fatty acid		SE		MSE	
		RT	%	RT	%
Palmitic acid	C16:0	40.74	12.19	41.02	14.06
Palmitoleic acid	C16:1	7.57	2.48	8.63	2.62
Stearic acid	C18:0	10.68	3.56	10.51	4.25
Oleic acid	C18:1	36.39	16.53	37.08	18.24
Linoleic acid	C18:2	40.29	34.40	41.32	35.12
Linolenic acid	C18:3	40.19	13.26	42.38	13.48
Total			**82.42**		**87.77**

While fortunella matgarita swingle fruit's fatty acid components was examined, the observation was that while dominant fatty acids were 82.42 % at SE tecnique, it increased to 87.77 % at MSE method. Dominant fatty acids' components were appeared as same components at both methods. Each C16:00 (Palmitic acid) and C18:00 (Stearic acid) from

these components is a saturated fatty acid. It is determined that sum of the saturated fatty acids at SE method is %15.75 , sum of the unsaturated fatty acids at SE methods is 66.67 %. Moreover; sum of the saturated fatty acids at MSE method is 18.31 %, sum of the unsaturated fatty acids at MSE methods is 69.46 %. It was examined that the unsaturated fatty acids were at the higher rates at both methods. It was seen that all the components increases even if it is in a little amount fort he MSE method. Generally, microwave supported analysises were obtained with more yield espacially for unsaturated fatty acids.

3.4 Fatty acid composition of Passiflora edulis

Table 4 shows the dominant fatty acids' compontents of *Passiflora edulis* fruit obtained by raw oils given to gas chromotography after methyl esters were obtained by both MSE and SE methods.

Table 4 Fatty acids' compontents of *Passiflora edulis*

Fatty acid		**SE**		**MSE**	
		RT	**%**	**RT**	**%**
Palmitic acid	C16:0	36.37	11.69	35.26	10.27
Stearic acid	C18:0	40.72	0.76	40.88	0.81
Oleic acid	C18:1	40.23	12.29	41.22	12.31
Linoleic acid	C18:2	40.15	50.42	41.78	54.56
Linolenic acid	C18:3	43.83	1.23	44.09	1.67
Total			**76.39**		**79.62**

While *Passiflora edulis* fruit's fatty acid components was examined, the observation was that while dominant fatty acids were 76.39 % at SE tecnique, it increased to 79.62 % at MSE method. Dominant fatty acids' components were appeared as same components at both methods. Each C16:00 (Palmitic acid) and C18:00 (Stearic acid) from these components is a saturated fatty acid. It is determined that sum of the saturated fatty acids at SE method is 12.45 % , sum of the unsaturated fatty acids at SE methods is 63.94 %. Moreover; sum of the saturated fatty acids at MSE method is 11.08 %, sum of the unsaturated fatty acids at MSE methods is 68.54 %. It was examined that the unsaturated fatty acids were at the higer rates at both methods. There is a increase at the MSE tecniques except Palmitic acid. There is a decrease for the Palmitic acid even it is a little. Generally, microwave supported analysises were obtained with more yield espacially for unsaturated fatty acids.

3.5 Saturated and unsaturated fat ratios of fruit samples

In the results of the analyses, at the SE method sum of the saturated fatty acids in *Citrus anurantifolia* fruit is 31.86 %, and the sum of the

unsaturated fatty acids is 52.37 %; sum of the saturated fatty acids in *Fortunella matgarita* Swingle fruit is 15.75 %, and the sum of the unsaturated fatty acids is 66.67 %; sum of the saturated fatty acids in *Passiflora edulis* fruit is 12.45 %, and the sum of the unsaturated fatty acids is % 63.94. Generally, it is determined that rate of saturated fatty acids in *Citrus aurantifolia* fruit is higher than the unsaturated fatty acid rate. At the MSE method, sum of the saturated fatty acids in *Citrus aunrantifolia* fruit is 32.04 %, and the sum of the unsaturated fatty acids is 54.77 %; sum of the saturated fatty acids in *Fortunella matgarita* Sswingle fruit is %18.31, and the sum of the unsaturated fatty acids is 69.46 %; sum of the saturated fatty acids in *Passiflora edulis* fruit is 11.08 %, and the sum of the unsaturated fatty acids is 68.54 %. Generally, it is determined that rate of saturated fatty acids in *Citrus aurantifolia* fruit is higher than the unsaturated fatty acid rate.

4. Conclusion

When the results of the investigation are examined, it is possible to determine the fatty acids that are the important components for the plants and especially the fruits with different extraction methods. Microwave supported extraction method, which is being often used in recent years, can do analysis when it is being added to soxhlet extraction method. Average 6 hours of analysis at locally done with soxhlet extraction method decreases to 30 minutes when it is done with microwave supported soxhlet extraction. It is seen that this method saves a lot of time. At the microwave supported soxhlet extraction, usage of solvent decreases in comparison to locally done soxhlet extraction, that method both decreases the solvent cost and has beneficial effects on nature so that makes MSE superior against SE. For the plants, the thing came out is that not only fatty acids but also other volatile components could be done with microwave supported analyses thus there will be both time and solvent savings.

References

[1] E. Murillo, D. Giuffrida, D. Menchaca, P. Dugo, G. Torre, A.J. Meléndez-Martinez, and L. Mondello (2013), "Native carotenoids composition of some tropical fruits", *Food Chemistry*, 140(4), 825-836.

[2] O. S. Enejoh, I. O. Ogunyemi, Bala, M. S., Oruene, I. S., Suleiman, M. M., & Ambali, S. F. (2015), "Ethnomedical Importance of Citrus Aurantifolia (Christm) Swingle", *The Pharma Innovation*, **4**(8, Part A), 1,.

[3] S. Parashar, H. Sharma and M. Garg, (2014), "Antimicrobial and antioxidant activities of fruits and vegetable peels: A review, *Journal of Pharmacognosy and Phytochemistry"*, **3(1),** 160-164.

[4] S. S. Patel (2009),"Morphology and pharmacology of Passiflora edulis: a review", *Journal of Herbal medicine and Toxicology*, **3(1**), 1-6,.

[5] S. Baki, A. N. Tufan, M. Altun, F. Özgökçe, K. Güçlü and M. Özyürek (2018), "Microwave-assisted extraction of polyphenolics from some selected medicinal herbs grown in Turkey", *Records of Natural Products*, **12(1)**, 29.

[6] *International Organization for Standardization*, (1988), "Oil seeds - Determination of oil content", ISO Geneva, Switzerland, Standard No. 659.

[7] IUPAC, "Standard Methods for Analysis of Oils, Fats and Derivates", *International Union of Pure and Applied Chemistry*, 7th ed. IUPAC Method 2.301, Blackwell Scientific Publications, (1987).

HYBRID (FUSION-FISSION) REACTORS

Mehtap Düz[*]

Introduction

Reactors where nuclear fusion and fusion reactions can be carried out together are called hybrid reactors. The purpose of hybrid reactors; to obtain high energy with fusion reaction and to meet the energy need, to produce useful fissile materials and energy from long-life radioactive products by making conversion and fission reaction to fertile materials such as ^{238}U, ^{232}Th in the reactor.

In order to obtain energy in hybrid reactors, the first step is fuel selection as in other fission and fusion reactors. As fuel, uranium in fission reactors, D-D or D-T fuels were preferred in fusion reactors. In hybrid reactors, D-D or D-T fuel is used as fuel in order to obtain high energy and carry out other reactions. The fusion reaction is applied to the D-D or D-T fusion fuels used at high temperatures in order to combine the nuclei and overcome the electrostatic push barrier. The fuel used with the fusion reaction is made into plasma. Plasma is magnetically limited by the help of toroidal and poloidal magnetic fields so that the plasma can stay in balance and not interact with the reactor materials (Figure 1.).

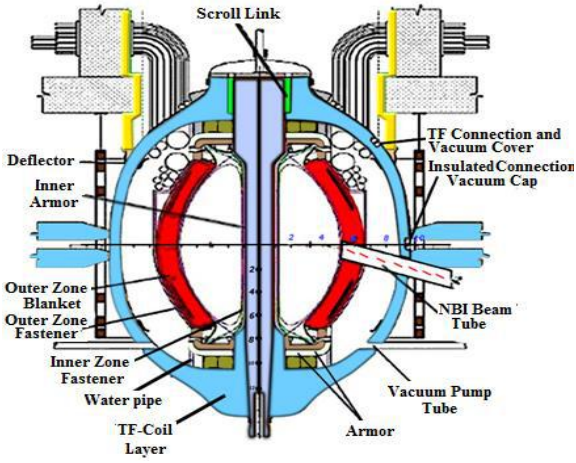

Figure 1. Illustration of a hybrid reactor (El-Guebaly & ARIES Team, 2018)

[*] (Associate Professor.); İnönü Üniversity, Faculty of Arts and Sciences, Department of Physics, Malatya-TÜRKİYE, e-mail: mehtap.gunay@inonu.edu.tr

D-T fuel is used as a fuel in hybrid reactors, where more energy is obtained than D-D fuel. With the fusion reaction of D-T fuel, 14.1 MeV fusion neutron and alpha particle with 3.5 MeV energy are released. The alpha particle transfers the energy it has to the plasma so that the fusion reaction can continue and the plasma does not cool. Since the energy of fusion neutrons with 14.1 MeV energy is very high, it is very difficult to control these neutrons (Baetsle, 2001; Şahin, 2007; Nygren, et al., 2004; Kadomtsev, 1992; Şahin, et al., 2001; Günay, 2016). For this reason, in order to use high energy fusion neutrons in a useful way and act in accordance with the purpose of hybrid reactors, the surrounding of the plasma is surrounded by a wall formed by ^{238}U or ^{232}Th fertile materials that cannot fission reaction with thermal neutrons but can react with high energy neutrons such as 14.1 MeV. Thus, 14.1 MeV high-energy fusion neutrons that come out of the plasma transform and fission reaction with the ^{238}U or ^{232}Th fertiles surrounding the plasma. At the end of the transformation reaction, if ^{238}U fertile is used in the wall surrounding the plasma, ^{239}Pu fissile, if ^{232}Th fertile is used, ^{233}U fissure is obtained. At the end of the fission reaction, fission neutrons and energy are also produced.

$$^{238}U(n,\gamma)^{239}U \xrightarrow{\beta^-} {}^{239}Np \xrightarrow{\beta^-} {}^{239}Pu$$

$$^{232}Th(n,\gamma)^{233}Th \xrightarrow{\beta^-} {}^{233}Pa \xrightarrow{\beta^-} {}^{233}U$$

While a small part of the fissile fuel produced in hybrid reactors is used to contribute to energy production in the reactor, the remaining amount is taken out of the reactor by suitable methods and used as fuel in fission reactors. In other words, high energy fusion neutrons transform and fission into fertile fuels (^{238}U, ^{232}Th), resulting in fissile fuel (^{239}Pu, ^{233}U), fission neutrons and energy production at the same time. Production of these fissile materials is important for hybrid reactors since ^{239}Pu and ^{233}U fissile materials are fuel raw materials used in fission reactors.

D-T fuel, which is used as a fuel in hybrid reactors, is easy to supply since deuterium is abundant in water. However, tritium is a radioactive element that can be produced in the laboratory. In order for the hybrid reactors to continue working, the D-T fusion reaction must also continue. However, since tritium reacts with deuterium, tritium supplementation is required to continue the reaction. For this, either the tritium produced in the laboratory must react with deuterium or the reactor must produce its own tritium. It is more logical for the reactor to produce the required tritium itself. Since tritium is produced by the reaction of lithium with neutrons, a reactor must contain a lithium-containing wall in the reactor in order for hybrid reactors to produce the required tritium. Accordingly, neutrons released from plasma and other nuclear reactions react with the lithium-containing wall,

thereby producing the required tritium for the fusion reaction to continue due to the operation of hybrid reactors.

Three types of nuclear reactions have occurred in hybrid reactors: fusion, fission and production (conversion) reactions for energy, fissile fuel and tritium production. Fusion reaction of hybrid reactors; It is made to obtain high energy in D-D or D-T fusion fuels. The fusion neutron with 2.45 MeV energy is obtained at the end of the D-D fusion reaction, and the fusion neutron with 14.1 MeV energy is obtained at the end of the D-T fusion reaction. Fission reaction; The reaction of fertile materials with the released high-energy neutrons is done to obtain energy and fission neutrons at the end. Thus, fusion neutrons with 14.1 MeV energy, which are released when using D-T fusion fuel, are reacted with radioactive ^{238}U or ^{232}Th fertilizers to produce energy and fission neutrons. Production (transformation) reaction; It is carried out to absorb fissile fuel and the required tritium production for the reactor by absorbing neutrons with the fast neutrons released. ^{239}Pu or ^{233}U fissile materials are produced by conversion by absorbing neutrons with 14.1 MeV energy fusion neutrons, radioactive ^{238}U or ^{232}Th fertiles, which are released by D-T fusion reaction. Hybrid reactors are 100% benefited from natural uranium by fission and conversion by ^{238}U fertile, which is less likely to react with thermal neutrons and left as waste in fission reactors, by reacting with rapid neutrons in hybrid reactors to obtain ^{239}Pu fissil. Thus, ^{239}Pu fissure, which is the fuel raw material in fission reactors, is obtained from the radioactive ^{238}U isotope. When D-T fuel is used in hybrid reactors, while deuterium is abundant, since tritium is a radioactive element that can be produced in the laboratory, it is necessary to produce the tritium necessary for the operation of hybrid reactors and for the D-T fusion reaction to continue. For this, the neutrons released from plasma and other nuclear reactions react with the lithium layer, resulting in the required tritium production for the reactor (Baetsle, 2001; Şahin, 2007; Nygren, et al., 2004; Kadomtsev, 1992; Şahin, et al., 2001).

Natural lithium consists of 7.56% ^{6}Li and 92.44% ^{7}Li isotope. $^{6}Li(n, \alpha)T$ reaction reacts with thermal neutrons, $^{7}Li(n, \alpha n')T$ reaction reacts with fast neutrons. Accordingly, neutrons released from plasma and other nuclear reactions first react with ^{7}Li isotopes in the lithium region. At the end of the reaction with ^{7}Li, tritium, ^{4}He and thermal neutrons are produced. Thermal neutrons released react with ^{6}Li to produce tritium and ^{4}He.

$$^{6}Li + {}^{1}n \rightarrow T + {}^{4}He + 4{,}784\ MeV$$

$$^{7}Li + {}^{1}n \rightarrow T + {}^{4}He + {}^{1}n - 2{,}467\ MeV$$

The reaction of the neutrons released from plasma and other nuclear reactions in the lithium layer ensures the tritium production required for the operation of hybrid reactors and the D-T fusion reaction to continue, from ^{6}Li and ^{7}Li.

In hybrid reactors, heat conducting coolers are used to prevent the reactor core from melting and to convert the released heat energy into electrical energy. Liquid and gas coolers are used as coolants. In hybrid reactors, heat energy is taken with liquid and gas coolers and transferred to the generators to obtain electrical energy. Liquid coolers should generally be liquid metals such as liquid lithium, liquid sodium due to their heat transmission and nuclear properties. Helium is used as the gas cooler.

In hybrid reactors, the reactor environment is surrounded by a reflector to capture the escaping neutrons and provide neutron economy. Graphite, Be, Fe materials are generally used as reflectors (Baetsle, 2001; Şahin, 2007; Nygren, et al., 2004; Kadomtsev, 1992; Şahin, et al., 2001; Canada, et al., 1994).

I. APEX Hybrid Reactor

In conventional fusion reactors, the fuel used by the fusion reaction in the core area of the reactor turns into plasma and high-energy fusion neutrons, gamma rays and charged particles are released from the plasma.

The first wall surrounding the plasma is exposed to high-energy fusion neutrons, gamma ray, and charged particle fluxes from the plasma. Applying high-energy neutrons to a structural material (solid) causes the atoms in the structural material to migrate to disrupt the mesh structure of the material, i.e. radiation damage. If the first wall is a structural material, it causes degradation of the structural material and reduced reactor life as the most damage is in this region (Abdou, et al., 2001; Ünalan, 1998; Youssef, et al., 1998; Blink, et al., 1985; Perlado, et al., 1995; Duderstadt & Moses, 1982; Şarer, et al., 2007; Youssef & Sawan, 2002). To reduce these adversities, Christofilos first proposed the idea that the first wall surrounding the plasma was a liquid wall rather than a solid wall (Christofilos, 1989; Moir, 1997).

The APEX (Advanced Power Extraction) hybrid reactor was developed in the U.S. in early 1998 to study fusion energy technology. The liquid wall concept proposed by Christofilos was used in APEX. Thus, the traditional first solid wall surrounding the plasma in APEX was replaced by a flowing liquid wall layer. The flowing liquid wall was used for regulating the performance of the APEX hybrid reactor, for energy transfer and tritium production. The most efficient obtaining methods for neutron wall charge

and surface flux have been developed in the APEX hybrid reactor (Abdou, et al., 2001; Abdou, et al., 2005; Abdou, 2004; . Şahin & Übeyli, 2004; Abdou, 2001; Abdou & The APEX Team, 1999; Abdou, et al., 1999; Youssef & Abdou, 2000; Wong, et al., 2004). Figure 2 shows the APEX hybrid reactor.

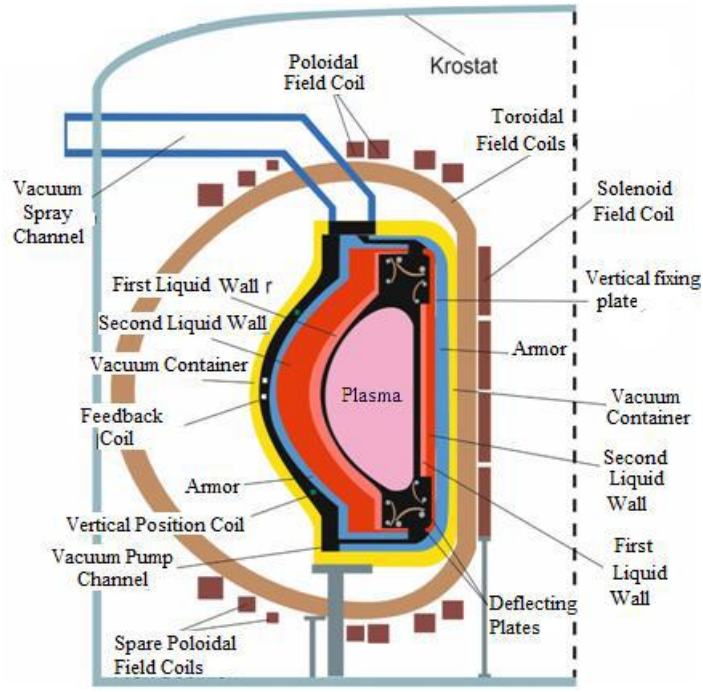

Figure 2. Illustration of APEX hybrid reactor (Neilson, 2013)

The purpose of the APEX hybrid reactor; by producing fusion and fusion reaction, obtaining high energy with fusion reaction, meeting energy requirement and making fusion energy attractive, producing fissile materials used as fuel raw materials from radioactive products in fission reactors by transforming and fusing into fertile materials in APEX as well as in hybrid reactors, and to be a competitive energy source by providing the necessary energy production for the reactor with fission neutrons. Unlike other reactors, fluid liquid wall was used instead of the first solid wall in APEX hybrid reactor. The advantages of using fluid liquid wall instead of traditional first solid wall in APEX are as follows;

a. Ensuring regularity in the balance and limitation of plasma,
b. It has high power density with its renewable wall feature,
Neutron wall load (neutron power falling on the surface)> 10 MW/m^2
Surface heat flux> 2 MW/m^2

c. It significantly reduces radiation damage and activation in structural materials, and increase the life of these materials,
d. Easy maintenance of the materials in the reactor vessel,
e. Provides high thermodynamic efficiency (> 40%),
Thermodynamic efficiency = (High temperature-Low temperature)/High temperature
f. It is the better production of tritium production.

In APEX, two liquid walls, the first (thin) liquid wall and the second (thick) liquid wall, are used. The first liquid wall is after the plasma, the second liquid wall is after the first liquid wall. Both thin and thick liquid walls are suitable for eliminating high surface heat flow. The first thin liquid wall in the reactor is 2 cm thick and at a speed of 20 m/s and traps charged particles. The thick liquid wall flowing a little slower just behind it is 40 cm thick and 8 m/s speed, significantly reducing radiation damage in the structural material and converting it to heat by trapping the radiation energy released due to neutrons (Abdou, et al., 2001; Abdou, et al., 2005; Abdou, 2004; Abdou, 2001; Abdou & The APEX Team, 1999; Abdou, et al., 1999; Youssef & Abdou, 2000; Ying, et al., 1999; Youssef, et al., 2002).

Unlike other reactors, the liquid wall concept was used in the APEX hybrid reactor. The liquid wall used is suitable for removing the high surface heat flow after the plasma, reducing the radiation damage in the structural material and converting the radiation energy into thermal energy by trapping charged particles. However, in order for the liquid wall to not damage the plasma and other layers, it is necessary to flow in the reactor with a certain stability. For this reason, some different fluid wall concepts have been developed by applying various forces to drive the fluid flow of the liquid wall and attach the liquid wall to a back solid wall (Abdou, et al., 2001; Abdou, et al., 1999). These liquid wall concepts;

a. Gravity-Momentum Driven (GMD),
b. Vortex Flow with GMD,
c. Electromagnetic Retention (EMR),
d. Magnetic Thrust are liquid wall concepts.

Of the developed liquid wall concepts, only the magnetic thrust liquid wall concept has not yet been explored for the APEX hybrid reactor. Other fluid wall concepts, along with APEX, have been explored for configurations with tolap, spherical torus and magnetic field constraints.

Gravity-Momentum Driven (GMD) fluid wall concept; the fluid forming the liquid wall is injected at a tangent angle from the top of the sheet towards the back solid wall. In this way, as seen in Figure 3, the fluid flows

towards the bottom of the layer by sticking to the wall with centrifugal force. For the reactor to work efficiently in APEX, the liquid wall must be continuous. In order for the liquid wall to be continuous and stable, the centripetal force that pushes the fluid to the back solid wall must be greater than the force of gravity.

Vortex Flow and GMD fluid wall concept; angular velocity is given to the fluid forming the liquid wall to provide rotational motion. The fluid rotating with angular velocity is attached to the back solid wall in the form of eddy flow. The eddy flow increases the centrifugal acceleration and ensures better adhesion of the fluid to the wall.

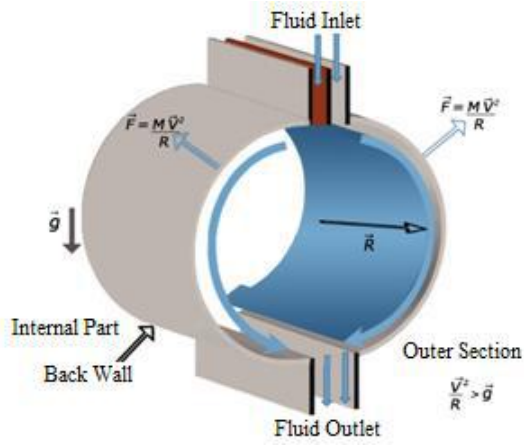

Figure 3. Liquid wall formation with gravity momentum drive (GMD) ($\vec{R}$= curve radius, $\vec{v}$= fluid velocity, $\vec{g}$= gravitational acceleration, $\vec{F}$= centripetal force) (Mirhoseini & Volpe, 2016)

Electromagnetically Restrained (EMR) in liquid wall concept; the fluid forming the liquid wall is injected in the poloidal direction from the top of the sheet towards the back solid wall. A poloidal stream ($\vec{J}$) is produced by injecting the fluid in the poloidal direction. As seen in Figure 4, the generated poloidal current interacts with the toroidal magnetic field ($\vec{B}$) to produce the electrical force ($\vec{F} = \vec{J}x\vec{B}$) that will hold the fluid to the back wall.

Magnetic Propulsion in the concept of liquid wall; the fluid forming the liquid wall is injected from the top of the sheet with an electric current towards the back solid wall. The toroidal magnetic field creates a pressure drive force with the interaction of the applied electric current. The resulting pressure change causes the flow to accelerate from the inner region, where the magnetic field force exists, to the outer region. In addition, an irregular

Lorentz force occurs with the irregularity of the toroidal magnetic field. The Lorentz force created provides an active feedback mechanism to stabilize the flow while keeping the fluid adhered to the solid wall. This fluid wall concept proposed by L. Zakhorov has not yet been studied for APEX (Abdou, et al., 2001; Abdou, et al., 2005; Şahin & Übeyli, 2004; Abdou, 2001; Abdou & The APEX Team, 1999; Abdou, et al., 1999).

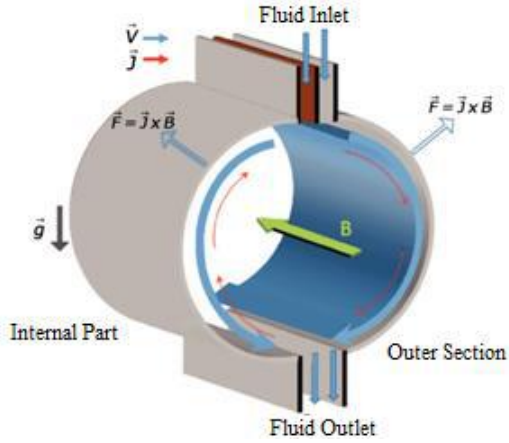

Figure 4. Electromagnetic retention (EMR) fluid wall concept representation ($\vec{B}$=Toroidal magnetic field, $\vec{J}$= Poloidal current density, $\vec{v}$= Fluid velocity, $\vec{F}$= Electromagnetic force) (Mirhoseini & Volpe, 2016).

In the APEX hybrid reactor, the selection of fuel, coolant and structural materials must be made correctly for the production of sufficient energy, fissile fuel, tritium.

II. Fuel

D-D or D-T fusion fuels that produce the fusion reaction are used as fuel in order to obtain high energy and carry out other reactions. As the energy obtained with D-T fuel is more than D-D fuel, D-T fusion fuel is generally preferred as fuel in APEX hybrid reactor. Plasma is formed by fusion of deuterium and tritium nuclei, which come together to realize the high temperature D-T fusion reaction. Fusion neutrons with 14.1 MeV energy and alpha particles with 3.5 MeV energy are released from the plasma. The alpha particle transfers the energy it has to the plasma to continue the fusion reaction and to heat the plasma. Fusion neutrons with 14.1 MeV energy are used to produce fissile fuel, energy and fission neutrons by performing conversion and fission reactions to fertile fuels. The neutrons produced from the plasma with the D-T fusion reaction and obtained by other nuclear reactions are reacted with the lithium layer, resulting in the production of tritium necessary for the D-T fusion to continue.

In APEX hybrid reactor; The use of D-T fuel provides high energy, fissile fuel production, which is the fuel raw material in fission reactors, the production of tritium necessary for the operation of the reactor and the D-T fusion reaction to continue (Ünalan, 1998; Youssef, et al., 1998; Blink, et al., 1985; Sawan & Abdou, 2006; Abdou, et al., 2005; Abdou, et al., 1986; Şahin and H. Yapıcı, 1998).

III. Cooler

Energy carrier materials that provide heat conduction to prevent the melting of the reactor core and to convert the heat energy released into electrical energy are called coolers. Liquid and gas coolers are used as coolants. Liquid coolers that are effective in heat conduction are generally used as coolers in APEX hybrid reactors. Features to be considered in choosing a good cooler are as follows;

1. Low density,
2. High thermal transmission,
3. Low vapor pressure,
4. High lithium atomic density for tritium production,
5. High chemical stability,
6. Low tritium resolution,
7. Low melting point,
8. It is necessary to provide low cost features.

In the APEX hybrid reactor using D-T fusion fuel, the reactor and the required tritium must be met for the D-T fusion reaction to work. Since tritium is produced as a result of reaction with lithium, the energy carrier liquid (coolant) must be a lithium containing liquid to ensure adequate tritium production. Accordingly, in the APEX hybrid reactor, the neutrons that come out of the plasma with the D-T fusion reaction and obtained by other nuclear reactions will react with the lithium layer and provide the required tritium production for the reactor.

Flibe (Li_2BeF_4), Flinabe melt salts and $Li_{20}Sn_{80}$, Li, $Li_{17}Pb_{83}$ liquid metals are used as coolants in the APEX hybrid reactor (Nygren, et al., 2004; Abdou, et al., 2001; Youssef, et al., 1998; Moir, 1997; Abdou, et al., 2005; Abdou, 2004; Abdou, 2001; Abdou & The APEX Team, 1999; Abdou, et al., 1999; Youssef & Abdou, 2000; Wong et al., 2004; Ying, et al., 1999; Youssef, et al., 2002; Yokomine, et al., 2007; Takeuchi, et al., 2006; Jung & Abdou, 1983; Nygren, et al., 2003; Morley, et al., 1999; Übeyli, 2004; Übeyli & Acır, 2007; Übeyli, 2004). In Table 1, some properties of energy carrier liquids which are tritium producer are shown.

Lithium is alkali metal, and it is the liquid metal that is preferred as a coolant because of its high tritium production. Natural lithium has higher

lithium atom density and neutron capture than other coolant candidates. That's why tritium production is good. However, heat conduction is not so good. In addition, lithium is likely to react with water and air. For this reason, the tritium production and chemical properties of materials other than lithium have been investigated as coolants (Moir, 1997; Abdou, et al., 2005; Abdou, 2004; Abdou, 2001; Abdou & The APEX Team, 1999; Abdou, et al., 1999; Youssef & Abdou, 2000; Wong et al., 2004; Ying, et al., 1999; Youssef, et al., 2002; Yokomine, et al., 2007; Takeuchi, et al., 2006; Jung & Abdou, 1983; Nygren, et al., 2003; Morley, et al., 1999; Übeyli, 2004; Übeyli & Acır, 2007; Übeyli, 2004). In Figure 5, Li liquid metal used as a coolant in the APEX hybrid reactor is shown in Figure 5 for the respective regions of the reactor in degrees.

Table 1. Some properties of tritium producing energy carrier fluids (Übeyli, 2004; Übeyli & Acır, 2007; Übeyli, 2004)

	Flibe	**Flinabe**	**$Li_{20}Sn_{80}$**	**Li**	**$Li_{17}Pb_{83}$**
Melting point (ºC)	459	240	330	180	235
Density (g/cm^3)	2	2	6,2	0,48	8,98
Li Density (g/cm^3)	0,28	0,12	0,09	0,48	0,062
Tritium Production	Good	Good	Good	Good	Very good
Chemical Stability	~Determined	~Determined	~Determined	Active	Middle
Tritium Resolution	Very low	-	-	High	Very low

In recent years, the tritium production of Flinabe melt salt and $Li_{20}Sn_{80}$ liquid metal coolants has been investigated. These refrigerant candidates were preferred because their melting points and vapor pressures were low. As can be seen from Table 1, Flinabe's lithium density is higher than $Li_{20}Sn_{80}$ liquid metal. However, due to the high neutron capture cross section of the Fluorine (F) element in Flinabe, the neutrons from the reaction with Flinabe decrease. Flinabe has a lower tritium production than $Li_{20}Sn_{80}$ liquid metal, as fewer neutrons will react for lithium production with tritium, as neutrons decrease with Flinabe. The temperatures of the Flinabe melt salt used in the APEX hybrid reactor as a coolant in Figure 6 and the $Li_{20}Sn_{80}$ liquid metal in Figure 7 are shown in degrees for the respective regions of the reactor.

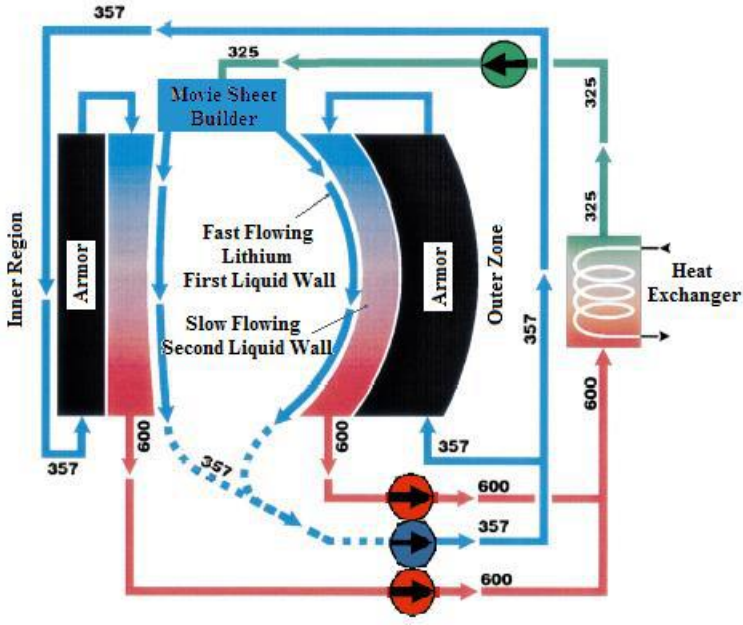

Figure 5. Temperature flow chart for Lithium (Morley, et al., 1999)

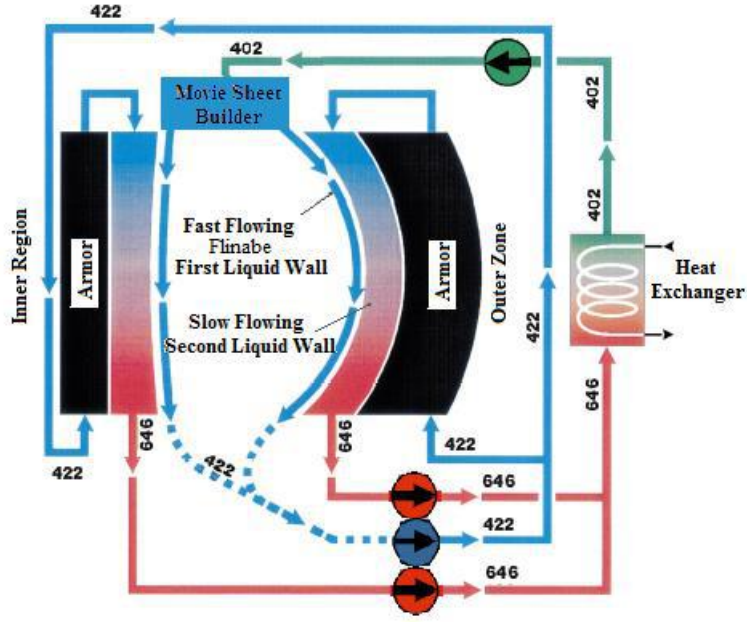

Figure 6. Temperature flow chart for Flinabe (Morley, et al., 1999)

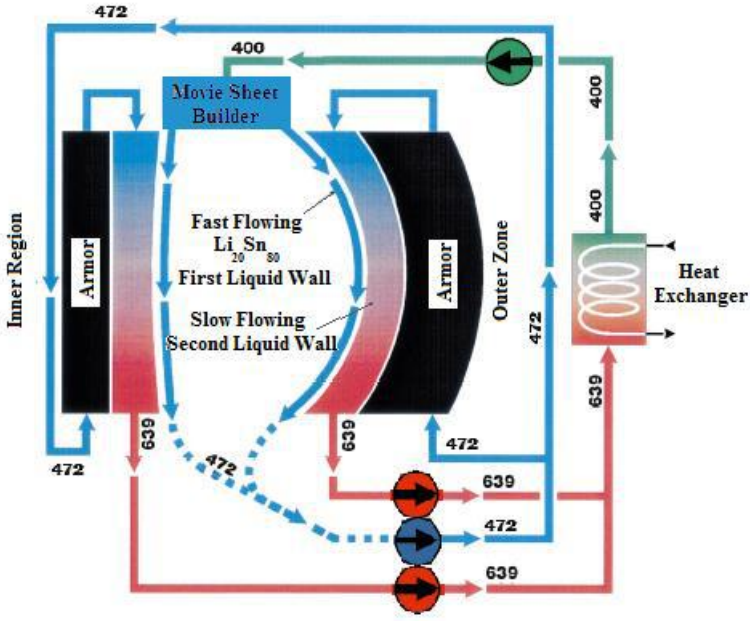

Figure 7. Temperature flow chart for $Li_{20}Sn_{80}$ (Morley, et al., 1999)

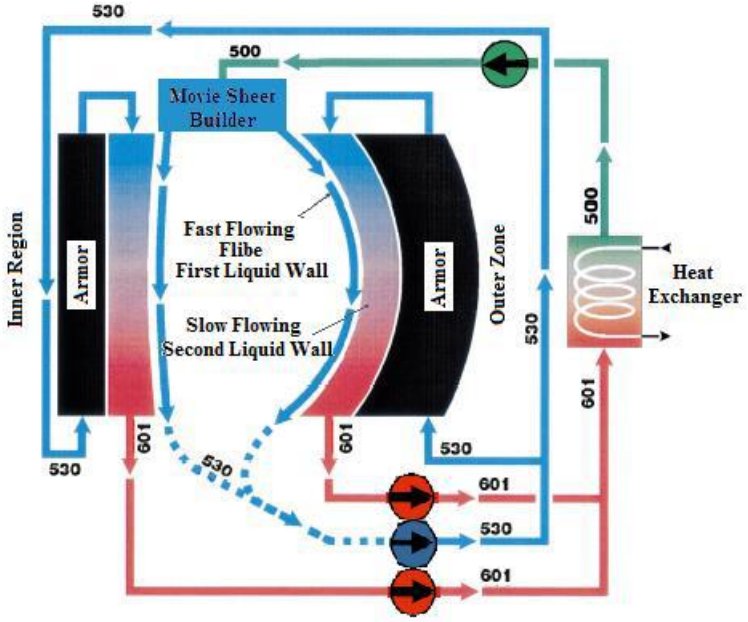

Figure 8. Temperature flow chart for Flibe (Morley, et al., 1999)

The vapor pressure of the $Li_{20}Sn_{80}$ liquid metal is lower than that of the $Li_{17}Pb_{83}$ liquid metal. The stability of the plasma varies depending on the

electrical conductivity of the energy carrier liquid. Flibe is preferred as a coolant due to its low activation and low electrical conductivity (Nygren, et al., 2004; Abdou, et al., 2001; Youssef, et al., 1998; Moir, 1997; Abdou, et al., 2005; Abdou, 2004; Abdou, 2001; Abdou & The APEX Team, 1999; Abdou, et al., 1999; Youssef & Abdou, 2000; Wong et al., 2004; Ying, et al., 1999; Youssef, et al., 2002; Yokomine, et al., 2007; Takeuchi, et al., 2006; Jung & Abdou, 1983; Nygren, et al., 2003; Morley, et al., 1999; Übeyli, 2004; Übeyli & Acır, 2007; Übeyli, 2004). The temperature of the Flibe melt salt used in the APEX hybrid reactor as a coolant is shown in Figure 8 for the relevant regions of the reactor in degrees.

IV. Structural Material

To improve the neutronic performance of the reactors, it is necessary to increase the power density of the hybrid reactor using a high neutron wall load. Structural material should be used in the reactor to achieve high neutron wall load. Features to be considered in choosing a good structural material are as follows;

1. High temperature,
2. Low radiation damage against high energy neutrons,
3. Low hydrogen and helium production by nuclear reactions,
4. High thermal transmission,
5. Low activation properties need to be provided.

Alloys and reflective metals are used as structural materials. As an alloy; Niobium (Nb), Tantalium (Ta), Chrome (Cr), Molybdenum (Mo) and Tungsten (W) are used. As reflective metal; Ferritic steel (9Cr-2WVTa), vanadium alloys (V-4Cr-4Ti) and SiC are used.

The proposed structural materials have high temperature, high neutron wall load and low activation properties. Reflective metals can also be used as fridges in fusion reactors due to their high temperature, good heat conduction and low activation properties (Abdou & The APEX Team, 1999; Abdou, et al., 1999; Youssef & Abdou, 2000; Wong, et al., 2004; Ying, et al., 1999; Nygren, et al., 2003; Morley, et al., 1999; Übeyli & Acır, 2007; Übeyli, 2004; Şahin & Übeyli, 2005).

Result

While fossil energy sources such as oil, coal, and natural gas used for energy production are found in limited quantities, the fact that these resources are consumed rapidly and cause environmental problems led countries to find cleaner and continuous energy resources. After the discovery of fission and fusion reactions, using the high energies obtained

from these reactions, a nuclear reactor was set up to meet the energy needs. It is seen that the alternative clean energy source of the future will be nuclear reactors and the energy need will be provided mostly from nuclear reactors due to the lack of source problems in the realization of fission and fusion reactions, providing high energy at the end of the reactions, meeting the energy need, and not causing environmental problems. For this reason, nuclear energy is considered as the most resource and quick response to human needs when it is considered in terms of economy, environment, security, dependency on foreign resources and sufficient amount of fuel. In addition, the use of nuclear technology will create a new vision not only in the nuclear field but also in the development of science and technology in the communities of the 21st century.

Today, only fission reactors have been applied. Fission and hybrid reactors are at the research and laboratory stage for now due to technological and economic deficiencies. The availability of abundant and easy raw materials used for the fusion reaction, the release of very high energy at the end of the fusion reaction, and the absence of radioactive wastes with the fusion reaction made fusion reactors more attractive than fission reactors. Due to scientific and technical difficulties after the discovery of the fusion reaction, the inability to perform the fusion reaction in a controlled manner showed a slow development in the realization of fusion reactors. For this reason, it is believed that with the sufficient maturity of knowledge and technology, these problems in fusion reactors will be eliminated and the energy source we will use in the 21st century as the clean, cheap, continuous energy source required.

It is now an imperative to turn to the search for a new resource from now on, so that there is no problem with nuclear fuel supply in the next century. Therefore, the amount of waste in nuclear fuel supply and storage areas hybrid reactor system has been proposed by many researchers on reduction, recycling and recycling to use the uranium elements found in spent fuel and making long-life fission products harmless. It is predicted that hybrid reactors will be preferred over fission and fusion reactors in the future, and hybrid reactors will be used as the clean, cheap, continuous energy source required.

References

ABDOU, M. A., et al., (1986), "Deuterium-Tritium Fuel Self-Sufficiency in Fusion Reactors", *Fusion Technology,* Vol. 9, pp. 250-285.

ABDOU, M. A., et al., (1999), "Chapter 1: Overview", *APEX Interim Report,* pp. 1-17.

ABDOU, M. A. and The APEX Team, (1999), "Exploring Novel High Power Density Concepts For Attractive Fusion Systems", *Fusion Engineering and Design*, Vol. 45, pp. 145-167.

ABDOU, M. A., (2001), "Research On Liquid Walls for Fusion Systems", *Applied Electromagnetics and Mechanics*, pp. 151-152.

ABDOU, M. A. et al., (2001), "On The Exploration of Innovative Concepts for Fusion Chamber Technology", *Fusion Engineering and Design*, Vol. 54, pp. 181-247.

ABDOU, M. A., (2004), "Preface", *Fusion Engineering and Design*, Vol.72, pp. 1-2.

ABDOU, M. A., et al., (2005), "Overview of Fusion Blanket R&D in The US Over The Last Decade", *Nuclear Engineering and Technology*, Vol. 37: 5, pp. 401-422.

ABDOU, M. A., et al., (2005), "U.S. Plans and Strategy for ITER Blanket Testing", *Fusion Science and Technology*, Vol. 47, pp. 475-487.

BAETSLE, L. H., (2001), "Application of Partitioning / Transmution of Radioactive Materials in Radioactive Waste Management", *Lectures given at the Workshop on Hybrid Nuclear Systems for Energy Production, Utilisation of Actinides and Transmutation of Long-lived Radioactive Waste Trieste*, 3-7 September, Belgium.

BLINK, A., et al., (1985), In: K. L. Essary, K. L. Lewis, editors, "High–Yield Lithium-Injection Fusion Energy (HYLIFE) Reactor", *UCRL-53559*, Lawrence Livermore National Laboratory.

CANADA, J., et al., (1994), "The Role of NIF in Developing Inertial Fusion Energy", *Energy and Technology Review*, Vol. 38.

CHRISTOFILOS, N. C., (1989), "Design for A High Power-Density Astron Reactor", *Journal of Fusion Energy*, Vol. 8, pp. 97-105.

DUDERSTADT, J. J. and MOSES , G. A., (1982), "*Inertial Confinement Fusion"*, New York: John Wiley & Sons.

EL-GUEBALY, L. A. and ARIES Team (2018), "Nuclear Assessment to Support ARIES Power Plants and Next-Step Facilities: Emerging Challenges and Lessons Learned", *Fusion Science and Technology*, pp. 1536-1555.

GÜNAY, M., (2016), "Monte Carlo Calculations of The Nuclear Effects of Certain Fluids in a Hybrid Reactor", *Progress in Nuclear Energy*, Vol. 86, pp. 103-109.

JUNG, J. and ABDOU, M., (1983), "Assessments of Tritium Breeding Requirements and Breeding Potential for The Starfire / Demo Design", *Nuclear Technology / Fusion*, Vol. 4, pp. 361-366.

KADOMTSEV, B. B., (1992), "Tokamak Plasma: A Complex Physical System", Çeviri editörü: E.W. Laing, Institute of Physics Publishing, Bristol and Philadelphia.

MIRHOSEINI, S. M. H. and *VOLPE*, F. A., (2016), "Resistive sensor and electromagnetic actuator for feedback stabilization of liquid metal walls in fusion reactors", *Plasma Physics and Controlled Fusion*, Vol. 58:12.

MOIR, R. W., (1997), "Liquid First Walls For Magnetic Fusion Energy Configurations", *Nuclear Fusion*, Vol. 37, pp. 557-566.

MORLEY, N. B., et al., (1999), "Chapter 7: Thin Liquid Wall Concepts and The CLiFF Design", *APEX Interim Report*.

NEILSON, H., (2013), "Issues and Paths to Magnetic Confinement Fusion Energy", *Symposium on Worldwide Progress Toward Fusion Energy AAAS Annual Meeting*, Boston.

NYGREN, R. E., et al., (2003), "A Fusion Chamber Design With A Liquid First Wall and Divertor", *20th Symposium on Fusion Engineering*, San Diego, CA, United States.

NYGREN, R. E., et al., (2004), "A Fusion Reactor Design With A Liquid First Wall and Divertor", *Fusion Engineering and Design*, Vol. 72, pp. 181-221.

PERLADO, M., et al., (1995), "Radiation Damage in Structural Materials. Energy from Inertial Fusion, *International Atomic Energy*, 272, Vienna.

SAWAN, M. E. and ABDOU, M. A., (2006), "Physics and Technology Conditions for Attaining Tritium Self-Sufficiency for The DT Fuel Cycle, *Fusion Engineering and Design*, Vol. 81, pp. 1131-1144.

ŞAHİN, S. and YAPICI, H., (1998), "Rejuvenation of Light Water Reactor Spent Fuel in Fusion Blankets", *Annals Nuclear Energy*, Vol. 25: 6, pp. 1317-1339.

ŞAHİN, S., et al., (2001), "Neutronic Performance of Proliferation Hardened Thorium Fusion Breeders", *Fusion Engineering and Design*, Vol. 54, pp. 63-77.

ŞAHİN, S. and ÜBEYLİ, M., (2004), "Modified APEX Reactor as A Fusion Breeder", *Energy Conversion and Management*, Vol. 45, pp. 1497-1512.

ŞAHİN, S. and ÜBEYLİ, M., (2005), "Radiation Damage Studies on The First Wall of a HYLIFE-II Type Fusion Breeder", *Energy Conversion and Management*, Vol. 46, pp. 3185-3201.

ŞAHİN, H. M., (2007), "Monte Carlo Calculation of Radiation Damage in First Wall of An Experimental Hybrid Reactor", *Annals of Nuclear Energy*, Vol. 34, pp. 861-870.

ŞARER, B. et al., (2007), "Three—Dimensional Neutronic Calculations For The Fusion Breeder Apex Reactor, *Fusion Science And Technology*, Vol. 52, pp. 107-115.

TAKEUCHI, J., et al., (2006), "Study of Heat Transfer Enhancement / Suppression for Molten Salt Flows in A Large Diameter Circular Pipe Part I: Benchmarking", *Fusion Engineering and Design*, Vol. 81, pp. 601-606.

ÜBEYLİ, M., (2004), "On The Tritium Breeding Capability of Flibe, Flinabe and Li_{20} Sn_{80} in A Fusion-Fission (Hybrid) Reactor", *Journal of Fusion Energy*, Vol. 22: 1, pp. 51-57.

ÜBEYLİ, M., (2004), "Neutronic Performance of New Coolants in A Fusion-Fission (Hybrid) Reactor", *Fusion Engineering and Design*, Vol. 70, pp. 319-328.

ÜBEYLİ, M. and ACIR, A., (2007), "Utilization of Thorium in A High Power Density Hybrid Reactor With Innovative Coolants", *Energy Conversion and Management*, Vol. 48, pp. 576-582.

ÜNALAN, S., (1998), "Rejuvenation of The LWR Spent Fuel in (D-T) Driven Hybrid Reactors", *Fusion Engineering and Design*, Vol. 38, pp. 393-416.

WONG, C. P. C., et al., (2004), "Molten Salt Self-Cooled Solid First Wall and Blanket Design Based On Advanced Ferritic Steel", *Fusion Engineering and Design*, Vol. 72, pp. 245-275.

YING, A., et al., (1999), "Chapter 5: Thick Liquid Blanket Concept", *APEX Interim Report*, pp. 1-172.

YOKOMINE, T., et al., (2007), "Experimental Investigation of Turbulent Heat Transfer of High Prandtl Number Fluid Flow Under Strong Magnetic Field", *Fusion Science and Technology*, Vol. 52, pp. 625-629.

YOUSSEF, M. Z., et al., (1998), "X-rays Surface And Volumetric Heat Deposition and Tritium Breeding Issues In Liquid-Protected FW In High Power Density Devices", *Draft copy paper presented at the 13th Topical Meeting on the Technology of Fusion Power*, Nashville, Tennessee, June 7-11.

YOUSSEF, M. Z. and ABDOU, M. A., (2000), "Heat Deposition, Damage and Tritium Breeding Characteristics in Thick Liquid Wall Blanket Concepts", *Fusion Engineering and Design*, Vol. 49-50, pp. 719-725.

YOUSSEF, M. Z. and SAWAN, M. E., (2002), "Radwaste Volume in Lithium and Flibe Thick Liquid Wall and Comparison to Conventional SW Concepts", *Fusion Engineering and Design*, Vol. 63-64, pp. 263-269.

YOUSSEF, M. Z., et al., (2002), "The Breeding Potential of "Flinabe" and Comparison to "Flibe" in "CLiFF" High Power Density Concept", *Fusion Engineering and Design*, Vol. 61-62, pp. 497-503.